G.O. SEPARATE

EPRI
Electric Power
Research Institute

Topics:
Geothermal power plants
Geothermal fluids
Scaling
Corrosion
Brines
Chemical analysis

EPRI AP-4342
Project 1195-12
Final Report
December 1985

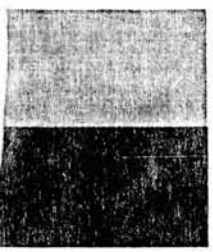

Chemistry, Scale, and Performance of the Hawaii Geothermal Project-A Plant

Prepared by
Hawaii Electric Light Company, Inc.
Hilo, Hawaii

REPORT SUMMARY

SUBJECTS: Geothermal, hydrothermal, geopressure systems / Power system operation

TOPICS: Geothermal power plants; Geothermal fluids; Scaling; Corrosion; Brines; Chemical analysis

AUDIENCE: Generation engineers / R&D scientists

Chemistry, Scale, and Performance of the Hawaii Geothermal Project-A Plant

A two-and-a-half-year monitoring study of a geothermal power plant showed that the chemistry of the resource fluid strongly influenced power plant performance. Changes in the fluid chemistry—such as higher salinity and lower pH—substantially increased the rate of scale formation and corrosion in plant components.

BACKGROUND

The Hawaii Geothermal Project-A (HGP-A) plant, funded by DOE and the state of Hawaii, is located on the Kilauea Volcano on the island of Hawaii. DOE initiated the project to demonstrate the technical feasibility of operating a baseload geothermal unit from a single well and to provide long-term operating data on the geothermal resource. Information on the changing chemical composition of well fluids, as well as on the effects of fluid chemistry on plant performance, was needed to provide guidance in designing, constructing, and operating future geothermal facilities having similar reservoir characteristics.

OBJECTIVES

To document changes in the chemistry of a geothermal plant's reservoir fluid over a two-and-a-half-year period and to evaluate the effects of fluid chemistry on plant scaling, corrosion, and performance.

APPROACH

From June 1981 through January 1984, researchers conducted 50 analyses of the chemical composition of the geothermal fluids entering the plant. They documented changes in the concentration of dissolved solids in the brine and related such changes to seawater intrusion and other reservoir events. During a plant overhaul in 1983, they performed chemical analyses of scale and corrosion deposits found on major plant components and correlated their findings with the chemistry of the fluid in the plant's steam- and brine-handling systems. Other experiments studied the rate of silica scale formation and the factors influencing it.

RESULTS

Scale deposition on plant components consisted primarily of metal sulfide minerals and silica. Metal sulfide deposits, largely pyrite, predominated in the steam system. Iron corrosion products from the pipe and hydrogen sulfide in the steam were causal in formation of the pyrite. Air entering the

pipeline during shutdowns transformed the iron sulfides to iron oxides and increased the rate of pipeline corrosion. Silica scale occurred principally in the brine system. A brine chemistry with low pH and high salinity significantly increased the rate of silica polymerization and flocculation.

Chemical analyses of the wellhead fluid showed that since the start of plant operation brine salinity had increased from approximately 3,200 ppm to 16,000 ppm total dissolved solids. Noncondensable gas content remained constant at about 0.11%. These findings suggested that the wellhead fluid came from two sources—a steam-producing aquifer near the bottom of the well and an overlying brine aquifer. Seawater entering the brine aquifer added to its salinity and lowered its pH, thereby increasing the potential for scale formation and corrosion in the future.

EPRI PERSPECTIVE

Before its 1983 overhaul, the HGP-A plant operated for 17 months with 93% availability, thereby demonstrating the feasibility of operating a baseload power plant on a single geothermal well. However, chemical changes in the resource during the two-and-a-half years of monitoring have already affected plant performance and are likely to cause problems in the future. In anticipation of this, the rigorous monitoring program begun in this study will continue. The close relationship between resource chemistry and plant scaling, corrosion, and performance presents a strong argument for implementing routine monitoring programs in geothermal plants to analyze and track chemical changes in the reservoir fluid.

PROJECT

RP1195-12
EPRI Project Manager: Mary E. McLearn
Advanced Power Systems Division
Contractor: Hawaii Electric Light Company, Inc.

For further information on EPRI research programs, call EPRI Technical Information Specialists (415) 855-2411.

Chemistry, Scale, and Performance of the Hawaii Geothermal Project-A Plant

AP-4342
Research Project 1195-12

Final Report, December 1985

Prepared by

HAWAII ELECTRIC LIGHT COMPANY, INC.
1200 Kilauea Avenue
Hilo, Hawaii 96720

Principal Investigators
E. C. Baughman
R. T. Uemura

A subsidiary of
HAWAIIAN ELECTRIC COMPANY, INC.
900 Richard Street
Honolulu, Hawaii 96813

Consultant
D. Thomas
HAWAII INSTITUTE OF GEOPHYSICS

Prepared for

Electric Power Research Institute
3412 Hillview Avenue
Palo Alto, California 94304

EPRI Project Manager
M. E. McLearn

Geothermal Power Systems Program
Advanced Power Systems Division

ORDERING INFORMATION

Requests for copies of this report should be directed to Research Reports Center (RRC), Box 50490, Palo Alto, CA 94303, (415) 965-4081. There is no charge for reports requested by EPRI member utilities and affiliates, U.S. utility associations, U.S. government agencies (federal, state, and local), media, and foreign organizations with which EPRI has an information exchange agreement. On request, RRC will send a catalog of EPRI reports.

NOTICE

Prepared by
Hawaii Electric Light Company, Inc.
Hilo, Hawaii

ABSTRACT

The objective of this study was to determine the effects of scale, corrosion, and erosion of the geothermal resource on HGP-A Geothermal Wellhead Power Plant. Analysis of the fluid chemistry was made to interpret the cause of corrosion and scale deposition in the brine and steam systems. It was found that metal sulfide scale formation occurred in the steam system and silica type scale formation in the brine system. The rate of scale deposition was strongly influenced by the chemical conditions in those systems. Although scale and corrosion did occur in the plant piping systems and equipment, they did not appreciably affect the performance of the plant. The results of this study will make the utilities more aware of the effects of geothermal fluid chemistry on scale deposition and corrosion which may increase plant efficiency and reduce maintenance of future plants.

CONTENTS

ILLUSTRATIONS

TABLES

SUMMARY

OBJECTIVE

The objective of this project was to document and evaluate the nature and extent of the impacts of fluids from the HGP-A geothermal well and the operation and maintenance of the first geothermal electric facility in the State of Hawaii. It is anticipated that this analysis will provide guidance in the design, construction and operation of future geothermal facilities both in Hawaii and in other geothermal systems having similar reservoir characteristics.

APPROACH

The study undertaken consisted of these primary tasks:

1. An analysis of the chemical composition of the geothermal fluids entering the HGP-A Wellhead Geothermal Power Plant and an interpretation of the evolution of the fluid chemistry in terms of its probable future impact on power plant operations.

2. A chemical and morphological analysis of the scale deposition and material erosion patterns in the facility.

3. An analysis of the impacts of the scale deposition and erosion on the operational conditions of the geothermal facility. The systems in the geothermal facility that were inspected and analyzed included the following:

    - Steam Flow Path
    - Brine Flow Path
    - Atmospheric Flash Tank
    - Main Steam Line
    - Control Valves
    - Main Condenser and Other Heat Apparatus
    - Steam Turbine Internals
    - Brine Piping and Valves

Upon completion of the inspection and analysis of the tasks, an effort was made to synthesize the findings of the individual tasks to enable projections to be made of future problems anticipated with the facility and with the geothermal reservoir. In addition, recommendations were made for changes in operating procedures in the HGP-A power plant or future geothermal power plants utilizing this reservoir.

FINDINGS

Task 1:

The analysis of the fluid chemistry has shown that the dissolved solids concentration in the brine has increased substantially during the operational history of the facility. The increased dissolved solids loading is attributed to seawater entry into the geothermal system tapped by HGP-A. The implications of seawater entry into the geothermal system include the following: reaction between seawater and reservoir may lower the pH of the geothermal fluids to very low levels (pH = 2 to 3) and thereby increase the corrosiveness of the brine phase; increased ionic strength of the brine phase may further compound the corrosiveness of the fluids; increased salinity will accelerate the deposition rate of silica scale in the brine handling equipment.

A more positive finding of this study is that a dry steam resource may be present in the geothermal reservoir encountered by the HGP-A well. The most important implication of this is that it may be possible to exclude the brine producing reservoir and thereby circumvent the majority of the scaling and corrosion problems encountered at the HGP-A geothermal facility.

Task 2:

Scale deposition in the geothermal facility was found to consist primarily of silicate and metal sulfide minerals (Table A). Although deposition of both was found to occur simultaneously in a few areas, each mineral type was found to generally predominate in different systems of the power plant facility. Amorphous silica was found to deposit primarily in the brine handling system, in the flash steam separator, brine disposal piping, and to a much heavier degree, in the atmospheric flash chamber and brine disposal ponds. Iron sulfide deposition was found in only limited quantities in the steam supply piping but much more extensively in the moisture separator and on the turbine casing walls.

Analysis of deposition rates and scale morphology suggests that scale deposition is strongly influenced by the chemical conditions present in the steam and brine systems: brine salinity and pH strongly influence silica deposition and access of atmospheric oxygen to the steam system plays a major role in metal sulfide deposition.

The specific mechanism associated with silica deposition can be described as follows: brine entering the flash steam separator is supersaturated with silica and, although polymerization of the silica occurs, surface charge effects strongly inhibit the growth of the polymers beyond the colloidal stage and their deposition onto a solid substrate. However, increases in brine salinity or pH reduce the surface charge effects and thereby accelerate the flocculation or deposition of the suspended polymerized silica. Hence, the increased brine salinity has allowed more rapid and more dense silica deposition to occur in the brine handling system during the operational history of the facility. In addition, pH changes associated with brine flashing in the pipelines and in the atmospheric flash tank have resulted in much higher rates of localized silica deposition than are found in the brine system as a whole.

Iron sulfide (predominantly pyrite) deposition in the steam supply system was mediated by the availability of chloride ion, from brine aerosol carryover, and atmospheric oxygen that was admitted to parts of the system during turbine upset conditions.

Erosion and corrosion of the internal surfaces of the steam and brine systems were found to be relatively limited. The areas of most significant corrosion were found to be those portions of the steam system that were composed of mild steel and were alternately exposed to high temperature steam and to atmospheric oxygen during operations and turbine upset conditions respectively. Only limited erosion or pitting of the turbine rotating surfaces was found; although some metal loss may have been the result of electrochemical attack, the majority appeared to be the result of aerosol impingement.

The impacts of the scale deposition and corrosion/erosion on the facility operating characteristics have been relatively minor. The most significant operating problem has been silica deposition in the brine disposal lines and control valves. This necessitated the installation of redundant pipelines and more frequent maintenance than would otherwise have been required. Scaling and

corrosion in the steam handling system have not caused any significant deterioration in the performance or output of the turbine. The general absence of major problems is reflected in the 93% availability factor for this facility during its first eighteen months of operation.

CONCLUSIONS AND RECOMMENDATIONS

The most important findings of this study are the following:

1. The chemical data for the well discharge suggest the presence of a high temperature dry steam geothermal resource in the reservoir tapped by the HGP-A well.

2. Increasing salinity of the brine phase produced by a lower temperature aquifer indicates that seawater is intruding into the shallow resource area.

3. The chemistry of the brine phase strongly influences the deposition of silica scale.

4. Access of oxygen to the steam system substantially increases the rate of corrosion and iron sulfide scale formation.

Even though current operations of the facility have not been substantially impacted by scale deposition or corrosion, the following recommendations are made to further reduce turbine down time and further optimize resource utilization.

1. The most cost effective means of eliminating the deposition of silica scale in a generation facility on this reservoir will be to exclude the brine phase from the wells by following a well casing program that will admit fluids only from the dry steam reservoir.

2. If brine production does occur, silica scale deposition can be minimized by maintaining close control over where and when boiling and associated pH changes occur.

3. Exclusion of atmospheric oxygen from the steam handling system will reduce the rate of iron sulfide deposition and rate of oxygen mediated corrosion in the mild steel portions of the steam system.

4. Knowledge of the chemistry of the fluids produced by the resource is critical for both the design of a power generation facility and for its continued maintenance and operation.

TABLE A

SUMMARY OF SCALE DEPOSITION

Subsystem	Scale		Morphology	Impact
	Type	Extent & Thickness		
Separator	Silica	Moderate 0.1-3cm	Granular cemented	Minor impact associated with separation efficiency; moderate impact resulting from constriction of brine discharge line.
Brine Piping	Silica	Moderate 0.1-2cm	Chalky to vitreous	Very minor impacts associated with decreased pipe diameter.
Brine Level Control Valves	Silica	Moderate 0.5-3cm	Granular to vitreous	Substantial impact upon operation of valves. Require more frequent service and overhaul.
Brine Flash Tank	Silica	Heavy 5-50cm	Granular to massive vitreous	Moderate impact associated with flash tank clean out and brine disposal.
Steam Piping	Metal sulfide	Light to moderate 0.05-25mm	Fine, granular	No impact.
Moisture Separator	Metal sulfide & oxide	Moderate to heavy 0.5-15mm	Fine grained foliar	Significant impact arising from exfoliation of the scale and accumulation around and plugging of bottom drain.
Control Valves	Metal sulfide	Light 0.5-1mm	Fine grained	No detectable impact.
Inlet Nozzles	Mixed sulfide silica	Moderate to heavy 0.1-2.0mm	Fine grained cemented	Partial plugging of inlet nozzles but no significant impact on performance
Turbine Internals	Metal sulfide	Light to moderate 0-0.8mm	Fine grained to granular	Generally very light coating - no significant impact on turbine efficiency.
Turbine Casing	Metal sulfide	Moderate to heavy 1-10mm	Foliar and friable	Substantial layer of pyrite throughout turbine casing - primary impact was wedging of diaphragms in place.
Condenser	Metal sulfide	Light 0-0.1mm	Fine grained	No impact.

Section 1

INTRODUCTION

The first scheduled overhaul of the HGP-A Wellhead Geothermal Power Plant occurred in August 1983 after approximately 17 months of base load operation. Because this was the first generator facility to have been installed on the geothermal resource discovered by the HGP-A research well, this overhaul provided a unique opportunity to document both the reservoir characteristics of the resource and their impacts on the operation and maintenance of a base load generator facility. Thus, the current study was undertaken is an effort to provide documentation and a preliminary analysis of:

1. the chemical and physical characteristics of the geothermal resource observed during the first 17 months of continuous reservoir production.

2. the operational parameters of the geothermal generator facility during this period.

3. the operations and maintenance impacts of the geothermal fluids on the major components of the generator facility.

The ultimate objective of this study, however, is to provide a data base upon which the design of future geothermal facilities can build.

BACKGROUND

The HGP-A Wellhead Geothermal Power Plant (Figure 1-1) was funded primarily by the United States Department of Energy (DOE) with additional contributions by the State and County of Hawaii. This plant is one of the first geothermal wellhead generator units to be installed in this country. As such, the plant was to demonstrate the technical feasibility of operating a base load geothermal unit from one well and to provide long term operating data on the geothermal resource. The facility is owned by the DOE and managed by the HGP-A Development Group, a joint venture of the State Department of Planning and Economic

Development (DPED), the County of Hawaii's Department of Research and Development, and the University of Hawaii's Hawaii Natural Energy Institute (HNEI). The Hawaii Electric Light Company, Inc. (HELCO) is under contract with the State to operate and maintain the plant as well as to purchase the electricity generated. The revenues gained by the State from the sale of electricity to the utility are used to offset the cost of operation and maintenance of the plant.

HGP-A Wellhead Geothermal Power Plant was synchronized into HELCO's electrical system grid in July 1981. After resolution of numerous start-up problems, the plant was placed in commercial operation in March 1982. Since commercial operation, the plant has had an availability factor of 93%.

The first overhaul of the HGP-A Wellhead Geothermal Power Plant was performed after its first seventeen months of operation. Due to financial and scheduling constraints the overhaul was performed in two phases. The first phase was performed in August 1983; work was done on all of the systems on the steam side of the flash separator which included the condensate, cooling water, and the hydrogen sulfide abatement systems. The second phase was performed in March 1984 when work on the brine side of the flash separator was done.

Figure 1-1. HGP-A Wellhead Geothermal Power Plant

Source: Hawaiian Electric Co., Inc.

Section 2

HGP-A WELL CHEMISTRY

The HGP-A well is located on the lower East Rift Zone of Kilauea Volcano (Figure 2-1). Kilauea is a very active shield type volcano made up of thousands of thin tholeitic basalt flows. The rift zone, with which the geothermal reservoir is associated, is a structural feature of the volcano and is made up of linear, vertical or near vertical dikes and fractures. This feature extends from the summit of the volcano through the submarine extension of the rift zone and, to a large extent, controls the recharge hydrology of the geothermal reservoir.

The HGP-A well was completed in 1976 to a depth of 1966 m (6450 ft.) and has a measured bottom hole temperature, under static conditions, of 358°C (676°F). The current casing configuration for the well is solid 17.78 cm (7 in) casing to a depth of approximately 915 m (3000 ft.) and 17.78 cm (7 in) slotted liner from that depth to bottom hole. Production is believed to come primarily from aquifers located at 1372 m (4500 ft.), 1768 m (5800 ft.), and bottom hole. The well is capable of producing approximately 49,900 kg/hr (110,000 lbs./hr.) of a mixed phase fluid (57% liquid, 43% steam) at a wellhead pressure of 1222 kPaa (175 psia).

During the period from 1976, when the well was completed, until 1981, only a very limited amount of production from the well occurred. A number of short duration tests, ranging from a few hours to a maximum of just over 40 days, were performed but the aggregate total production time did not exceed 150 days. In June 1981, upon completion of the HGP-A Wellhead Power Plant Facility, the well was put into a much longer term of production. Equipment failure necessitated the suspension of production from September 1981 until December of that year when production resumed. On June 1, 1984 the total duration of production, since June 1981, amounted to 986 days.

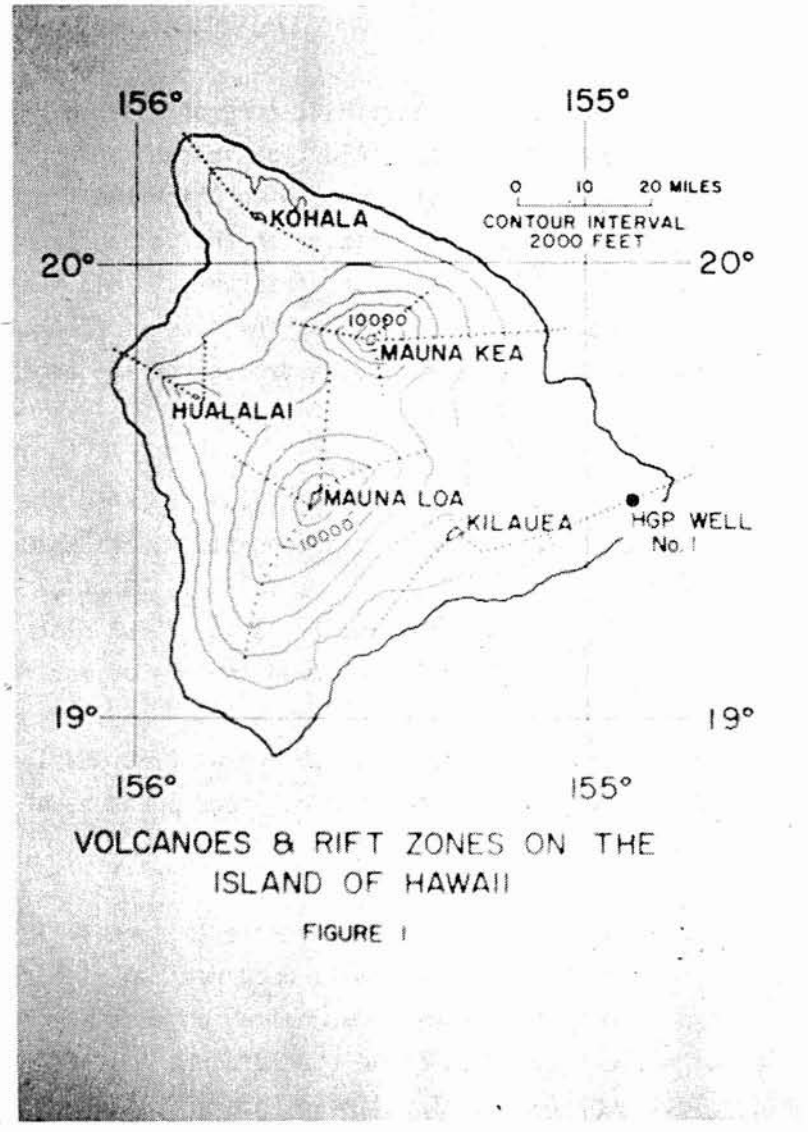

Figure 2-1. Map of Island of Hawaii

Source: Hawaiian Electric Co., Inc.

FLUID CHEMISTRY

The fluids from the HGP-A well have been sampled and analyzed for a variety of constituents since initial production began (Table 2-1). Analysis of the brines during the early flow testing of the well indicated that the total dissolved solids concentration was much lower than expected, in the range of 3000 to 4000 mg/kg in the brine, and was dominated by sodium and chloride ions (Kroopnick et al, 1977). Silica concentrations in the brine were quite high (ranging to 750 mg/kg) but well below the expected concentrations for reservoir temperatures of 358°C (676°F). Prior to testing, the production fluids were anticipated to have a TDS concentration approximately equal to that of seawater largely because the production zones in the well ranged from 1100 m (3600 ft.) to more than 1700 m (5577 ft.) below any Ghyben-Herzberg fresh water lens in this area. The low TDS fluids encountered indicated that the simple Ghyben-Herzberg lens model is not valid for the Kilauea East Rift and that substantial amounts of fresh water are entering the geothermal reservoir. Since the beginning of production testing, the concentrations of dissolved solids have shown an increasing trend but, up to the present time, the TDS level remains well below that of sea water.

Figure 2-2 presents a plot of chloride ion concentration versus time in the brine phase from HGP-A during the production periods June 11, 1981 to September 4, 1981 and December 12, 1981 to the most current data available. Several aspects of the data deserve comment. The chloride concentrations during both production periods exhibit a rapid increase with time during the first 1000 hours of production but, over this period, the rate of increase declines. The initial rapid increase of the chloride concentration in the brine is believed to be due, in part, to the change in steam quality as the steam generation front moves into the reservoir. As this front moves into the formation more heat can be "mined" from the rock as the residual brine moves inward toward the wellbore. As more steam is flashed from the residual brine phase, the remaining brine becomes more concentrated in the non-volatile salts. This type of phenomenon should abate as the flash front stabilizes in the reservoir yielding a relatively constant steam quality and residual brine chemistry. The gradual increase in the chloride concentration in the later production period is interpreted to be due to infiltration of seawater into the reservoir as a result of withdrawal of fluids from the well. It is also noteworthy that the chloride concentrations in the fluids decline during periods when production from the

TABLE 2-1

HGP-A WELL-BRINE CHEMISTRY

(January 12, 1984)

PARAMETERS

Temperature: 190°C TDS: 15,800 mg/L.

Pressure: 170 psi pH: 6.6

Conductivity: 23,000 umhos/cm

CHEMICAL SPECIES (mg/L)

Ag:	< 0.010	Cr:	< 0.001	Mg:	0.26	Sb:	0.6
Al:	0.1	Cu:	< 0.002	Mn:	0.21	Si:	386
As:	0.09	Fe:	< 0.010	Mo:	< 0.001	Sn:	< 0.020
Ba:	4.6	Hg:	< 0.050	Na:	4927	Sr:	6.5
Ca:	358	K:	756	Ni:	< 0.010	Ti:	< 0.003
Co:	< 0.001	Li:	1.1	Pb:	< 0.010	V:	0.002
						Zn:	0.016

B:	4.3	$CO_3^=$:	< 0.1 (as CO_2)	NH_3/NH_4^+:	< 0.01 (as N)
Br^-:	44(±4)	HCO_3^-:	18.5 (as CO_2)	$S^=$:	15(±4)
Cl^-:	8968	F^- :	0.25(± 0.10)	SO_4 :	24(±4)

Total Carbonate: 18.5 (as CO_2)

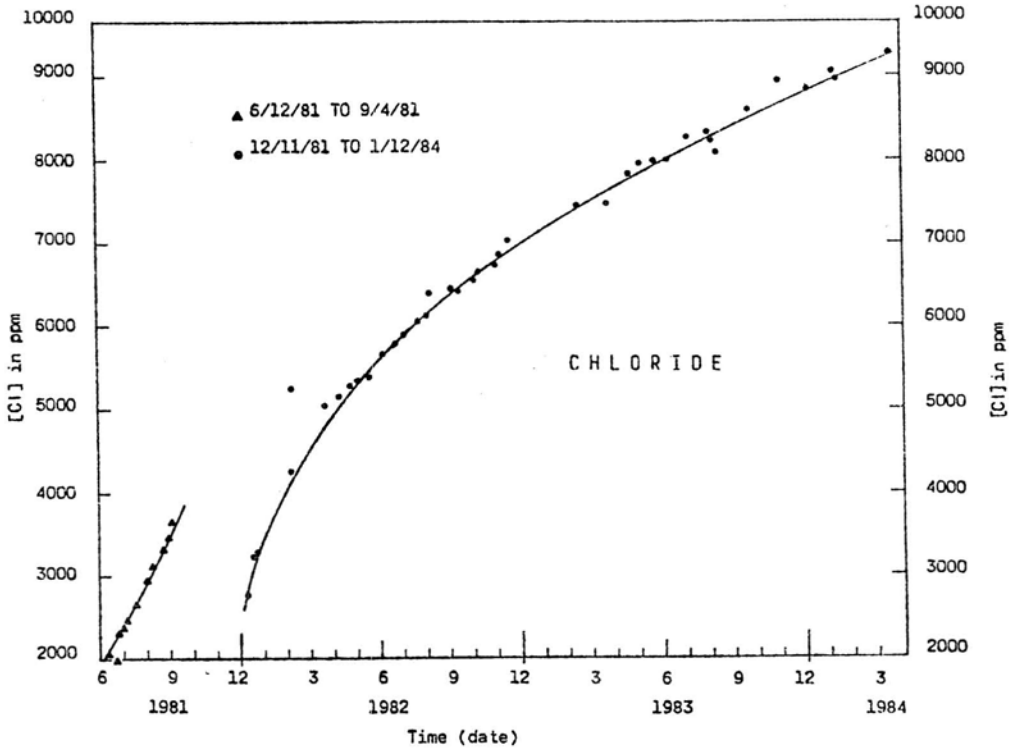

Figure 2-2. Chloride Ion Concentration Versus Time

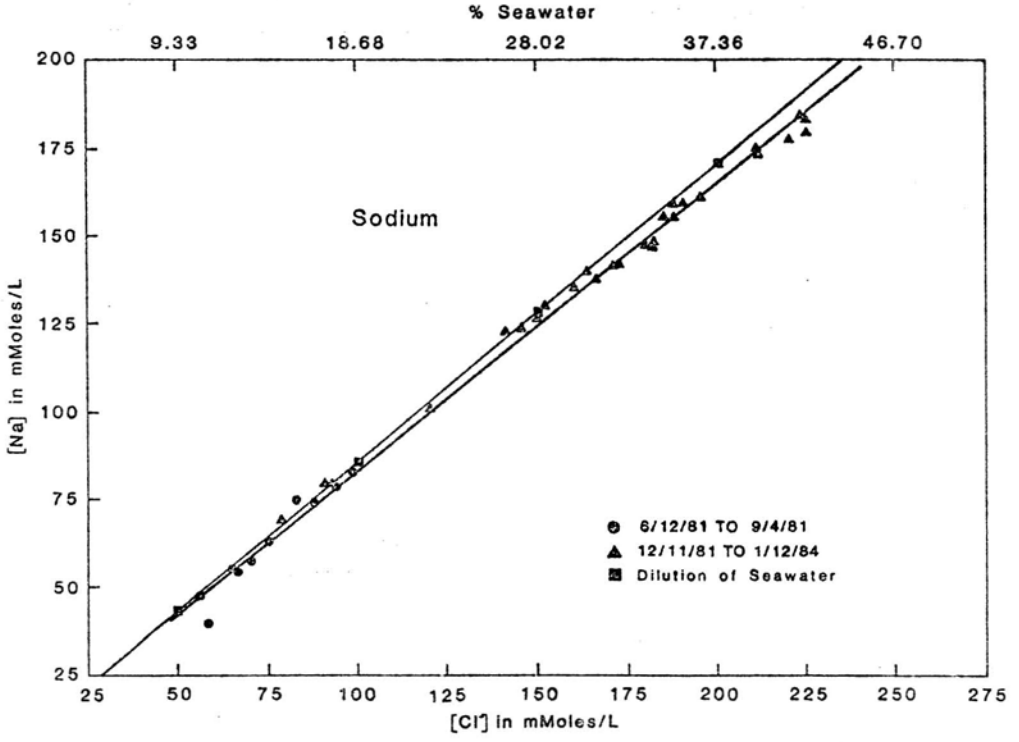

Figure 2-3. Sodium Versus Chloride

well is suspended (e.g. between the early short duration flow tests and when flow was suspended between September and December 1981). This decline is thought to be the result of natural recharge to the reservoir by low salinity geothermal fluids of meteoric origin.

The sodium ion concentration has increased along a trend almost identical to that of the chloride ion (Table 2-2). Figure 2-3 presents a plot of sodium versus chloride for the HGP-A fluids and for varying dilutions of seawater. It is apparent that the sodium to chloride ratios are virtually identical to those observed for seawater. Experimental seawater basalt reactions performed at high temperatures (Mottle and Holland, 1978; Mottle et. al., 1979) have shown that sodium should act as a conservative element, (i.e., should be neither enriched nor depleted significantly). On this basis it can be concluded that the chloride and sodium ion increases in the geothermal fluids are almost exclusively from seawater intrusion into the thermal reservoir.

In contrast to sodium, both lithium and potassium ion concentrations in the geothermal fluids (Table 2-2, Figures 2-4 and 2-5) show marked variation from simple seawater dilution lines. Both ions are present in substantial excesses above seawater concentrations: the lithium to chloride ratio exceeds that of seawater by a factor of 20, whereas, potassium to chloride ratios are greater by a factor of more than 5. These enrichments are consistent with those found for seawater basalt experiments performed at low water to rock ratios at temperatures in the range of 300°C (572°F) to 500°C (932°F).

Calcium and magnesium ion concentrations (Figures 2-6 and 2-7) have also been found to exhibit deviations from seawater dilution. The causes for the deviations, however, are less straightforward. Although calcium was heavily depleted relative to the seawater Ca to Cl ratio during the early production, it has more recently shown a substantial enrichment above the seawater ratio. Similar behavior has been observed in experimental studies (Mottle and Holland, 1978) wherein seawater calcium is depleted by the deposition of anhydrite as seawater is heated but, as reaction between water and rock proceeds, calcium is released by alteration of calcium bearing mineral phases (e.g. plagioclase) and eventually becomes enriched above its initial concentration. Although this may explain the observed behavior, other alternative explanations are also possible. Primary among these is that calcium ion is being released by remobilization of anhydrite (present as vein mineralization) from the reservoir rocks as the temperature

TABLE 2-2
(Sheet 1 of 2)

CHEMICAL ANALYSES OF HGP-A BRINES

Date	Concentrations in ppm					
	Li	Na	K	Ca	Mg	Cl^-
06/12/81	0.36	900	200	25.5	0.008	2065
06/18/81	0.34	1100	200	25	0.006	1986
06/20/81	0.38	1280	220	30	0.008	2319
06/29/81	0.39	1250	265	36	0.009	2360
07/04/81	0.41	1320	255	39.5	0.012	2468
07/16/81	0.45	1460	255	46.5	0.013	2655
08/03/81	0.49	1710	265	55	0.027	2935
08/12/81	0.52	1700	270	58	0.023	3107
08/22/81	0.56	1810	280	60.5	0.026	3307
08/29/81	0.59	1900	305	63	0.029	3469
09/04/81	0.61	1890	295	66.5	0.029	3622
12/11/81	0.51	1590	300	33	0.012	2763
12/17/81	0.56	1850	310	48.5	0.016	3207
12/22/81	0.58	1820	295	56	0.015	3290
02/05/82	0.73	2320	405	90.5	0.056	4265
02/08/82	0.84	2410	410	95.5	0.060	5243
03/22/82	0.84	2820	470	-	0.069	5017
04/12/82	0.85	2840	495	112	0.058	5151
04/26/82	0.86	2920	490	115	0.057	5294
05/03/82	0.88	2970	495	120	0.055	5323
05/17/82	0.88	2990	500	120	0.052	5378
06/07/82	0.94	3120	525	122.5	0.051	5667
06/23/82	0.95	3210	520	128.5	0.054	5796
07/05/82	0.98	3150	525	134	0.056	5898
07/19/82	0.98	3240	535	140	0.058	6051
08/02/82	0.98	3260	565	149	0.058	6117
08/06/82	1.00	3400	560	153	0.063	6390
09/07/82	1.02	3420	565	158	0.072	6441
09/14/82	1.02	3420	605	165	0.073	6402
10/04/82	1.02	3590	620	175.5	0.081	6549
10/11/82	1.02	3590	615	181	0.082	6654
10/12/82	1.03	3650	610	181.5	0.084	6657
11/01/82	1.04	3650	585	205	0.088	6729
11/08/82	1.06	3720	620	205	0.095	6879
11/16/82	1.07	3940	650	217	0.104	7029
02/15/83	1.08	4020	665	242	0.118	7473
03/23/83	1.08	3980	630	247	0.124	7482
04/18/83	1.12	4090	670	255	0.139	7842
05/04/83	1.14	4220	675	270	0.152	7965
05/24/83	1.12	4120	685	268	0.158	7990
06/09/83	1.13	4480	660	269	0.140	8000
07/05/83	1.11	4270	685	275	0.160	8275
07/28/83	-	4611	622	309	0.136	-
07/31/83	1.11	4660	695	-	0.164	8320
08/05/83	1.08	4600	675	280	0.160	8220
08/12/83	-	5034	639	306	0.148	8092
09/20/83	-	5982	718	321	0.179	8599
10/31/83	1.22	4450	791	320	0.180	8929
12/05/83	1.25	4650	763	319	0.210	8827
01/06/84	1.26	4750	808	377	0.220	9061
01/12/84	1.10	4927	756	358	0.260	8968

TABLE 2-2
(Sheet 2 of 2)

CHEMICAL ANALYSES OF HGP-A BRINES

Date	Concentrations in moles					
	Mg (10^{-6})	Ca (10^{-3})	Cl (10^{-3})	Na (10^{-3})	K (10^{-3})	Li (10^{-6})
06/12/81	0.329	0.636	58.24	39.15	5.12	51.9
06/18/81	0.268	0.623	56.02	47.85	5.12	49.0
06/20/81	0.321	0.748	65.41	55.68	5.63	54.8
06/29/81	0.370	0.898	66.57	54.37	6.78	56.2
07/04/81	0.494	0.985	69.61	57.42	6.52	59.1
07/16/81	0.535	1.160	74.89	63.51	6.52	64.9
08/03/81	0.111	1.372	82.79	74.38	6.78	70.6
08/12/81	0.946	1.446	87.64	73.95	6.91	74.9
08/22/81	1.07	1.509	93.33	78.73	7.16	80.7
08/29/81	1.19	1.571	97.85	82.64	7.80	73.5
09/04/81	1.19	1.658	102.16	82.21	7.54	87.9
12/11/81	0.494	0.823	77.93	69.16	7.67	73.5
12/17/81	0.658	1.209	90.46	80.47	7.93	80.7
12/22/81	0.617	1.400	92.80	79.16	10.10	83.6
02/05/82	2.30	2.257	120.30	100.91	10.36	105.2
02/08/82	2.47	2.382	147.89	104.83	10.49	105.2
03/22/82	2.84	0.0249	141.51	122.66	12.02	121.1
04/12/82	2.39	2.793	145.29	123.53	12.66	122.5
04/26/82	2.34	2.868	149.32	127.01	12.53	123.9
05/03/82	2.26	2.993	150.14	129.19	12.66	126.8
05/17/82	2.14	2.993	151.69	130.06	12.79	126.8
06/07/82	2.10	3.055	159.85	135.71	13.43	135.5
06/23/82	2.22	3.217	163.48	139.63	13.30	136.9
07/05/82	2.30	3.292	166.36	137.02	13.43	141.2
07/19/82	2.39	3.491	170.68	140.93	13.68	141.2
08/02/82	2.39	3.716	172.54	141.80	14.45	141.2
08/06/82	2.59	3.815	180.24	147.89	14.32	144.1
09/07/82	2.96	3.940	181.68	148.76	14.45	147.0
09/14/82	3.00	4.115	180.58	148.76	15.47	147.0
10/04/82	3.33	4.389	184.72	156.15	15.86	147.0
10/11/82	3.37	4.514	187.69	156.15	15.86	147.0
10/12/82	3.46	4.539	187.77	158.76	15.60	148.4
11/01/82	3.62	5.112	187.80	158.76	14.96	149.9
11/08/82	3.70	5.112	194.03	161.81	15.86	152.8
11/16/82	4.28	5.411	198.26	171.38	16.62	154.2
02/15/83	4.52	6.035	210.79	174.86	17.01	155.6
03/23/83	5.10	6.160	211.04	173.12	16.11	155.6
04/18/83	5.72	6.360	221.19	177.90	17.14	161.4
05/04/83	6.25	6.733	224.66	183.56	17.26	164.3
05/24/83	6.50	6.683	225.37	177.90	17.52	161.4
06/09/83	5.76	6.708	225.65	194.87	16.88	162.8
07/05/83	6.58	6.858	233.41	185.73	17.52	160.0
07/28/83	-	-	-	-	-	-
07/31/83	6.75	0.025	234.68	200.09	17.77	160.0
08/05/83	6.58	6.983	231.86	200.09	17.26	155.6

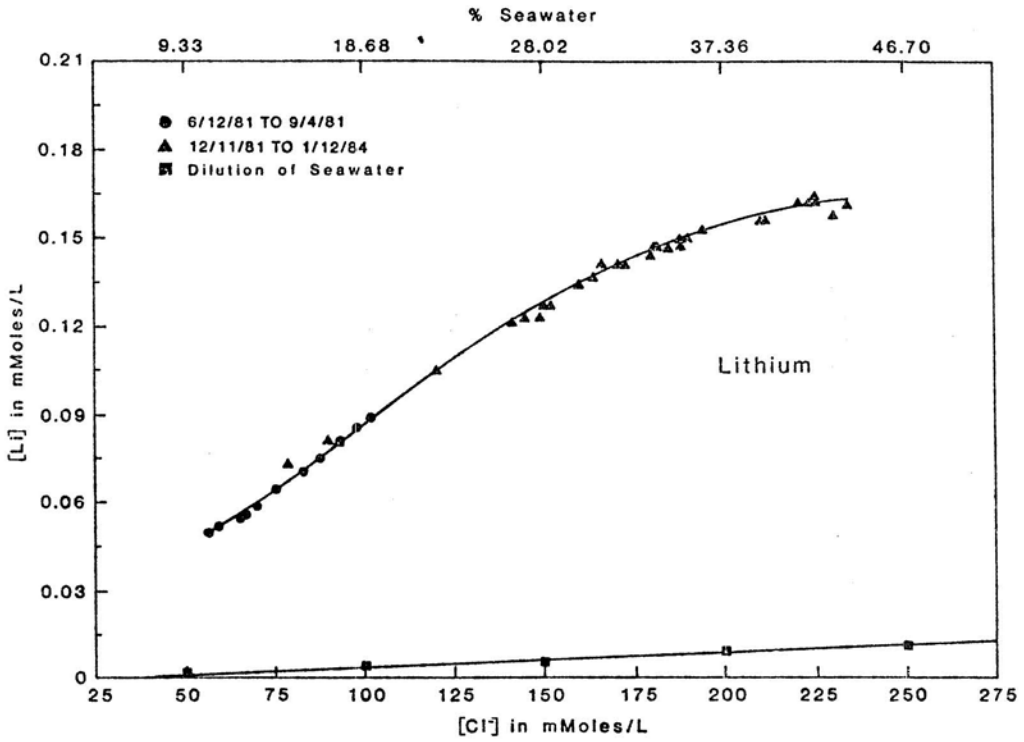

Figure 2-4. Lithium Versus Chloride

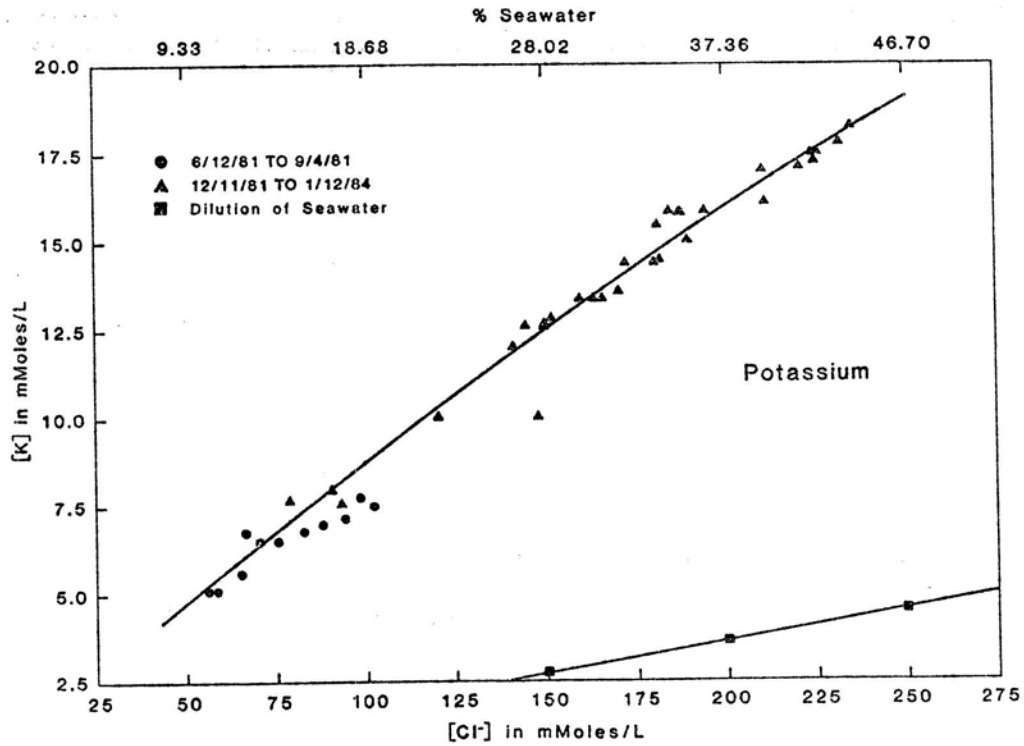

Figure 2-5. Potassium Versus Chloride

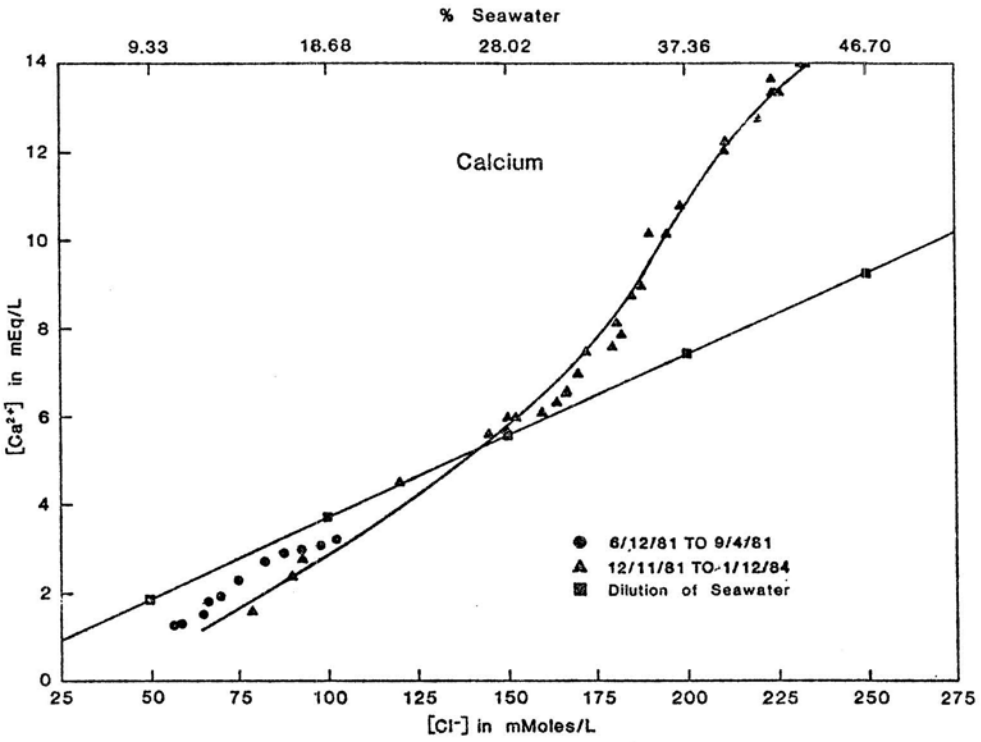

Figure 2-6. Calcium Versus Chloride

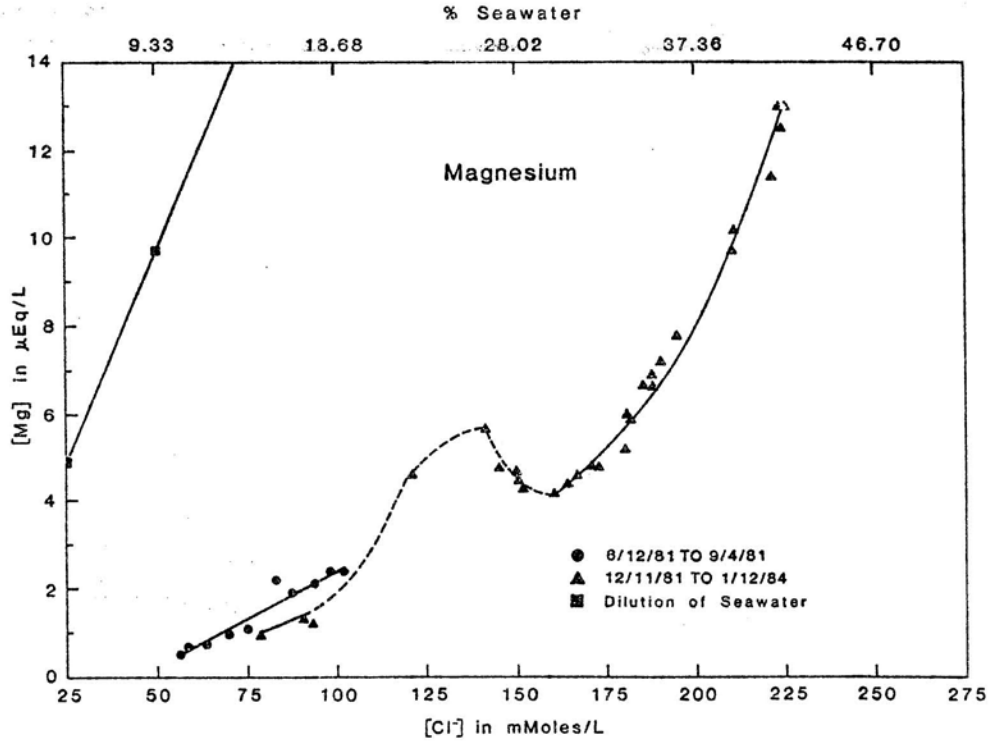

Figure 2-7. Magnesium Versus Chloride

in the formation declines due to steam formation and removal. Further monitoring of the chemistry of the well fluids will be required to resolve this question.

Magnesium ion concentrations have also been heavily depleted relative to seawater concentrations throughout the production history of HGP-A. Loss of magnesium is attributed to the formation of magnesium bearing alteration minerals such as chlorite in the reservoir. The marked deviation from a smooth curve at the intermediate chloride concentrations is believed to be the result of a small temporary influx of cooler unaltered seawater into the wellbore. The decline of this source may be the result of self sealing of the entry fractures by the precipitation of anhydrite.

Silica concentrations observed in the geothermal fluids have generally been lower than anticipated for the measured reservoir temperatures - ranging up to only about 850 mg/kg. The only occasions where these levels have been exceeded were during initial flow of the well when the silica concentrations were measured at approximately 1200 mg/kg. The calculated silica geothermometer temperature for the lower silica concentrations is approximately 267°C (513°F) and only 297°C (566°F) for the higher values. The lower than expected silica concentrations may be the result of rapid silica precipitation in the reservoir during production. However, it is now considered more likely that the low silica concentrations accurately reflect the temperature of an intermediate temperature aquifer supplying a mixed steam and water phase to the well bore.

Discussion

The brine chemistry observed at HGP-A during the first 24 months of operation has several implications with regard to reservoir engineering, power plant design, and maintenance.

The most important aspect of the brine chemistry relevant to an understanding of the reservoir is that the total dissolved solids indicate that the naturally occurring (pre-production) reservoir is recharged primarily from meteoric rainfall. The near absence of seawater in the reservoir at depths of nearly 1800 m below sea level, as noted above, was entirely unexpected and requires that a model different from the Ghyben-Herzberg theory be applied to this reservoir. The model proposed is as follows:

The structure of the Kilauea East Rift Zone is made up of a series of vertical or near vertical dikes extending from near the surface to depths of several kilometers. The major trend of the dike system is along an east-west strike. Within the dike system are numerous vertical or near vertical fractures that developed as a result of the emplacement of intrusive bodies in the rift system. The trend of the fracture system is also east-west. The East Rift Zone, because of the dike and fracture system orientation, will have a profound impact on the hydrologic circulation system in this area. The dike system will impede water flow in the north-south direction and will tend to impound or channel recharge along the east-west trend, whereas the vertical fracture system will have the effect of enhancing water flow both vertically and in the east-west direction. Thus the major water flow pattern within the Rift Zone will be in both the vertical and east-west horizontal direction with virtually no fluid flow across the strike of the rift. Therefore, seawater entry into the rift will be strongly impeded and vertical meteoric recharge will be enhanced. The thermal structure of the rift will have further impacts on water recirculation patterns. The heat source deep in the rift zone will heat intruding fresh and saline water and the density of both will be less than that of cold fresh water. Thus, a continuous circulation of deep reservoir fluids to the surface will tend to enhance recharge from the major flow direction along the vertical fractures.

Finally, a chemical effect associated with high temperature seawater basalt interactions will serve to further exclude seawater from the system. Calcium and sulfate ions are both present in seawater at concentrations well below the saturation point for anhydrite. However, the solubility of anhydrite decreases with increasing temperature and as seawater is heated, the anhydrite saturation point is exceeded and this mineral begins to precipitate out.

Therefore, seawater entering the geothermal reservoir through cross-cutting fractures in the Rift Zone will precipitate anhydrite as it reaches high temperatures. This precipitation may have the effect of gradually choking off seawater entry points as they form. Thus, the hydrologic circulation model of the geothermal reservoir associated with the Kilauea East Rift is a system in which the vertical and east-west, horizontal movement of meteoric recharge, driven by thermal convection, predominates and where north-south migration of deep geothermal fluids and of intruding seawater is strongly impeded both by the impermeable dike system and by vein-filling anhydrite precipitation resulting from the heating of the infiltrating seawater.

The fact that seawater is currently entering the well suggests that the production zone may be a relatively young feature or that it may have originally been an outflow aquifer prior to fluid production from the well. The decline in salinity of the initial production fluids observed after a period of suspended production suggests that the latter possibility is a reasonable interpretation.

The entry of seawater into the reservoir encountered by HGP-A has a number of potential implications relevant to future productivity from the well and to power plant maintenance. If the above proposed model for anhydrite deposition is valid, there is a possibility that the sea water zone may choke itself off after a period of time. As noted above, the rate of TDS increase has declined throughout the production history; however, we have not yet observed any indication that the TDS concentrations have stabilized or declined. A continued increase of seawater entry into the wellbore could lead to substantial problems with power plant maintenance (to be discussed below) and possibly to increased corrosion or scaling in the well casing. There is, at present, no way to determine whether seawater salinities will, in the long term, be achieved. A simple projection of recent chloride increases with time suggests, however, that brine salinities will not equal those of seawater for at least another five years.

The observed silica concentrations are similarly cause for concern. As indicated above, calculated silica geothermometer temperature indicates that an intermediate temperature aquifer is supplying a mixed steam-water phase to the well bore causing the silica concentrations in the brine phase to be substantially lower than anticipated for the bottom hole temperatures observed at HGP-A. One interpretation of these data is that silica is depositing in the reservoir as the single phase reservoir fluid flashes to a two phase brine-steam mixture. If this interpretation is correct it is likely that silica plugging of the production aquifers may occur and thus eventually choke off one or more production zones in the well bore. No substantial decay of the well bore production has yet been observed but continued monitoring is underway to detect this phenomenon if it is occurring.

The changing brine chemistry could also have substantial impacts on power plant operations and maintenance. The sources of greatest concern are the potential for accelerated corrosion and increased silica scale deposition in the brine handling system. The possibility of accelerated corrosion in the brine system is of concern from both the increased salt concentration and an anticipated decline in brine pH. The latter phenomenon could result from seawater-basalt reactions in which the buffering capacity of the basalt is exceeded. Laboratory studies on high temperature seawater-basalt reactions (Mottle and Holland, 1978) have observed pH decreases from 7.5 down to 2 under some conditions. A slight pH decline has been observed during the HGP-A operational history, from pH 7.4 to pH 6.8, and continued decreases are clearly possible. Whether the decline will continue, or at what rate, will be governed by the rate of increase of seawater entry into the reservoir around HGP-A.

The increasing rate of silica scaling is also tied to the increasing salinity of the production fluids. Even though silica concentrations have been nearly constant during the production life of the well, silica is present in the geothermal brine as a meta-stable colloidal polymer. Drastic changes in pH or in ionic strength (i.e. salinity) can destabilize the colloid resulting in much more rapid deposition of silica. Although no such drastic changes are anticipated in the near future, the character of the silica being deposited on the pipe walls has already begun to change from its original depositional pattern. Continued monitoring of scale formation is currently underway to determine whether substantial problems are beginning to develop.

Summary and Conclusions

The data that have been acquired on the brine chemistry at HGP-A indicate that the reservoir hydrology is strongly influenced by the Kilauea East Rift Zone fracture and dike complex. The reservoir fluid chemistry within the rift may have dissolved solids concentrations well below those of seawater although some seawater entry is clearly possible. It is apparent that the seawater entering HGP-A has been heavily altered by high temperature reactions with the basaltic reservoir rock. Laboratory studies conducted on seawater-basalt reactions (Mottle and Holland, 1978) suggest that, although seawater entry may choke itself off due to anhydrite deposition, other alterations in the seawater chemistry may bring about drastic declines in fluid pH. The result may be an increase in corrosiveness of the fluids and possibly an increase in silica scale deposition. However, the currently available data for the HGP-A brine chemistry indicate that the rate of change of the brine is slow. This observation suggests that major problems with the brine are not likely to occur in the immediate future.

NON-CONDENSABLE GAS CHEMISTRY

The concentration and composition of the non-condensable gas (N.C.G.) present in the steam phase produced by HGP-A have been monitored since the initial production testing on the well. Although a number of difficulties in monitoring were encountered during the earlier phases in the sampling and analytical procedures for the N.C.G., which resulted in poor analytical results, more recent data have yielded several valuable insights of importance both to plant design and operation and to reservoir engineering.

The total N.C.G. concentration in the HGP-A steam has been found to be relatively low: approximately 0.25% by weight in the steam phase or 0.11% by weight in the total discharge. The major constituents present are carbon dioxide (0.12% by weight), hydrogen sulfide (0.09% by weight), nitrogen (0.0125% by weight) and hydrogen (0.0011% by weight). A number of other trace gases have also been found including methane, helium, argon, and radon. It is of note, however, that neither ammonia nor boron has been detected to the limits of our analytical capabilities in the steam produced by HGP-A.

It is also significant that both the absolute concentration of the N.C.G. and the relative proportions of the individual gases have remained relatively

constant through the recent production history of the well (Table 2-3). Although substantial variability of both the absolute concentration and the relative concentrations of the N.C.G. were noted during the early start-up of the well, the sampling and analytical difficulties encountered during this period render the data obtained too inaccurate to interpret with any reliability and hence the data are not included in the present data set.

Discussion

Power Plant Engineering. The most notable aspect of the N.C.G. present at HGP-A with regard to power plant engineering has been the absence of ammonia and boron in the steam phase. Their absence has resulted in much more efficient control of hydrogen sulfide (H_2S) in the turbine exhaust steam. Partitioning of H_2S in the condenser ejector system has been found to strongly favor the gas phase with less than 0.7% of the H_2S remaining in the steam condensate. The very low H_2S carryover into the liquid phase results in only minor sulfide control efforts being required for use of condensate as make-up water to the cooling tower. An additional advantage of the low boron content in the HGP-A steam has been that the environmental impacts of cooling tower drift encountered in the Geysers field have not been observed at HGP-A.

The scaling and corrosion aspects of the N.C.G. present in the HGP-A steam will be discussed at length in Section 3 of the present report and will not be repeated here. However, it is of note that the observed sulfide scaling present at HGP-A has resulted in fewer difficulties than those encountered with borate fouling at either the Geysers or the Lardarello fields.

Reservoir Engineering. The origins of the individual components of the non-condensable gas fraction of the steam phase have not yet been fully determined, although several possible sources are considered to be candidates. Potential sources for carbon dioxide include magmatic gases, marine carbonates deposited between lava flow units, dissolved marine carbonate entering with seawater, or atmospheric/biogenic CO_2 either deposited by circulating meteoric recharge and subsequently remobilized or dissolved CO_2 being cycled through with recharge. Although no firm conclusion can be drawn with regard to the primary source of CO_2, some constraints can be imposed using the small amount of isotopic data that is available. Carbon-13 data on some of the early production gases analyzed indicated an isotope ratio intermediate between seawater and magmatic carbon although atmospheric CO_2 was also a possible contributor.

TABLE 2-3

GAS CHEMISTRY

Date	CO_2	H_2S	N_2	H_2
07/05/82	1337	936	120.3	10.75
07/12/82	1369	979	161.9	14.0
07/19/82	1360	952	137.2	11.9
07/26/82	1313	944	120.9	10.67
08/02/82	1303	949	115.1	10.4
08/09/82	1271	958	123.3	11.0
08/16/82	1199	967	119.9	11.08
08/23/82	1105	970	115.4	10.6
08/31/82	1483	935	130.5	10.5
09/07/82	1470	893.8	125.3	10.34
09/14/82	1496	923	143	11.6
09/20/82	1467	949	131.8	9.91
09/27/82	1439	949	132.4	10.8
10/04/82	1492	951	138.2	11.1
10/11/82	1410	948	127.2	10.8
10/18/82	1459	946	149	12.0
10/25/82	1381	957	128	10.8
11/02/82	1338	941	122.8	11.1
11/08/82	1500	931	162	12.1
11/15/82	1344	939	120.8	10.3
01/31/83	1125	942	127.9	11.59
03/15/83			124.1	10.64
04/18/83			126.7	11.29
05/24/83			133.2	11.21
06/24/83	1508	842	124.6	11.22
07/28/83			126	10.16
08/03/83(1)	1244	912	166.9	13.6
--	1199	882	123.8	10.3
08/12/83	1221	914	129	10.6
08/13/83(2)	1198	697	-	-
08/19/83(3)	1135	884	117.4	10.32
09/20/83	1122	872	110.6	10.73
08/10/83	1082	845	109.3	10.24
08/10/83	1092	850	107.3	10.13
10/31/83	1300	862	125.5	10.8
12/05/83	1272	903	168.4	11.97
01/06/84	1263	903	152.1	12.1
02/29/84	1279	914	143.5	11.7
03/19/84	1120	905	144.6	12.3
03/19/84	1150	905	136	11.6
03/19/84	1151	910	134.2	11.8

Notes: (1) At 190 psi
(2) At 180 psi
(3) At 175 psi

Carbon-14 data for CO_2 produced during early testing indicated that the activity of the CO_2 was approximately 25% of modern carbon; more recent data have shown an increase in activity to approximately 30% of modern carbon. Although these activities place a maximum age of the CO_2 at approximately 11,000 and 9,000 years, respectively, they also indicate a maximum contribution of 70% magmatic CO_2 and a minimum contribution of 30% from surface meteoric or recent marine sources. Further radioand stable-isotope analyses will be required before a firmer interpretation will be possible, however.

The two principal candidate sources for the sulfides present are magmatic sulfur, either stripped from the reservoir rock matrix or outgassed by a cooling magma body, or marine sulfate that has been reduced by high temperature reaction with the iron minerals present in the reservoir rocks. Analysis of cores and cuttings from the deeper sections of the well identified substantial amounts of both pyrite and anhydrite in fractures and veins indicating that abundant sulfur is present in the reservoir rock matrix. Isotopic analyses of the sulfur, although not yet complete, have indicated that the H_2S present may be in equilibrium with the sulfate and pyrite minerals present. This suggests that we will be unable to uniquely identify a magmatic or marine source for the sulfur. However, in light of the nearly constant concentrations of hydrogen sulfide being produced and the ten-fold increase in seawater contribution to the HGP-A brine, it would appear that an active contribution of sulfide from seawater sulfate reduction is unlikely. Further analysis of the sulfide concentrations and sulfur isotopic composition will be required to more closely identify the sulfide source in this well.

The minor gases, nitrogen and hydrogen, are believed to be the result of atmospheric contributions and water/basalt equilibrium reactions respectively. Neither has been studied isotopically and hence little other information is available for interpretation of their probable sources.

One further aspect of the overall gas chemistry that should be examined more closely with regard to reservoir interpretation is the near constancy of the total gas concentrations. As noted above, sampling and analytical difficulties during the early production of fluids from HGP-A prevented us from determining the initial gas chemistry to within a factor of approximately two. Even within

this constraint, however, the fact that the total non-condensable gas fraction present in the well discharge has changed by less than a factor of two during a time period when the total dissolved solids concentration has changed by a factor of approximately 4.5 indicates that the steam chemistry is almost entirely independent of the water chemistry. This in turn suggests that HGP-A, although producing a mixed fluid at the well head, may be producing single phase fluids from two independent aquifers in the reservoir. It is postulated that a single phase steam aquifer is producing dry steam from near the bottom of the well and that an overlying aquifer is producing lower temperature water or brine at a shallower level in the well bore.

Summary and Conclusions

The total non-condensable gas fraction produced by HGP-A is in the low-to-moderate range when compared with other geothermal fields worldwide. Although the hydrogen sulfide concentration relative to the other non-condensable gases is somewhat higher than is typically found, no major engineering difficulties have been encountered due to its concentration. The virtual absence of ammonia and boron in the steam phase produced by HGP-A has been found to have a substantial impact on the partitioning of hydrogen sulfide in the steam exhaust system allowing for much more efficient removal of the sulfide from the steam condensate that ultimately is recycled to the cooling tower, as make-up water.

Although a complete analysis of the reservoir implications of the gas chemistry data is not yet possible, the primary sources for the non-condensable gases are indicated to be meteoric recharge, marine recharge, or magmatic exhalations. The invariability of the N.C.G. concentrations during the recent production history of HGP-A, when compared to a more than four-fold change in brine TDS, suggests that a single phase steam production horizon is present in the well that is overlain by a liquid production zone and that the two zones are mutually independent. If this interpretation is correct, the presence of a dry steam resource in Puna will have substantial implications for both the technical and economic feasibility of developing this resource. Proper casing programs, if utilized in future wells, may be able to exclude the brine resource entirely and thereby totally eliminate a number of operational and maintenance problems encountered in the brine handling system at HGP-A.

Section 3

MAIN STEAM SYSTEM

SYSTEM DESCRIPTION

The piping system that transports the geothermal fluid from HGP-A is illustrated in Figure 3-1. The two phase flow of geothermal fluid from the well is piped to a flash separator where the steam is separated from the brine phase.

The steam exits from the top of the flash separator and passes through a venturi meter (FT-1) which measures the flow rate of the steam. The steam is then passed through a moisture separator where water droplets, which may have formed in the line, are removed prior to the steam entering the turbine. The steam turbine operates at an inlet pressure of 175 psia (12.3 kg/cm^2) and exhausts vertically into the exhaust ducting to the main steam condenser. The turbine rotates at 5,800 rpm and is geared down to a generator speed of 1,800 rpm.

The main condenser is a surface type condenser designed to operate at an absolute pressure of 2 psia (0.14 Kg/cm^2). Non-condensable gas is pumped from the condenser with steam ejectors and is piped to the hydrogen sulfide abatement system. The condensate is pumped into the condenser cooling water return header that flows to the top of the cooling towers. Caustic soda is injected into the condensate line and mixed with the condensate by a static pipeline mixer to maintain a neutral or slightly alkaline solution condition in the circulating water. This allows the use of carbon steel piping for the condensate system.

Steam can be diverted from the turbine during reduced load conditions or upon turbine trip by a turbine by-pass line. This line is operated to maintain separator outlet steam pressure. Steam that is bypassed is treated with sodium hydroxide to abate hydrogen sulfide and muffled in a rock muffler before being released to the atmosphere.

The effects of the geothermal fluids on the steam system are discussed below. The steam/condensate systems were overhauled in August 1983 and the brine system in March 1984 which allowed the detailed inspection of the plant equipment.

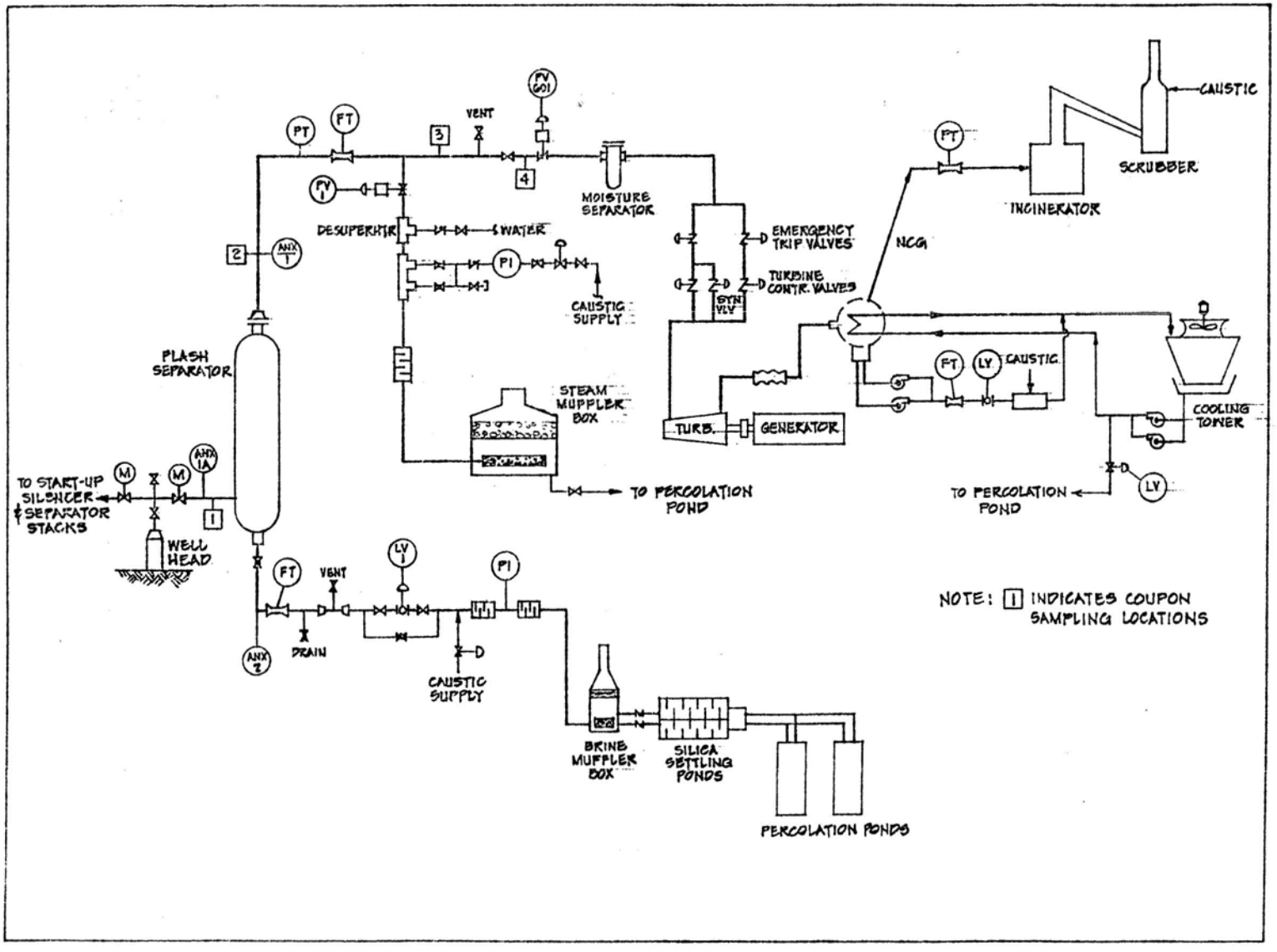

Figure 3-1. HGP-A Geothermal Power Plant-Flow Diagram

CHEMICAL ANALYSIS OF SCALE MATERIAL - STEAM SUPPLY SYSTEM

The current discussion of scale deposition in the steam handling system is divided into three sections (see Figure 3-1): 1) the steam supply system between the flash separator and the moisture separator; 2) the moisture separator - inlet manifold - turbine internal surfaces; and 3) the turbine exhaust system. These divisions are based on the nature of the "atmosphere" to which each part has been exposed. The steam supply system has been exposed to only high temperature steam and N.C.G. since operations began in December 1981; the moisture separator through the turbine internals has been exposed alternately to high temperature steam and N.C.G. during normal operations and to atmospheric oxygen during turbine outages; the turbine exhaust has been exposed to low temperature steam (less than 212°F (100°C)) and N.C.G. and to varying amounts of air due to minor vacuum leaks and during interruptions of turbine operation.

Scale deposits identified in the steam system were predominantly iron sulfides; in some sections exposed to atmospheric oxygen the sulfides were accompanied by varying proportions of iron oxides. Siliceous scale was found to be predominant only at the turbine inlet handwheel chamber; it was also found at low concentrations in the inlet nozzles and first stage diaphragm. The deposited scale material varied widely in thickness and in chemical composition. The thicknesses of the sulfide and oxide deposits varied depending upon both the physical conditions that the surfaces were exposed to (e.g., stationary vs. rotating surfaces) and the chemical conditions experienced at each location. Iron sulfides and oxides predominated but were accompanied by smaller amounts of siliceous deposition in the nozzle block chamber and first stage rotating blades.

MAIN STEAM LINE

The investigation of scale formation in the steam supply system included sampling and removal of circular coupons from the steam supply pipe walls in three locations (as noted in Figure 3-1). The pipe coupons were removed from the top of the pipe and the internal conditions of the sides and bottom were inspected visually at each location. In only one location, at ANX 1 (point 2 in Figure 3-1), was there sufficient scale accumulation on the bottom of the pipe to be sampled.

The scale deposition observed at the first location is presented in Figure 3-2. The thickness of the scale layer observed was approximately 0.04 inches (1 mm). The scale is easily friable and has a somewhat foliated texture. The bottom of

the pipe at this location showed a significantly greater accumulation of scale that appeared to be deposited as a narrow channeling along the bottom of the pipe. Although it was not possible to photograph the scale at this location large samples of scale were removed intact and photographed in the approximate orientation observed in the pipe (Figure 3-3). The gross morphology of the scale deposition observed at this location suggests that pyrite formation is enhanced at the steam-liquid interface along the very small volume of brine streaming along the bottom of the pipe.

X-ray diffraction analysis indicates that the scale material is composed of nearly 100% pyrite with only trace amounts of pyrrhotite and silica present. The micromorphology of this material, as indicated by scanning electron microscopy, is of intermediate to small, well-formed crystals interspersed with much smaller fragments and micro-crystalline material. Scale deposited on the pipe walls was found to have an essentially identical micromorphology (Figures 3-4 and 3-5).

The second pipe coupon was removed at an elbow bend in the pipe located at point 3 in Figure 3-1. Scale deposition was noticeably thinner at this location (Figure 3-6) and did not allow a valid thickness measurement to be made. Inspection of the bottom of the pipe and the outer edge of the elbow did not reveal any significantly thicker scale deposition in these locations nor was detectable erosion of the pipe evident. The uniform deposition of scale at this location suggests that very minimal amounts of liquid were present in the steam line and that a bottom stream of condensate carryover was not present in the pipe.

The micromorphology of the scale present at this location was of an extremely fine texture that was too small to resolve with the scanning electron microscope (Figure 3-7). Although there was not enough scale present to perform x-ray analysis, the material is clearly an iron sulfide and is very probably pyrite or pyrrhotite.

The last pipe coupon removed for inspection was located just upstream of stop valve PV601 at point 4 in Figure 3-1. The scale layer formed at this location was even thinner than at the second location and appeared to be discontinuous, having been unable to develop a complete coating on the inner pipe walls. There

was no evidence of thicker scale accumulation on the walls or bottom of the pipe, suggesting a relatively uniform deposition mechanism.

Scanning electron microscopy of the scale from this location showed the texture to be layered (Figure 3-8) but, even at high resolution, crystalline structures were not resolvable. The amounts of scale present at this location were again inadequate to allow an x-ray diffraction analysis of the mineralogy.

MAIN STEAM MOISTURE SEPARATOR

The main chamber of the moisture separator had severe oxide scaling. About 30 pounds of scale were found on the bottom of the separator (Figure 3-9). The inlet and outlet perforated plates were also heavily scaled with iron sulfide and oxide of 1/16 to 1/8 inches (0.16 to 0.32 cm). The mist pack was coated with oxides of approximately 0.020 to 0.060 inches (0.05 to 0.15 cm) in thickness but was still effective. The bottom drain was effectively plugged as seen in Figure 3-10.

The scale material was friable and did not adhere strongly to the walls of the moisture separator vessel. X-ray diffraction analysis of this material identified pyrite as the primary material with lesser amounts of iron oxides being present as well.

CONTROL VALVES

The steam manifold through the trip and control valves carried a light coating of friable scale that was easily scraped from the pipe walls (Figure 11). The bottom of the horizontal lines also carried an accumulation of macro-crystalline material that was in sharp contrast to that found on the pipe walls. The latter material was found on the butterfly control valve surfaces as well. Thickness found on the pipe walls ranged from 0.040 to 0.060 inches (1.0 to 1.5 mm).

X-ray analysis determined that the deposition was composed of pyrite and pyrrhotite. The former was predominant in the macro-crystalline material accumulated at the bottom of the pipe and on the control valve surfaces.

STEAM TURBINE

The turbine inlet hand wheel chamber and nozzle block were found to have a thicker accumulation of scale material that had a distinctly different character

from that found in the remainder of the turbine system. The hand wheel chamber was coated with a 2 mm layer of vitreous siliceous scale whereas the inlet nozzles were coated with somewhat less vitreous appearing scale that ranged from 0.010 to 0.100 inches (2.5 to 25 mm) in thickness (Figures 3-12, 3-13, and 3-14). Although this thickness of scale appeared to restrict the nozzles somewhat, the scale had no apparent impact on the turbine operation. In both locations the scale material was firmly attached to the metal surfaces and had to be chipped free.

The gross morphology of the scale indicated that the former was nearly all silica whereas the latter consisted of iron sulfides accompanied by much smaller amounts of silica. X-ray analysis indicated that the more vitreous scale was composed of approximately 80% silica with the remainder being mixed iron sulfides and oxides. The scale present on the inlet nozzles was found to be predominantly pyrite (80%) and pyrrhotite (15%) that was cemented together with only a small amount ($\leq$ 5%) of silica.

Turbine Blades and Wheels

The turbine blades had a hard coating of pyrite with a maximum thickness of 0.015 inches (0.04 cm.). This coating was predominant at the minor blade diameters (see Figure 3-15). The outer blade diameters were relatively clean due to particle impingement and water washing.

The turbine wheels, shaft and inter-stage seals were coated with pyrite varying from over 0.030 inches (0.08 cm) thick on the inlet side of the wheel #2 to only a surface coating a few thousandth of an inch thick on the outlet side of wheel #6.

The turbine blade pitting mechanism is probably electrochemical and its activity is dependent upon the presence of moisture. The largest diameter pits were 0.030 inches (0.08 cm) which were located on the inlet side of row #2. The pit density was greatest on the outlet side of blades 3 and 4. The deepest pits were on the inlet edges of blade #4. See Figure 3-16.

There does not appear to be a correlation between scale thickness or location or pit depth and density as seen in Table 3-1. All blade stellite shields on rows 5 and 6 were intact and in good shape.

TABLE 3-1

PITTING AND SCALE - TURBINE SPINDLE AND DIAPHRAGMS
(Maximum Ranges, in Inches)

	Spindle					
	Rows					
	1	2	3	4	5	6
SPINDLE						
A. Pit Diameter						
inlet	.012L	.030L	.012H	.015H	.010H	.013H
outlet	.014L	.010L	.010VH	.010VH	.014H	.015H
B. Scale Thickness						
inlet	.012	.010	.015	.008	.006	.006
outlet	.012	.010	.015	.013	.010	.012
DIAPHRAGMS						
A. Pit Diameter						
inlet	.004L	.007L	.013M	.015M	.030H	
outlet	.012M	.020H	.030H	.030H	.025H	
B. Scale Thickness						
inlet	.008	.040	.028	.035	.030	
outlet	.033	.050	.025	.040	.025	

Density Legend: L = light, M = medium, H = high, VH = very high

Turbine Diaphragms

The diaphragms were coated with a porous to hard scale in the non-blade areas. This material was predominantly mixed iron sulfides.

The diaphragm blades were coated with pyrite similarly to the turbine wheel blades as seen in Figures 3-17, 3-18, and 3-19. The outer blade diameters were swept clean and the minor blade diameters contained coatings of pyrite from 0.008 to 0.040 inches (0.02 to 0.1 cm) thick. Pitting depth and density increased through the inlet stage (Table 3-1). Pitting diameters on the outlet side were greater than on the inlet side but depth and density followed the same pattern (Figure 3-20).

The mineralogy of the scale present in the turbine was virtually uniform throughout the turbine, being composed of 70% to 90% pyrite and 10% to 30% pyrrhotite. In only one location was the composition substantially different: macro-crystals of approximately 0.02 inches (0.5 mm) diameter were found to be growing on the outer edge of the third stage blade ring and were composed of at least 90% pyrrhotite with only minor pyrite accessory minerals.

The micromorphology of the scale material was also quite similar throughout the turbine internals. All samples, with the exception noted above, were made up of extremely fine grained micro-crystalline material; the individual grain sizes for all samples were too small to resolve at SEM magnifications of 5000 or more.

EXHAUST DUCT

Figures 3-21 and 3-22 show the condition of the turbine exhaust when the 36 inch (91.4 cm) diameter outlet pipe was removed. The scale was much lighter than that found upstream and consisted predominantly of iron sulfide with pyrite granules. The inside of the 36 inch (91.4 cm) diameter outlet pipe was coated with only a light, soft material that could be wiped off.

The exterior of the #1 and #2 gland was in fairly good shape with scale being predominantly mixed iron sulfides.

MAIN STEAM CONDENSER

The exteriors of the stainless steel tubes in this condenser were very clean and required no cleaning. The side walls of the condenser hot well were very clean

down to the water line. A dark stain was present below this line. The floor of the condenser hot well contained a light loose deposit of iron sulfide which was rinsed clean.

TURBINE GENERATOR AUXILIARY SYSTEMS

The turbine generator auxiliary systems were also inspected for scaling and corrosion that may have resulted from the use of steam condensate as cooling tower makeup water.

Condenser Recirculation System

The condenser has a four pass configuration with cooling tower water entering from the bottom and flowing out the top. The top fourth section of tubes was free of slime but exhibited a dark stain which required a sharp edge to penetrate. It is believed that this stain is the result of gas buildup during the August to December outage in 1981 when the system was left filled with cooling tower water. There was no detectable pitting of the tube interiors in this area.

The middle half section of tubes contained a slime coating rich in iron oxide. This slime was easily removed with a tube brush and a high pressure water rinse. A porous iron oxide coating was left in the tubes which will require mechanical removal.

The lower fourth section of tubes contained a lesser thickness of slime coating rich in iron oxide. A lighter porous coating was also evident.

Pitting under the iron oxide coating was evident in the bottom three-fourth section of tubes. The total extent of this pitting was undetermined due to the porous iron oxide coating. Selected tubes were mechanically cleaned at the tube sheet area for closer examination. Pitting of 0.010 to 0.012 inches (0.025 to 0.03 cm) deep was found on all examined tubes.

Lube Oil Cooler

The tubes were heavily fouled on the inlet side with debris from the cooling tower (Figure 3-23). The inlet/outlet box epoxy coating had failed and the steel underneath had begun to corrode (Figure 3-24). The tubes were flushed

with a high pressure, 3000 psig (211 kg/cm^2), water blaster. All loose material and slime were flushed clear. These tubes exhibited a porous oxide coating and pitting similar to the main condenser.

Generator Air Cooler

This finned tube bundle type heat exchanger was removed from the generator for cleaning. Both water heads were removed and all tubes flushed with a high pressure, 3000 psig (211 kg/cm^2), water blaster. These tubes exhibited a porous oxide coating and pitting similar to the main condenser.

Non-Condensable Gas Ejector Condensers

The two condensers were hand cleaned with a rod and brush and then flushed with water. The interiors came clean except for a minor scale which appeared to be the original mill scale. These condensers are the only piece of heat exchange apparatus on the cooling tower system that had a drain valve which had been opened during the August - December 1981 outage.

COOLING TOWER

The north top PVC fill had collapsed when steam from the brine sparger was drawn into this section and no cooling water was circulated. This PVC fill was removed and a new one installed. The tower was drained after settling for two days and a 3-inch (7.6 cm) deep sludge covered the bottom. This sludge was predominantly iron oxide. All cooling tower fan blades were removed, cleaned and resurfaced with epoxy after the eroded edges were rebuilt.

Discussion

The primary component of scale deposited in the steam supply system is the iron sulfide mineral, pyrite (Table 3-2). The depositional morphology in the upstream position of the steam line strongly suggests that pyrite formation is favored or promoted by the presence of both liquid water-borne iron ions and steam-borne hydrogen sulfide. In addition, the much thicker layer of scale found in the upstream location suggests that the presence of other dissolved salt ions in the liquid phase may also promote the scale formation process. The interpretation of these observations is that the salts present in the brine carried over from the separator vessel are promoting corrosion of the mild steel pipeline which provides dissolved iron ions to the accumulated liquid phase in the pipe. Reaction between the dissolved iron and the H_2S present in the steam phase at

TABLE 3-2

SCALE FORMATION - HGP-A STEAM SYSTEM

Location	Scale Formation
Valve in steam line	> 90% pyrite (FeS_2)
Upstream of moisture separator	minor pyrrhotite (Fe_1S)
Moisture separator	80% - 90% pyrite 10% - 20% iron oxides (Fe_2O_3)
Inlet nozzle block hand wheel chamber	80% silica (SiO_2) minor iron sulfides (FeS_2, FeS, Fe_2O_3)
Inlet nozzle	80% pyrite 15% pyrrhotite 5% silica
First stage blades	70% - 90% pyrite 10% - 30% pyrrhotite
First stage diaphragm	90% pyrite 10% pyrrhotite
Second stage	90% pyrite 10% pyrrhotite
Third stage (outer edge of blade ring)	98% pyrrhotite minor pyrite
Fourth stage	80% pyrite 20% pyrrhotite
Fifth stage (trailing edge of blades)	60% iron oxides 40% pyrrhotite
Sixth stage (trailing edge of blades)	60% iron oxides 40% pyrrhotite sides of turbine casing
Sides of turbine casing	60% pyrite 40% pyrrhotite
Bottom of condenser boot	> 90% goethite ($Fe_2O_3 \cdot H_2O$)
Sides of condenser boot	> 90% pyrite minor pyrrhotite

the steam-liquid interface brings about the deposition of the pyrite scale at this location and would account for the channel-like deposition found on the bottom of the upstream section of pipe.

It should be emphasized that the source of iron for sulfide scale formation is believed to be the pipe walls. Iron carryover to the steam line, either in the brine phase or in the steam phase, has been proposed as the source for the iron sulfides. There is virtually no evidence to support this interpretation and data available for the chemistry of the steam or brine phases strongly argue against such an interpretation.

The loss of the majority of the brine carryover, both at the bypass line downcomer (Figure 3-1) and at the condensate drop-out lines, removes most of the dissolved ions carried over with the brine leaving only a very low TDS steam condensate in the downstream portion of the piping. The low salinity condensate is unable to promote corrosion in the mild steel as effectively as the brine carryover and hence fewer iron ions are available for reaction with the H_2S in the steam phase.

The major component found in the scale deposited between the moisture separator and the turbine system was again the iron sulfide pyrite. The most notable difference between the scale deposition here and the upstream portion is the substantially higher deposition rates observed. This difference is believed to be due to both physical and chemical factors. The major physical factors controlling iron sulfide/oxide scale deposition are the occurrence of "drop-out" points (such as the moisture separator vessel), centrifugal deposition from the turbine rotating members, temperature cycling of the turbine system, and erosion of turbine blade material. The major chemical controls are the presence of liquid water and the intermittent access of air oxygen during turbine outage periods.

The latter factor, access of air to this subsystem, is believed to be responsible for the much larger amounts of scale present in the turbine system than was found in the steam supply system. The role that air oxidation plays is similar to that of salt carryover from the brine immediately downstream of the separator. During turbine outage periods, when this system is vented with

atmospheric air, the iron sulfides rapidly oxidize to iron oxides and varying amounts of elemental sulfur, sulfurous acid and sulfuric acid. The latter promotes corrosion of the mild steel piping and turbine housing; pit corrosion of the turbine blade tips was evident during inspection of the turbine spindle. This corrosion produces free iron that is available for rapid reaction with H_2S to form additional sulfides when steam is admitted to the system during the subsequent start up. Once present, the sulfuric acid may linger in cracks and between scale layers in the turbine for considerable periods of time before condensate formed in the turbine can carry it away. The rapidity of the oxidation process, even at room temperature, was observed during analysis of the collected scale samples. Repeat analysis of two aliquots of the same sample separated by a period of several days found a substantial conversion of the iron sulfides originally present to predominantly iron oxides.

The presence of water undoubtedly promotes the chemical (corrosion) reactions required to generate the iron ions initially and allow the reaction between iron ions and hydrogen sulfide to proceed. Additionally, it appears that crystal formation is, to some extent, controlled by the presence of water. In those areas where liquid water is constantly present, such as in a bottom stream of condensate in the inlet manifold piping, macro-crystalline pyrite was found whereas, on the pipe walls, where condensate may be present intermittently, only micro-crystalline pyrite is observed.

The major physical process promoting sulfide scaling in the turbine internal system is believed to be erosion of material from impacted surfaces. Pitting, although of limited extent, was clearly evident on the forward surfaces of nearly all the turbine blades. A semi-quantitative analysis of the scale from the turbine using x-ray fluorescence substantiates this mechanism. Although iron was the primary component in all samples, the relative proportions of trace amounts of chrome and manganese were observed to increase toward the back of the turbine (Table 3-3). Erosion also served to control the location of scale formation. In most cases the turbine blades and rotating members carried the lightest accumulation of scale material whereas the inter-stage diaphragms and the turbine housing carried the heaviest accumulations.

Thermal cycling of the turbine may also play a role in scale formation. Cooling of the internals allows condensation of liquid water in locations where it is not normally present and thus allows the chemical reactions noted above to

TABLE 3-3

NET X-RAY INTENSITY (COUNTS)

Element	P5120	P5121	P5122	P5123	P5124	P5125
S	32065	2756	32762	28787	29538	31453
CL	0	1800	0	0	0	0
K	59	701	0	137	24	35
CA	427	8049	1047	574	640	705
CR	706	4912	5382	7227	12793	38509
MN	262	36427	357	2810	3932	4613
FE	2202516	571766	1952776	2380403	2473864	1842987
NI	288	461	5173	2460	2114	1438
CU	727	752	1597	3622	2571	1196
ZN	184	160	122	363	0	350
AS and PB	434	6323	1819	1084	1490	629
SE	259	3416	6348	7948	6286	8253
BR	0	846	0	0	0	174
RB	* 700	*	*	*	*	
SR	* 9858	*	*	*	*	
MO	803	630	1668	1589	2993	676
BA	0	300	103	0	98	71

X-RAY INTENSITY NORMALIZED TO FE = 2473864 COUNTS

Element	P5120	P5121	P5122	P5123	P5124	P5125
S	36015.38	11924.40	41504.37	29917.25	29538	42219.75
CL	0	7788.073	0	0	0	0
K	66.26875	3033.022	0	142,3790	24	46.98093
CA	479.6060	34825.67	1326.386	596.5368	640	946.3301
CR	792.9786	21252.79	6818.158	7510.751	12793	51691.10
MN	294.2782	157609.0	452.2636	2920.328	3932	6192.086
FE	2473864.	2473864.	2473864.	2473864.	2473864.	2473864.
NI	323.4813	1994.612	6553.388	2556.586	2114	1930.245
CU	816.5657	3253.684	2023.151	3764.209	2571	1605.405
ZN	206.6686	692.2731	154.5551	377.2524	0	469.8093
AS & PB	487.4684	27357.77	2304.391	1126.561	1490	844.3144
SE	6286	0 11078.10	290.9086	14780.03	8041.930	8260.060
BR	0	3660.394	0	0	0	233.5623
RB	*	3028.695	*	*	*	*
SR	*	42652.68	*	*	*	*
MO	901.9289	2725.825	2113.097	1651.388	2993	907.4031
BA	0	1298.012	130.4850	0	98	95.30417

*Not Determined Due To Interference From High Fe Concentration.

Guide:
- P5120: Moisture separator bottom drain
- P5121: Inlet nozzle to turbine
- P5122: First stage rotating blades
- P5123: Backside 3rd stage diaphragm top
- P5124: Back of 4th stage diaphragm
- P5125: Trailing edge of 6th stage blades

proceed. An additional consideration is that the thermal cycling disrupts the existing sulfide coating present on pipe walls, turbine internal surfaces, etc., and thus exposes new, clean surfaces to attack by, and reaction with, H_2S. Spallation of the disrupted surface sulfide coating may also allow it to be carried into the drop out points at the moisture separator and on the turbine casing walls.

The cause of the silica scale observed in the turbine hand wheel chamber and on the inlet nozzles is not completely understood at present. The only hypothesis that suggests itself is that an isothermal pressure drop at the turbine nozzles may allow the small amount of residual brine aerosol to evaporate thus forcing deposition of dissolved salts present in the aerosol liquid. Visual inspection of the turbine nozzle deposits indicated that they were hygroscopic suggesting that other salts were present as well.

The virtual absence of scale deposition within the turbine exhaust duct and condenser system is attributable to the fact that this system is constructed of stainless steel. The typically lower temperatures encountered in this system may also contribute to the absence of scaling or significant corrosion. The small amount of iron oxide sludge identified in the condenser boot is probably the result of spallation and steam carryover of oxide or sulfide scale from the turbine casing.

Conclusions and Recommendations

The deposition of scale material in the steam supply system, the turbine internals, and the exhaust system was found to be quite limited even after 17 months of operation. The major sources of scale formation are believed to be the result of reactions between H_2S present in the steam and iron supplied by corrosion of the mild steel piping and turbine internals and by erosion of turbine blades. A minor source of scale forming materials was found to be brine aerosol carryover through the flash separator and the moisture separator vessel.

The major problems that arose from the observed scale formation were as follows:

1. Partial plugging of the bottom drain of the moisture separator.
2. Partial plugging of turbine inlet nozzles.
3. In-filling of crevices between "slip-fit" faces on turbine diaphragms.

Plugging of the bottom drain of the moisture separator vessel can compromise the ability of this vessel to remove entrained water from the steam phase. Relocation of the drain outlet to a short standpipe configuration should minimize the potential for accumulation of deposits in the drain line.

The deposition of siliceous scale in the hand wheel chamber and in the nozzle block can clearly lead to a loss in turbine efficiency and higher maintenance requirements. Periodic washing of the turbine inlet system may reduce the required frequency of major maintenance and descaling overhaul. Re-design of the turbine inlet system to allow individual maintenance of this portion of the unit without a complete teardown of the turbine would considerably reduce the time required for servicing this particular problem.

Infilling of "slip-fit" facings between the turbine diaphragms and their mating surfaces in the turbine housing resulted in substantial difficulties in turbine "tear-down." Removal of the diaphragms from the turbine housing had the greatest manhour requirement of any operation associated with overhauling the turbine. In an effort to alleviate this problem in subsequent overhaul operations, teflon tape was installed between the mating surfaces on the turbine housing and diaphragm units (Figure 3-25).

Several other procedures can also be recommended that may lead to a reduction in scale formation in the steam supply system.

1. Install additional brine/condensate dropout points downstream of the primary separator.
2. Install automatic nitrogen blanketing capability for use during turbine outages.
3. Install automatic anti-oxidant injection capability for use during turbine outages.

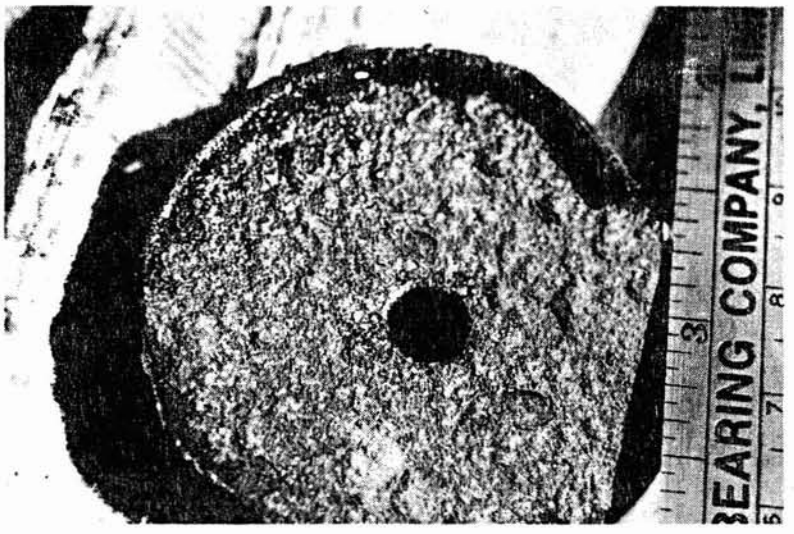

Figure 3-2. Top Sample of Main Steam Line Before Venturi. Scale consists predominantly of pyrite. Scale thickness is approximately 1mm.

Source: Hawaiian Electric Co., Inc.

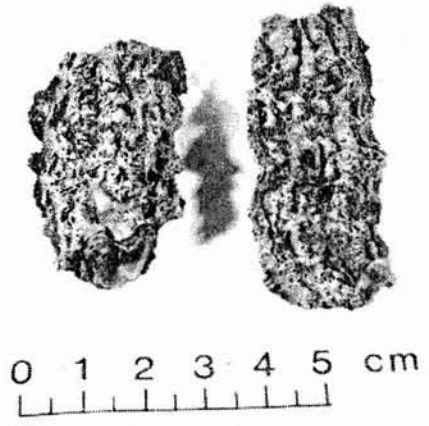

Figure 3-3. Scale Deposits - Main Steam Line Before Venturi. Scale consists of pyrite with traces of pyrrhotite and silica.

Source: Hawaii Institute of Geophysics

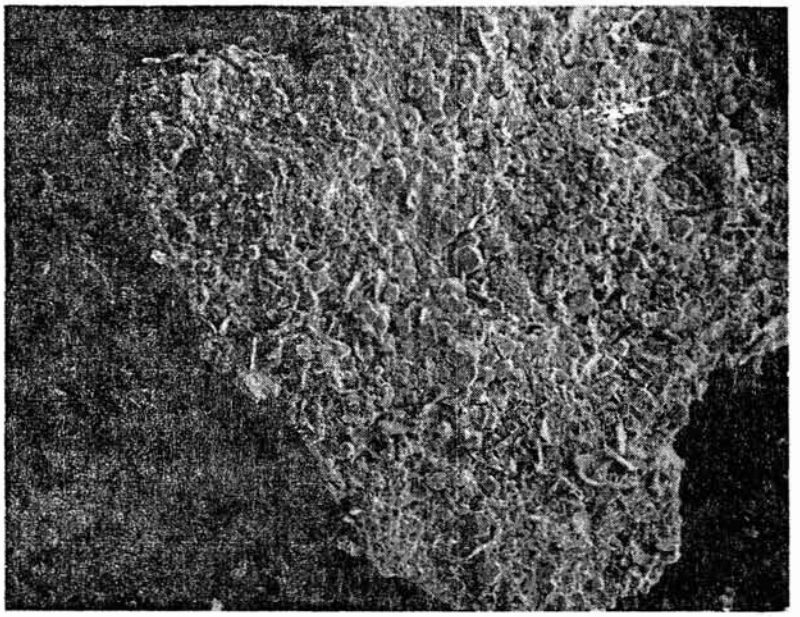

Figure 3-4. Micromorphology of Scale Deposits - Main Steam Before Venturi (110 x* Magnification)

Source: Hawaii Institute of Geophysics

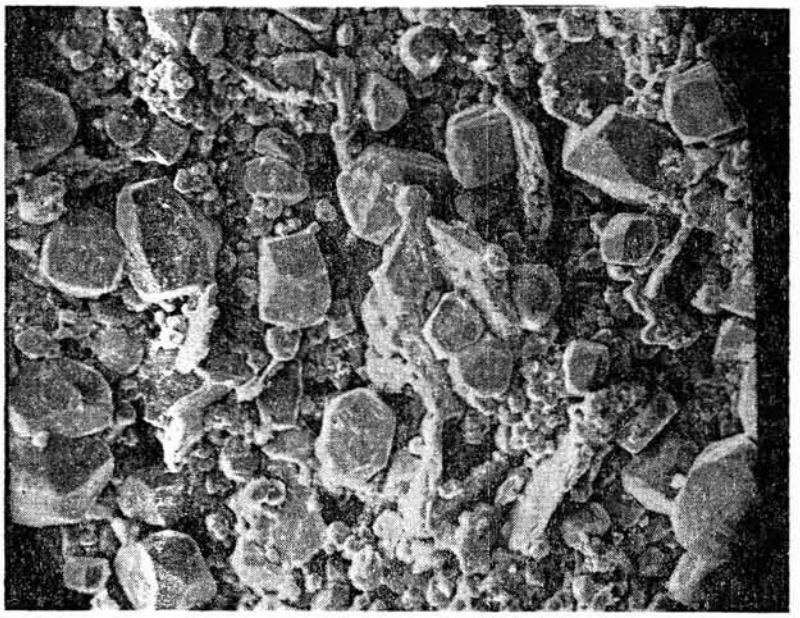

Figure 3-5. Micromorphology of Scale Deposits - Main Steam Line Before Venturi (540 x* Magnification)

Source: Hawaii Institute of Geophysics

* Please note that the illustration(s) on this page has been reduced 10% in printing.

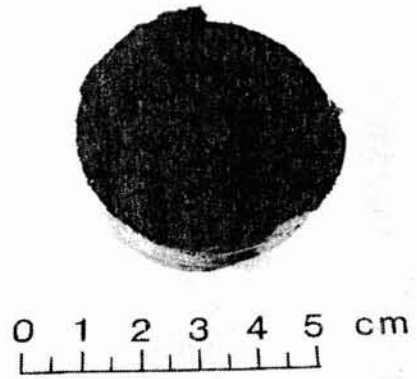

Figure 3-6. Top Sample of Main Steam Line at Second Elbow

Source: Hawaii Institute of Geophysics

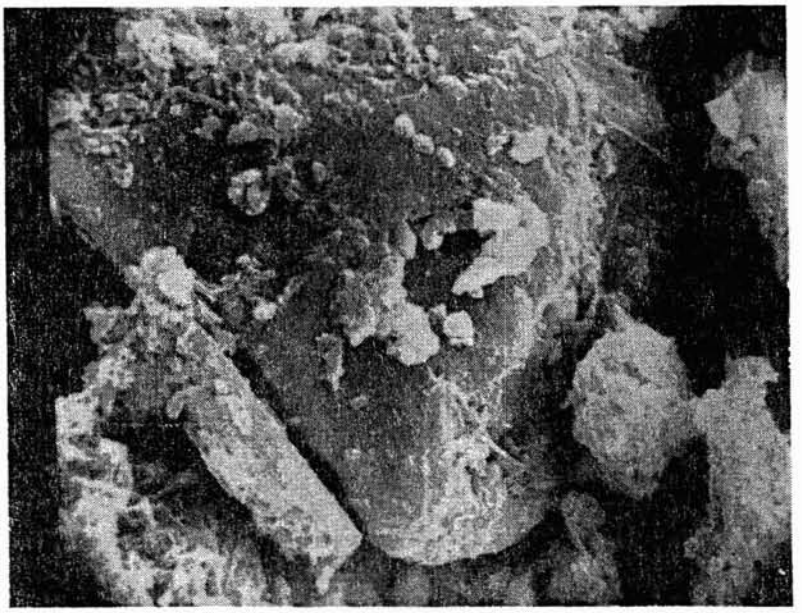

Figure 3-7. Micromorphology of Scale Deposits - Main Steam Line at Second Elbow (540 x* Magnification)

Source: Hawaii Institute of Geophysics

* Please note that the illustration(s) on this page has been reduced 10% in printing.

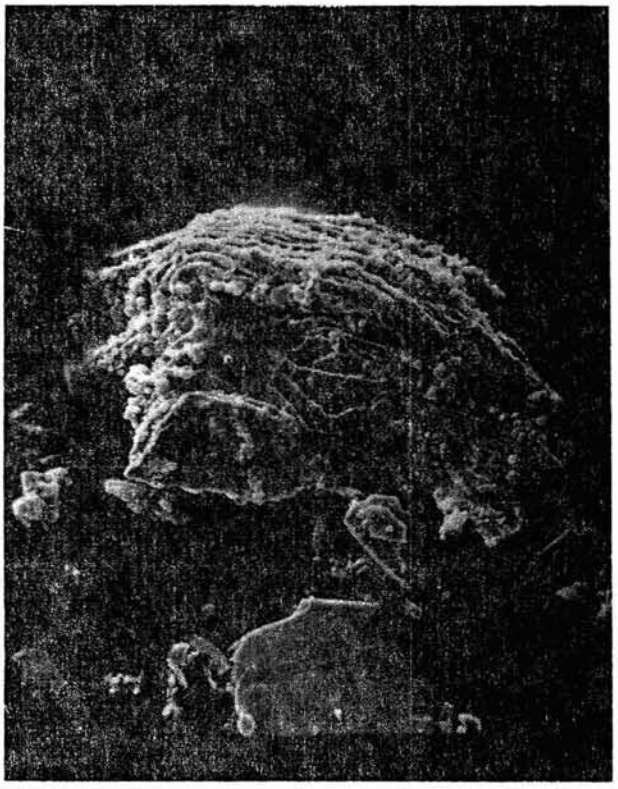

Figure 3-8. Micromorphology of scale deposits - Main Steam Line Before PV601 (620 x* Magnification)

Source: Hawaii Institute of Geophysics

* Please note that the illustration(s) on this page has been reduced 10% in printing.

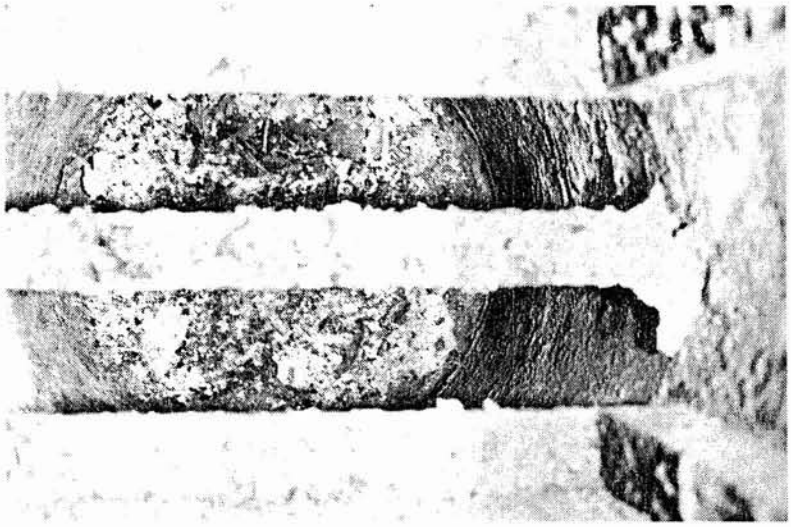

Figure 3-9. Moisture Separator - Chamber Bottom. Mixed iron sulfide and iron oxide scale accumulation over bottom drain.

Source: Hawaiian Electric Co., Inc.

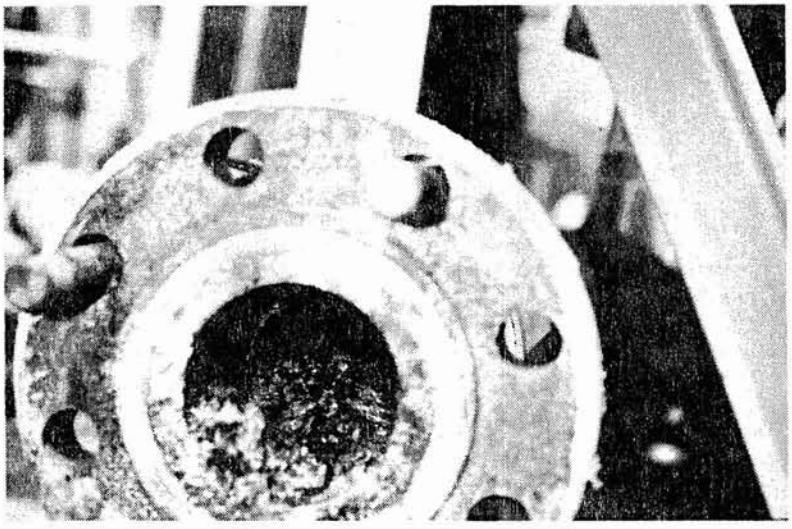

Figure 3-10. Moisture Separator - Bottom Drain. Mixed iron oxide, iron sulfide scale.

Source: Hawaiian Electric Co., Inc.

Figure 3-11. Main Steam Line Bottom - Inlet to Control Valve

Source: Hawaiian Electric Co., Inc.

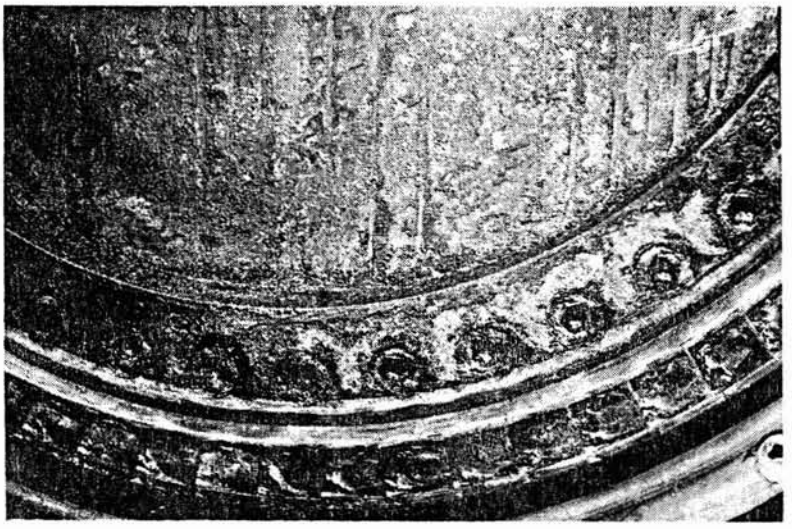

Figure 3-12. Nozzle Block Overview. Scale consists of mixed iron sulfide accompanied by silica. Scale thickness ranged from 0.025cm to over 0.25cm.

Source: Hawaiian Electric Co., Inc.

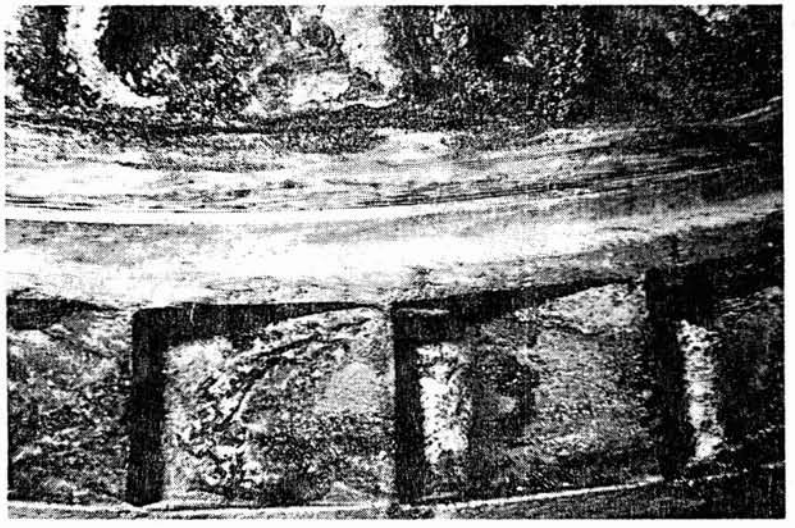

Figure 3-13. Nozzle Block - Close-up. Scale deposition consists of iron sulfides and silica.

Source: Hawaiian Electric Co., Inc.

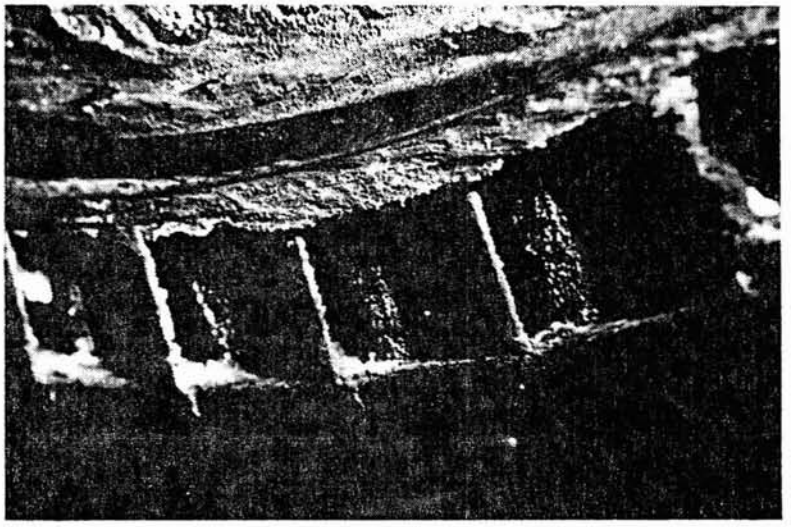

Figure 3-14. Nozzle Block - Close-up of Nozzle Opening. Scale material consists of the iron sulfides, pyrite, and pyrrhotite, and silica. Scale thickness ranged from 0.25mm to 25mm.

Source: Hawaiian Electric Co., Inc.

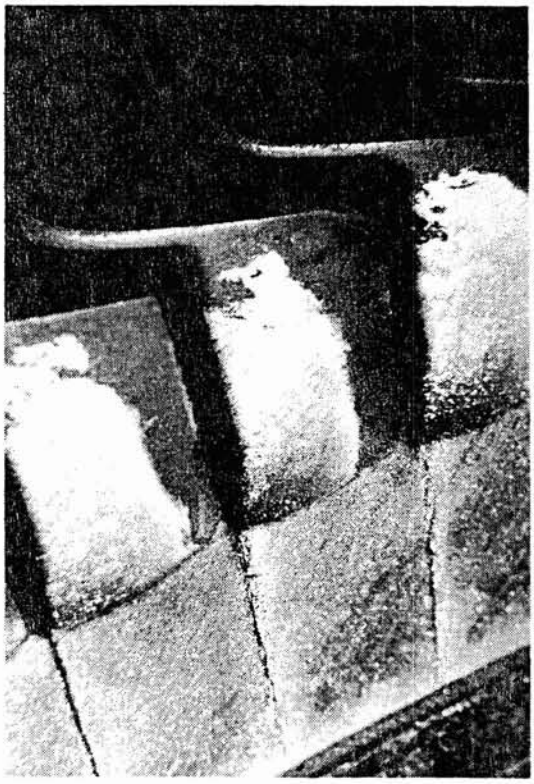

Figure 3-15. Turbine Wheel #1 Outlet Blade Side. Scale consists of the iron sulfides, pyrite and pyrrhotite. Maximum scale thickness is 0.04cm.

Source: Hawaiian Electric Co., Inc.

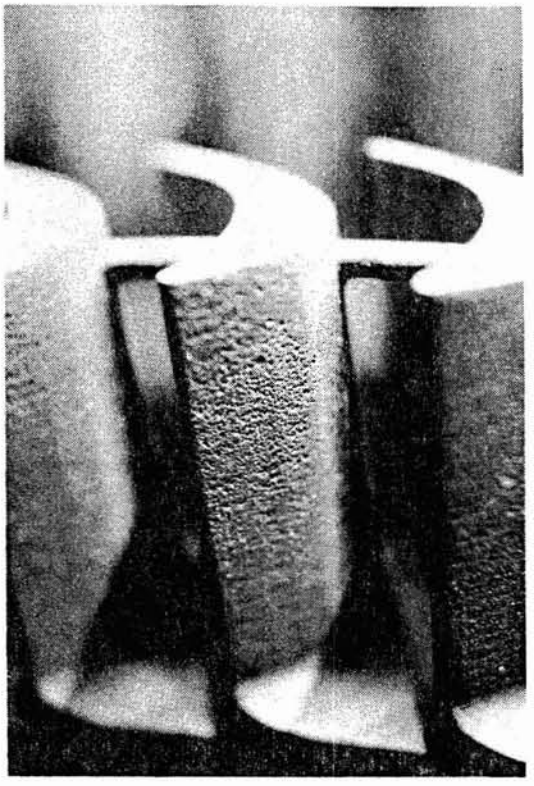

Figure 3-16. Turbine Wheel #3 Inlet Blade Side - Pitting

Source: Hawaiian Electric Co., Inc.

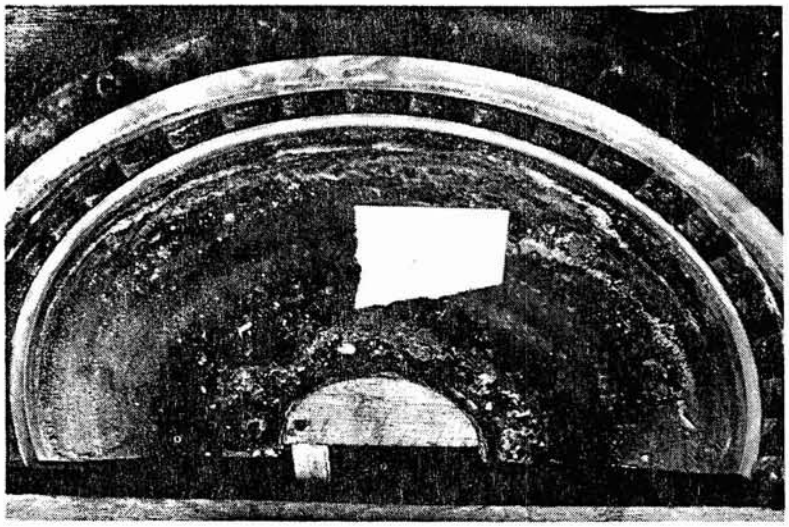

Figure 3-17. Diaphragm #1 Outlet Side - Overall View. Scale consists of pyrite and pyrrhotite.

Source: Hawaiian Electric Co., Inc.

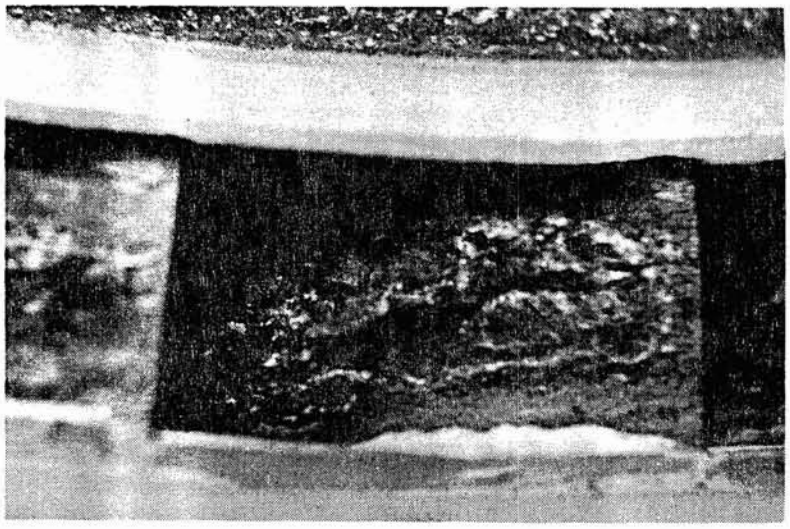

Figure 3-18. Diaphragm #1 Outlet Side - Top Section

Source: Hawaiian Electric Co., Inc.

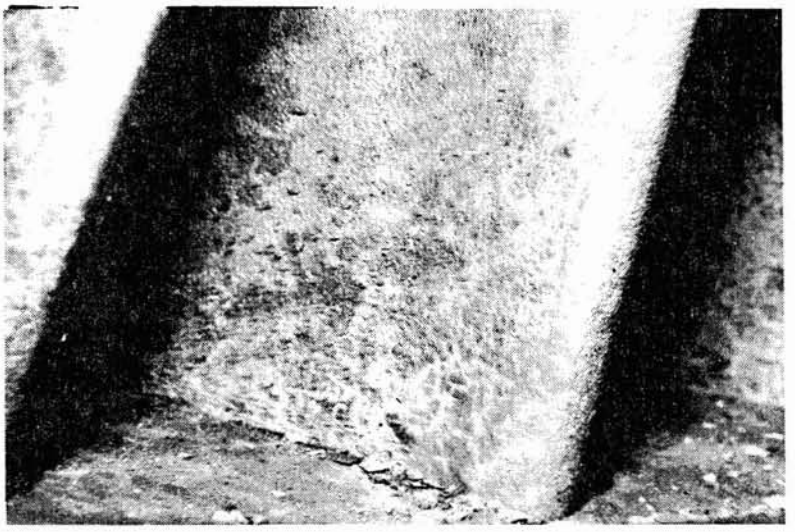

Figure 3-19. Diaphragm #4 Inlet Blade Side

Source: Hawaiian Electric Co., Inc.

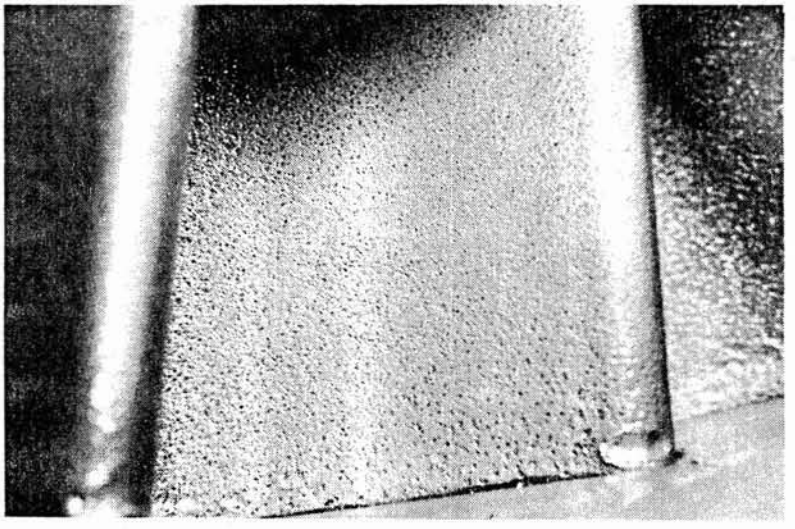

Figure 3-20. Diaphragm #3 Inlet Blade Side

Source: Hawaiian Electric Co., Inc.

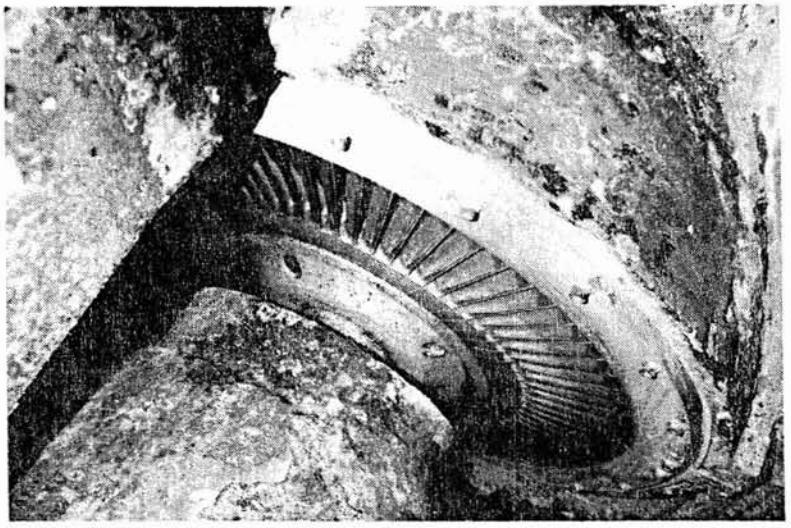

Figure 3-21. Turbine Exhaust Outlet. Scale consists of pyrite, pyrrhotite and mixed iron oxides.

Source: Hawaiian Electric Co., Inc.

Figure 3-22. Turbine Exhaust Top End of Outlet

Source: Hawaiian Electric Co., Inc.

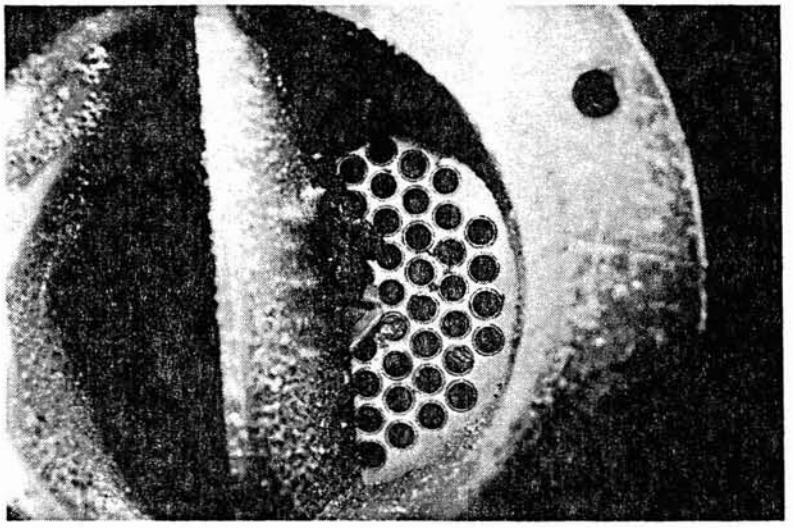

Figure 3-23. Lube Oil Cooler Inlet Side

Source: Hawaiian Electric Co., Inc.

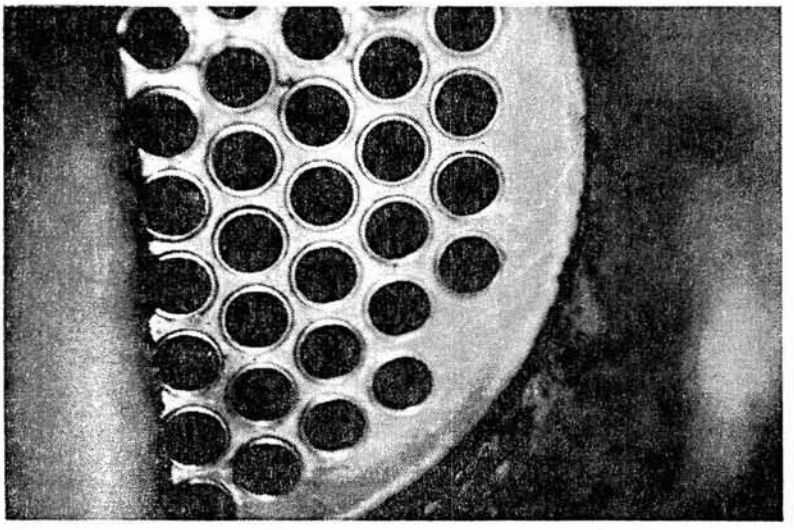

Figure 3-24. Lube Oil Cooler Outlet Side After Cleaning

Source: Hawaiian Electric Co., Inc.

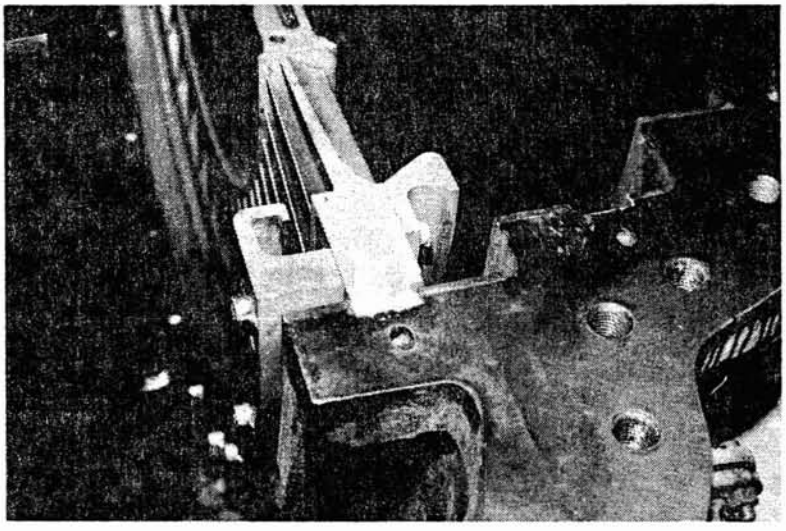

Figure 3-25. Diaphragm Resetting on Assembly with Teflon Tape

Source: Hawaiian Electric Co., Inc.

Section 4

BRINE SYSTEM

SYSTEM DESCRIPTION

Brine is separated from the two phase flow in the flash separator (Figure 3-1). A venturi is located in the brine discharge piping from the flash separator to measure flow rate. Level in the flash separator is controlled by a level control valve located in the brine discharge piping.

The hot, pressurized brine flows to a muffler box where the noise from the flashing process is abated when the brine's pressure is reduced to atmospheric pressure before disposal. The brine exits the muffler box and flows through the baffled settling ponds for about 45 minutes to allow precipitation of silica to take place. The brine then overflows into the percolation ponds via an open culvert where it is disposed by seeping into the ground. Overflow from the cooling tower and the waste discharge from the H_2S abatement system are also discharged into percolation ponds.

During the secondary flashing process of the brine, CO_2 and H_2S are released into the steam phase increasing the brine pH from about 7.0 to about 8.0. As a result of the temperature and pH change, colloidal silica formation is induced in the low temperature brines. During initial operations the colloidal silica showed little tendency to precipitate but, more recently, as the salinity of the fluids has increased, the precipitation of vitreous, sinter-like, silica scale within and downstream of the muffler box has increased substantially. This has led to plugging problems downstream of the muffler box, the piping, and the brine disposal ponds.

ANALYSIS OF BRINE SYSTEM SCALE MATERIAL

The geothermal fluid chemistry at the HGP-A facility presented at length in Section 2 is summarized below:

1. The silica concentration present in the HGP-A brines is approximately 850 mg/kg;

2. The salinity of the fluids produced from the HGP-A well has increased with time from a TDS concentration of approximately 3200 mg/kg to approximately 16,000 mg/kg;

3. The pH of the geothermal brine exiting the flash separator has declined from 7.4 to approximately 6.6-6.8;

4. The temperature of the fluids exiting the flash separator is approximately 374°F (190°C); and

5. The concentration of H_2S in the steam phase is approximately 950 mg/kg.

The chemical conditions present in the brine handling system clearly indicate a high probability for corrosion and for silica scale deposition. The former can be anticipated due to the high dissolved solids concentration, whereas, the latter would be expected because silica is present in the brine at approximately two to three times its saturation point. The overall analysis conducted at HGP-A found that silica scaling was present but relatively little evidence of corrosion was found in the air-free parts of the brine system.

MIXED PHASE LINE

The first sampling point in the geothermal piping is located immediately downstream of the wellhead wing valve and upstream of the primary plant separator (point 1 in Figure 3-1). A disc was cut from the 10-inch diameter pipe wall directly above a sampling flange point (ANX-1A). At this location, the pipe is exposed to the unseparated geothermal discharge composed of approximately 43% steam and 57% liquid brine (by weight) at a temperature of approximately 383°F (195°C). Two types of scale were identified at this location; a very thin coating of vitreous silica scale, approximately 0.02-inch (0.5 mm) thick, coated the inner surface of the 10-inch (25.4 cm) pipe (Figure 4-1) whereas the arm of the sampling flange had accumulated a significant amount of particulate material from the well that was cemented into a solid cake with silica (Figure 4-2).

Mineralogical analysis of the thin siliceous scale on the 10-inch (25.4 cm) pipe walls, using X-ray diffraction, indicated that this material was almost exclusively amorphous silica. Similar analysis of the caked material at the

sampling flange identified amorphous silica (60% to 70%), pyrrhotite (20%) and pyrite (10%). The latter deposit also contained small pebbles and rock fragments that presumably originated in the reservoir. Scanning electron microscopy of samples of scale from the pipe walls found the silica to be vitreous and acrystalline (Figures 4-3 and 4-4). Neither solution cavities nor inclusions were observed in the material sampled.

The very thin layer of silica scale observed and the vitreous nature of the scale suggests that the deposition of dissolved silica on this part of the piping system is either quite slow or has begun only very recently.

FLASH SEPARATOR

The second sampling point in the process stream evaluated was the primary brine separator. This vessel is approximately 4 feet-7 inches (1.4 m) in diameter and 17 feet-10 inches (5.4 m) high. Access to the separator was through a manhole located approximately 3 ft. (0.9 m) above the bottom of the vessel. Removal of the manhole cover revealed a thick accumulation of silica in the "dead-space" between the cover and the walls of the vessel (Figure 4-5). This material had an extremely rough surface (Figures 4-6 and 4-7) and consisted of poorly cemented particulates that were easily friable. The interior walls of the separator were coated with a similar appearing scale ranging in thickness from a few millimeters in the upper section of the separator to approximately 2 cm near the bottom. This material was more solidly cemented and more firmly attached to the vessel walls than was the accumulated material at the manhole. It was also apparent, however, that slabs of the former had broken free of the vessel walls and had formed an accumulation near the bottom of the separator that had subsequently been cemented into a nearly solid mass (Figure 4-8).

Removal of the silica scale from the vessel required the use of a heavy post hole digging iron; the vessel internal vortex breaker was uncovered. Nine two-gallon (7.6 liters) size pails of mineral were removed in this phase. A five-pound hammer and chisel were then used to break the hard mineral out of the four vortex breaker openings. It was impossible to clean these four openings due to the design of the vortex breaker. It was necessary to remove the 4-inch (10.2 cm) diameter bottom drain pipe section at the first elbow to facilitate flushing the smaller particles clear of the flash separator.

The gross surface morphology of the scale material, as indicated in Figure 4-6, consisted of wave-like protusions growing out of the overall mass. These protusions appear to be growing into the direction of water flow and have been observed in other parts of the brine handling system (see below). The implication of this fact is that accretion of the silica scale is affected by impact phenomena and hence turbulent flow of the brine fluids may promote silica scale formation.

X-ray analysis of the scale from the separator indicated that this material was composed primarily of silica; however, hand lens examination, as well as the coloration of this material, indicated that small amounts ($< 5\%$) of iron sulfides are present as well. Scanning electron microscopy showed the scale to be a mixture of extremely fine particulates mixed with larger fragments of cemented particles (Figures 4-9 and 4-10).

BRINE DISPOSAL LINE

The brine piping system between the separator discharge point and the level control valve (Figure 3-1) was sampled at three locations for scale deposition. The general findings were that the scale material was primarily siliceous with only very minor ($< 1\%$) amounts of iron sulfides present. The thickness of the scale ranged from 0.4-0.8 inches (1-2 cm) at the upstream end of the piping to less than 0.2 inches (0.5 cm) at the level control valve.

The observed decrease in scale thickness toward the downstream portion of the piping was unexpected since cooling of the fluids after leaving the separator would tend to increase the degree of silica supersaturation in the fluids. Subsequent to the completion of this work however, it was found that throttling of the brine flow was occurring at the exit point of the plant separator and not at the level control valve. On this basis we have concluded that flashing was occurring in the brine piping immediately downstream of the separator exit point. Steam formation and subsequent collapse and resorption accompanied by pH changes and increased turbulence may account for the increased silica scaling observed.

A second phenomenon that has been observed in this pipe run has been the rapid plugging or bridging of small diameter nipples or connection points on the 3-inch (7.6 cm) diameter line. Figures 4-11 and 4-12 show a brine piping connection point and a cut away view of a plug formed in a 1/2-inch (1.3 cm)

diameter auxiliary line approximately 10 feet (3.05 m) from the separator. Neither line was in continuous service and both were used only intermittently for brine withdrawal. The specific cause of the plug formation is not currently understood. At least two separate mechanisms are possible: 1) the small diameter pipe connection may act as a heat sink cooling fluids that may circulate within the connection and thereby promote silica precipitation or 2) the discontinuity in the pipe wall at the connection point may promote turbulent deposition of silica at the pipe surface. At the present time there is no obvious means of distinguishing between these possible mechanisms.

Figures 4-13 and 4-14 show the silica deposition in the brine piping approximately 10 feet (3.05 m) from the separator exit point. The silica layer is approximately 0.234 inch (0.594 cm) and appears to be of two distinct types. The outer layer (adjacent to the pipe wall) is chalky and moderately friable whereas the inner layer is more vitreous and harder. Both layers show a wave-like surface texture with the sharp edge of the waves facing into the direction of flow.

The micromorphology of the scale at this location shows a clear difference between the inner and outer layers of scale. The outer layer, Figures 4-15 and 16, is composed of a very open network of deposited material whereas the inner layer is much more solid (Figures 4-17 and 4-18) with fewer fluid cavities and channels. This change in structure of the deposit clearly reflects a change with time in the deposition characteristics and possibly in the mechanism of deposition. Increasing silica deposition rates with time have been observed downstream in the brine retention pond suggesting that the mechanisms responsible for scale formation may have become more rapid or efficient with time due to changes in brine chemistry.

X-ray diffraction analysis of this material indicates that both scale layers are composed predominantly of silica; only traces of iron sulfides are detected. The dark gray banding in the silica layers indicates, however, that sulfides are definitely present in small amounts.

The second section of pipe removed from the brine line about 80 feet (24.4 m) downstream of the flash separator (Figure 4-19) is quite similar to the first with the primary difference being that the thickness of the scale deposition is somewhat less. The measured thickness of the scale layer is approximately

0.136 inches (0.345 cm) and the surface morphology is of a pebbled texture rather than the wave-like protrusions observed upstream. The surface layer of scale is again glassier than the older scale layers and is substantially darker. The composition of both layers is again predominantly silica.

The last pipe section removed from about 175 feet (53.3m) (Figure 4-20) is virtually identical to the second piece described above. The scale thickness has decreased to 0.106 inch (0.269 cm) and the scale has the same layered appearance. The inner layer is again darker and glassier than the outer layer adjacent to the pipe walls and both are composed predominantly of silica with trace amounts of iron sulfides.

After the brine exits the pressurized portion of the disposal system, it is allowed to cool to 212°F (100°C) by boiling in an atmospheric flash chamber (Figure 4-21). It then passes through a retention pond and into a surface percolation pond. The physical and chemical changes occurring to the brine phase during this boiling process have a substantial impact on the silica deposition rate. These changes include the following: 1) a decrease in volume of the brine due to steam loss increases the silica concentration from about 850 mg/kg to more than 1100 mg/kg; 2) cooling of the brine from 370°F (188°C) to 212°F (100°C) substantially reduces the silica solubility due to the latter's strong temperature dependence; and 3) the loss of CO_2 and H_2S associated with the boiling process increases the brine pH which increases the silica deposition rate. The overall effect of these changes, in addition to major turbulence caused by the boiling process, is to dramatically increase the deposition rate of the silica present.

Figure 4-22 shows the silica deposition that formed in the discharge line from the atmospheric flash chamber over a period of approximately 12 months of use. The scale is predominantly silica and is almost entirely of the vitreous type. Wave-like protrusions on the surface of the scale are clearly evident and are oriented into or toward the direction of flow. The interpretation is that the scale is depositing by an impact type phenomenon from the very strongly supersaturated residual brine.

Silica deposition continues in the brine retention pond and was observed to form a thick layer of somewhat friable dendritic scale on the walls of the pond. Nucleation apparently began at the air-water interface at the pond

surface and subsequently grew outward from the thin layer originally formed. It is also of note that the outer friable layer was underlain by a thinner layer of massive vitreous silica; these features are clearly evident on Figures 4-23 and 4-24 where the more vitreous layer appears in the outer dark gray layer. The inner gray layers correspond to slightly higher concentrations of sulfides in the silica matrix.

The micromorphology of these two types of silica is shown in Figures 4-25 to 4-28. The dendritic scale in Figures 4-25 and 4-26 is clearly an open structure with numerous solution cavities whereas the vitreous material is more solid with virtually no porosity. It is hypothesized that the more open scale structure precipitates initially and is subsequently cemented into a solid mass as brine circulates through the solution cavities present in the original structure.

Discussion of Silica Deposition

Brine Piping System. In addition to the observations made on the silica scale deposition within the brine disposal line, several other characteristics regarding brine silica behavior have been noted during the operational history of HGP-A. These characteristics can be briefly summarized as follows: 1) Brine samples withdrawn from the pressurized brine disposal line and cooled to ambient temperature in a heat exchanger are clear and colorless whereas brine that has been allowed to cool by steam formation develops a turbid milky blue to opaque white character. 2) Addition of caustic to unflashed brine brings about a similar change at an intermediate pH and ultimately causes the precipitation of a gelatinous floc from the brine. Analysis of this material indicates that it is composed primarily of silica and calcium carbonate. 3) The rate of silica deposition in the brine retention pond has increased with time.

Our current interpretation of these observations is that silica polymerization in the geothermal fluids proceeds at a relatively slow rate and that this rate is strongly pH dependent. The unflashed geothermal brines, at a pH of approximately 7, are quite stable to colloidal silica formation for periods of hours to days. However, the slight increase in pH (to about 8.5) brought about by the flashing process and consequent acid gas (CO_2 and H_2S) loss produces almost instantaneous formation of a polymerized silica colloid.

Greater increases in pH result in further destabilization of the colloidal polymer which eventually allows the formation of a gelatinous floc.

Studies of the flocculated material have found that each particle carries a strong surface charge that is pH dependent. The surface charge is strongly negative, approximately -15 millivolts, at a low pH but gradually declines to a zero surface charge at a pH of approximately 11.5 that then rapidly increases to a positive surface charge at even higher pH levels (Table 4-1). This pH dependence of the silica polymer surface charge is believed to be the key to many of the characteristics of silica scale formation at HGP-A.

TABLE 4-1

ZETA POTENTIAL OF SILICA PARTICLES
(in H_2S free brines)

pH	Zeta Potential	Average Z.P. (to nearest 5)
8.5	-16, -19, -20	-20
9.0	-19, -20	-20
9.5	-17, -11	-15
10.5	-15, -17	-15
11.5	0, 0, +5	0
11.8	0, 0, 0, +8	0
12.0	+15, +16	+15

It is hypothesized that the strong surface charge formed on the dissolved silica at low pH very effectively inhibits the growth of larger silica polymers or their rapid deposition onto surfaces and hence silica precipitation under these conditions may proceed slowly. Turbulent mixing of the brine may allow a collision type of deposition to overcome the surface charge repulsions of the silica polymers in solution. Hence turbulence in the piping system, such as at nipple connections or at surface imperfections may promote growth of silica scale; growth into the direction of flow may account for the wave-like protrusions observed in the scale layers as well. An increase in pH, brought about by flashing or the addition of caustic to the brine, reduces the surface charge on the silica allowing the growth of larger

colloidal silica polymers and, at even higher pH, massive flocculation of the colloid.

The observed changes with time in both the nature of the silica deposited (to a more massive vitreous form) and the rate of scale formation may also be tied to the interaction between the surface charge on the silica polymer and the changing salinity of the geothermal fluids. During the early production of brine from the well, silica deposition onto the pipe surfaces was apparently inhibited by electrostatic repulsion between the similarly charged silica polymer in solution and the surface of the previously deposited scale. This electrostatic repulsion would be lower at protrusions or imperfections than it would be on flat surfaces and hence a more open network or dendritic scale growth would be favored. However, as the salinity (or ionic strength) of the brines increased, the dielectric constant of the brines would also increase and hence electrostatic shielding between the surface charges on the polymers and on the deposited scale would be more effective. The net result of the improved electrostatic shielding would be that silica deposition in general would increase and that the dendritic growth pattern would be less favored over deposition on flat surfaces. This may account for the apparent transition from a more open, friable, silica scale on the wall of the brine piping system to the more massive, vitreous silica deposited in the inner (more recent) layers of scale.

Experimental Studies of Silica Deposition

In order to further investigate the response of silica in the brine system to varying conditions of pH and salinity, two experiments of a very preliminary nature were performed. One experiment consisted of suspending glass slides in the brine retention tank for periods ranging from one to several weeks and recording weight changes due to silica deposition. The second experiment investigated the rate of silica deposition from the brine as a function of pH.

The results of the first experiment are presented in Table 4-2. The data represent the initial and final weights of the glass slides on the dates indicated. Slide 1 was placed in the upstream end of the retention pond and was replaced weekly with a new slide; slide 2 was also placed in the upstream end of the pond but was returned to the pond after being dried and weighed; slide 3 was placed in the downstream end of the retention pond and was replaced with a new slide weekly.

TABLE 4-2

SILICA DEPOSITION IN BRINE RETENTION POND

SAMPLE NUMBER	DATE IN	WEIGHT IN (g)	DATE OUT	WEIGHT OUT (g)	WEIGHT CHANGE	COMMENTS
1	3-09-83	4.7	3-16-83	5.0	0.3	
2	3-09-83	4.7	3-16-83	5.0	0.3	
3	3-09-83	5.0	3-16-83	5.0	0	
1	3-16-83	4.9	3-23-83	5.1	0.2	
2	3-16-83	5.0	3-23-83	5.4	0.4	
3	3-16-83	4.5	3-23-83	4.5	0.0	
1	3-23-83	4.8	3-30-83	5.13	0.33	
2	3-23-83	5.4	3-30-83	-	-	Sample lost
3	3-23-83	4.7	3-30-83	-	-	Sample lost
1	3-30-83	4.47	4-06-83	4.88	0.41	
2	3-30-83	4.64	4-06-83	5.04	0.40	
3	3-30-83	4.56	4-06-83	4.61	0.05	
1	4-06-83	4.53	4-14-83	7.71	3.18	
2	4-06-83	5.04	4-14-83	9.58	4.54	
3	4-06-83	4.97	4-14-83	5.13	0.16	
1	4-14-83	4.72	4-21-83	5.04	1.32	
2	4-14-83	9.58	4-21-83	11.54	1.96	
3	4-14-83	4.94	4-21-83	5.00	0.06	
1	4-21-83	4.56	4-27-83	4.81	0.25	
2	4-21-83	11.54	4-27-83	12.95	1.41	
3	4-21-83	4.75	4-27-83	-	-	Sample lost
1	4-27-83	4.49	5-04-83	11.58	7.09	
2	4-27-83	12.95	5-04-83	24.80	11.85	
3	4-27-83	4.94	5-04-83	5.76	0.82	
1	5-04-83	-	8-24-83	-	-	
2	5-04-83	-	8-24-83	-	-	
3	5-04-83	4.70	8-24-83	-	-	See Plate 3
1	8-24-83	4.72	9-06-83	11.96	7.24	
2	8-24-83	4.50	9-06-83	10.29	5.79	
3	8-24-83	4.96	9-06-83	9.83	4.87	
1	9-07-83	4.73	9-14-83	6.35	1.62	
2	9-07-83	10.29	9-14-83	18.78	8.49	
3	9-07-83	4.96	9-14-83	5.55	0.59	
1	9-14-83	4.72	9-28-83	10.50	5.78	
2	9-14-83	18.78	9-28-83	64.68	45.90	
3	9-14-83	4.56	9-28-83	6.91	1.35	
1	9-28-83	4.53	10-12-83	7.30	2.77	
2	9-28-83	4.92	10-12-83	7.60	2.68	
3	9-28-83	5.02	10-12-83	7.27	2.25	

The data suggest several conclusions. There is clearly an increase in the silica deposition rate with time. Although this increase appears to be quite variable, we believe that the majority of the variability is the result of changing brine flow conditions in the retention pond. Silica scaling in the discharge line from the Brine Muffler Box gradually choked off flow through the pond and the discharge line was eventually replaced. Subsequent to this date continued scaling in the pond eventually necessitated the diversion of brine flow through an alternative flash chamber and led to the termination of the experiment.

The second conclusion suggested by the data is that silica deposition was occurring most rapidly at the upstream end of the brine retention pond. In nearly every set of samples the upstream silica accumulation was substantially greater than that observed downstream. This may be due to the greater degree of dissolved silica supersaturation present in this location or possibly to greater turbulence occurring in this part of the pond.

The nature of the silica deposited was very similar to the nature of that found on the sides of the pond: very delicate open structures. Deposition was most rapid at the edges of the glass slides but gradually covered the entire surface. The rate of deposition was also clearly a function of available surface area; as the high surface area scale formed on the slide the rate of weight gain increased markedly. Figures 4-29 to 4-32 demonstrate the progression of silica deposition. The last in this series is the sample exposed for approximately three and one half months. Figures 4-33 and 4-34 show the appearance of the brine retention pond at the termination of this experiment.

The second silica experiment investigated the silica precipitation/ flocculation response with changes in brine pH. The experimental procedure was to add a known volume of sodium hydroxide to one liter of brine and decant the solution into a 1-liter graduated cylinder. The settling rate of the silica precipitate was monitored by noting the volume occupied by the silica floc as it settled and the total amount of silica removed from solution was determined by sampling and analysis of the clear supernatant at the termination of the settling experiment. It should also be noted that all of these experiments were performed at room temperature since convective mixing was found to inhibit silica settling in experiments attempted in hot brines.

Several general observations can be made regarding the results of this experiment. Below a pH of approximately 8.7, no silica precipitate was observed to settle. The amount of the silica precipitation generated at pH 8.7 and above was heavily dependent upon the solution pH as was the rate at which it settled. Table 4-4 presents the silica precipitation rate data from these experiments. The far left hand column represents the volume occupied by the precipitated silica floc as determined by a clear line in the turbidity of the mixture; the numbers in the rows across from these volumes represent the time in minutes required for settling of the floc to that volume. The top row corresponds to the pH of the brine sample for each individual experiment. Table 4-3 presents the analytical data for the silica concentrations present in the supernatant liquid at the termination of each experiment. The results demonstrate the strong pH dependency of the silica polymerization and precipitation rate. Whereas the former shows the sharpest breaks between pH 7.7 and 9.0 and again between 11.4 and 12.5, the latter shows a more gradual change with a maximum floc volume formed at approximately 11.5. It is noteworthy that the later pH is near the point of zero surface charge for the silica particulates formed (see Table 4-1).

TABLE 4-3

SILICA CONCENTRATIONS IN SUPERNATE
(at various pH's in H_2S free brine)

Hot Brine (100°C)		Cooled Brine (25°C to 30°C)	
pH	SiO_2, ppm	pH	SiO_2, ppm
10.2	291	7.7	1084
11.2	230	8.7	430
12.3	< 15 to 40	9.0	403
		9.1	395
		9.3	389
		10.2	368
		10.5	287
		10.8	305
		11.0	344
		11.4	214
		12.1	55
		12.5	88
		12.5	81

TABLE 4-4

SILICA PRECIPITATION RATES AT VARIOUS PH'S

Time in minutes at room temperature (25-30°C) unless otherwise specified.

	PH's																	
Ml	1.3	8.3	8.7	9.0	9.1	9.3	10.2	10.2*	10.5	10.8	11.0	11.2*	11.4	11.5	12.1	12.3*	12.5	12.5
1000	0-10	0-60	0	0		0		0	0	0	0	0	0	0	0	0	0	0
950												4			1			
900				0.75	1					1	1.5	94@8	2	1.5	1.67	2	1.5	1.67
												920@51						
800								2.5		2	2.67		3.5	2.5	2.5	2.5	2.5	3
700									4.5	2.5	3.67		4.5	4	3.33	720@4.5	3.5	4
600								3.5	5	3.5	5		6	9.5	4.5		5	5.25
550														23.5	7		7	540@6.5
525															11		24	
500								4.5	6	4.5	6		9		520@20			7.5
480																		9.5
450																		460@13.5
400							420@17		6.5	5.5			16					450@15.5
370											7.5							
350										7.5	340@8		26					
300							30	5.5	7.5	11.5	9							
250							50			17.5	11							
200						3	230@61	8.5	10	230@13								
										200@16								
170				2.75	3													
160				3				12.5	16									
150				3.5, 4	6													
				3.75														
140				4.5	5													
130				6.5	6													
120					8													
110					11	20												
100			15		18													
90			95@19,13															
			90@12															

*Run conducted at brine temperature of 100°C.

Conclusions

The silica scale deposition rates experienced at the HGP-A Generator facility have not been inordinately high in the majority of the brine handling system. Localized problems have been generated where brine has been allowed to boil or where the brine pH has been increased to levels above 8.5 by the addition of caustic.

The polymerization and flocculation rate of silica in the brines has been found to be strongly dependent upon the brine pH. Deposition of silica as a dendritic or vitreous scale is also dependent upon the ionic strength (or salinity) of the brines produced by the well. In light of the increasing brine salinity it is expected that the rate of silica deposition in the brine disposal system will increase and that the material deposited will become more vitreous and solid as compared to the more dendritic formations observed up to the present time.

Projections and Recommendations

The expected increase in silica precipitation rate that is anticipated in HGP-A could pose severe operational problems for this facility both with regard to brine system maintenance and with eventual disposal of the brines.

The following are recommended actions that should be undertaken to minimize the anticipated difficulties at the HGP-A facility.

1. Continue monitoring fluid salinity and silica precipitation rates in the brine retention pond;
2. redesign or refit the power plant separator to minimize the possibility of brine flashing at the exit point from the separator;
3. determine whether a crystallizer settler will permit efficient removal of polymerized silica from the geothermal effluent; and
4. investigate the feasibility of installing some other type of treatment system to remove dissolved silica from the geothermal fluids.

The applicability of the experience gained at HGP-A to other future geothermal facilities on Kilauea will depend upon both the nature of the resource encountered - whether water or steam dominated systems - and upon the chemistry of the geothermal brines produced. Lower salinity brines will, in

all probability, show similar scaling potential to that observed in HGP-A during the early operations. Higher salinity brines will, however, probably show a more rapid silica deposition rate than that currently observed at HGP-A.

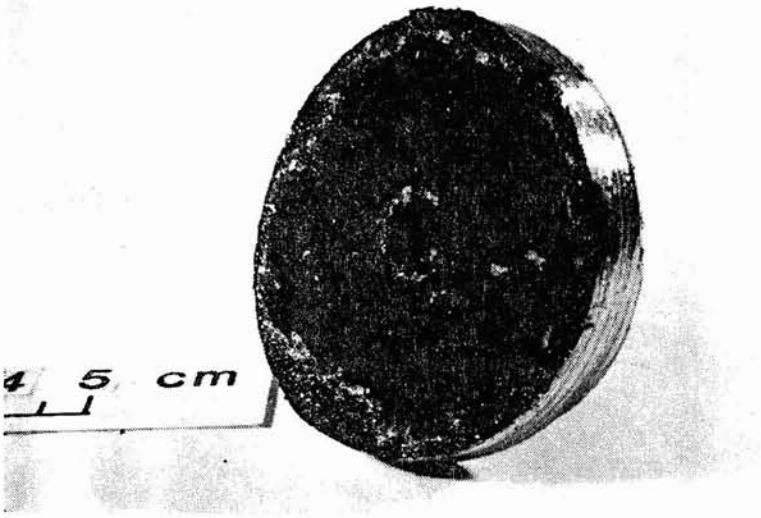

Figure 4-1. Disc Cut-out Two Phase Flow Pipe

Source: Hawaii Institute of Geophysics

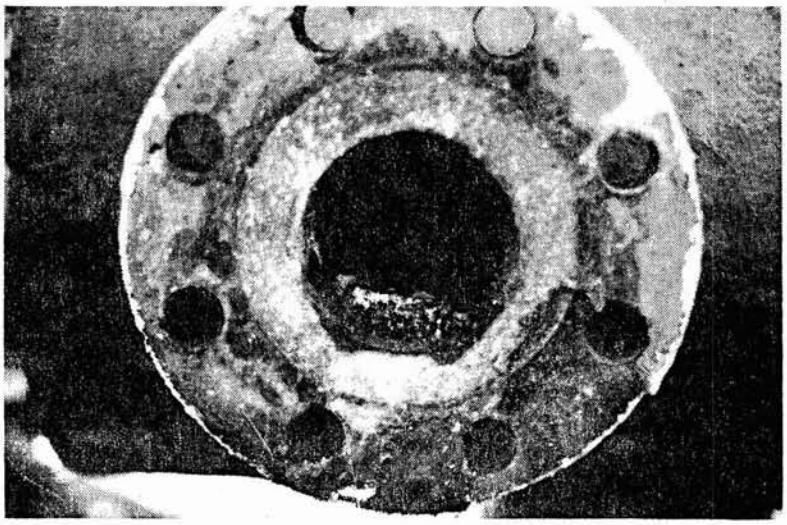

Figure 4-2. Two Phase Flow Sample Connection

Source: Hawaii Institute of Geophysics

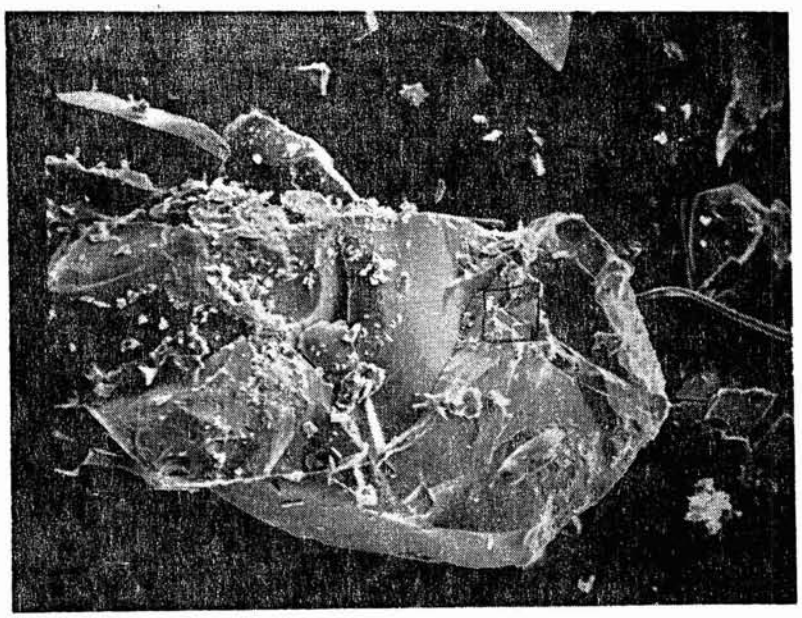

Figure 4-3. Micromorphology of Silica Scale Deposits - Upstream of Flash Separator (130 x* Magnification)

Source: Hawaii Institute of Geophysics

Figure 4-4. Micromorphology of Silica Scale Deposits - Upstream of Flash Separator (1300 x* Magnification)

Source: Hawaii Institute of Geophysics

* Please note that the illustration(s) on this page has been reduced 10% in printing.

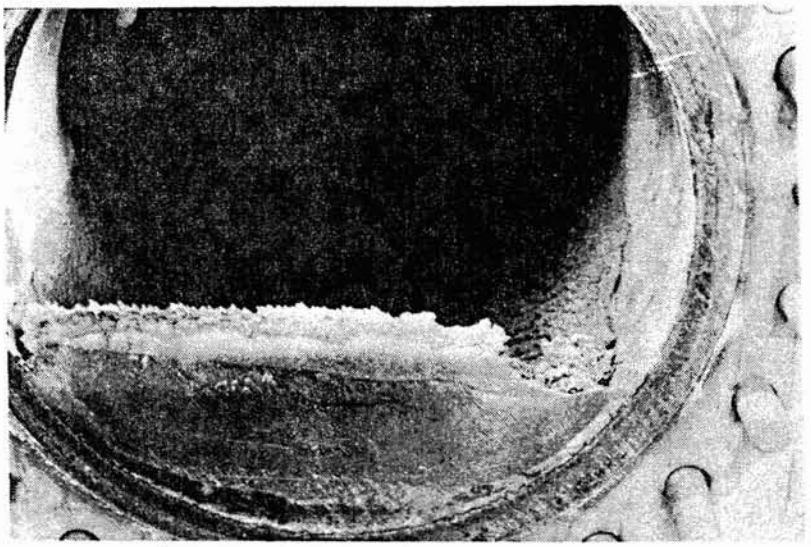

Figure 4-5. Flash Separator Manhole Doorway. Scale is predominantly silica. Thickness of scale ranged from near zero above water line to 2-3 cm in lower portion of separator.

Source: Hawaiian Electric Co., Inc.

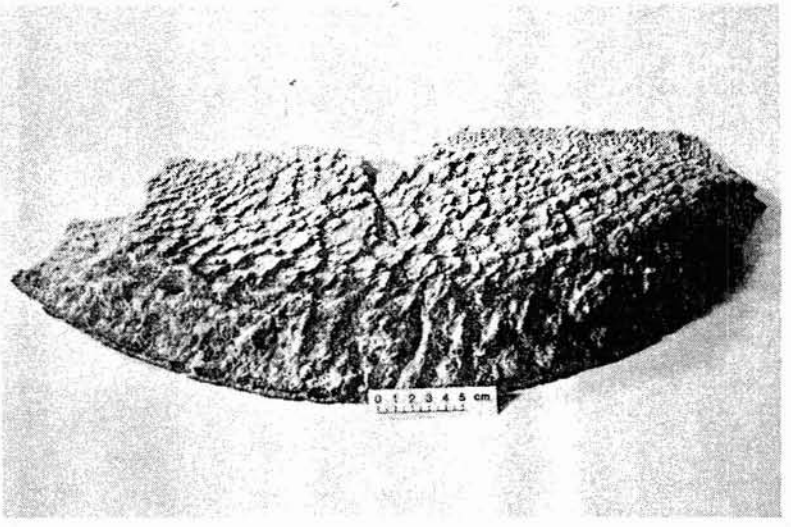

Figure 4-6. Scale Deposits taken from entry into Flash Separator

Source: Hawaii Institute of Geophysics

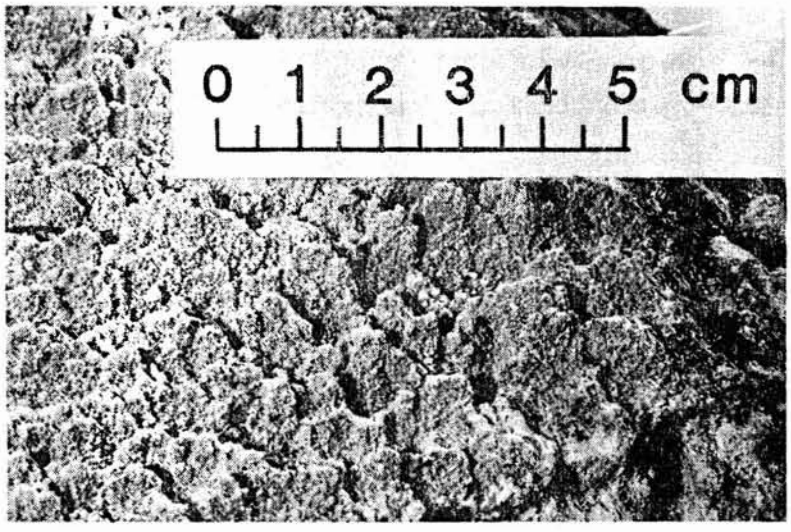

Figure 4-7. Scale Deposits - Flash Separator (Close-up)

Source: Hawaii Institute of Geophysics

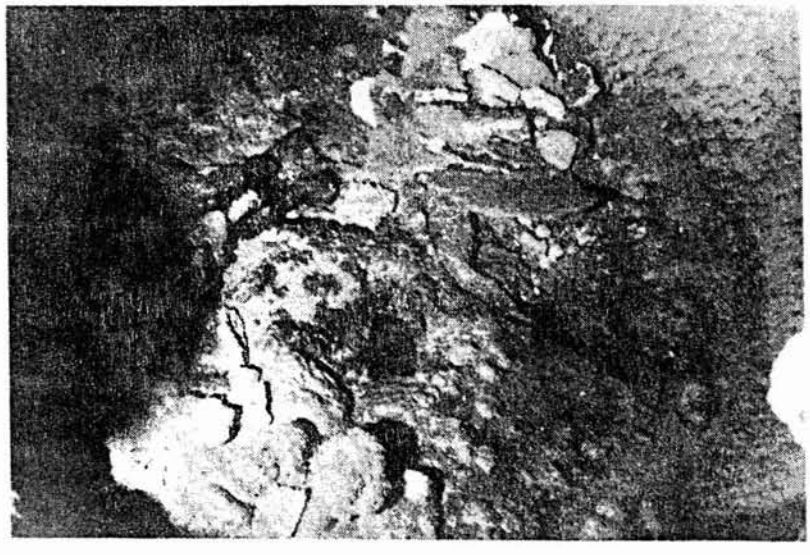

Figure 4-8. Flash Separator Floor

Source: Hawaiian Electric Co., Inc.

Figure 4-9. Micromorphology of Silica Scale - Flash Separator (420 x*Magnification)

Source: Hawaii Institute of Geophysics

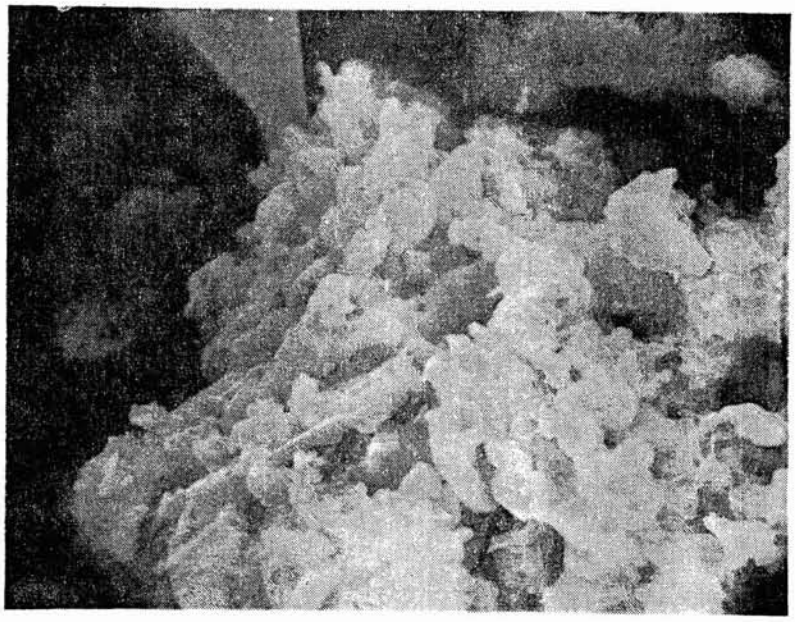

Figure 4-10. Micromorphology of Scale - Flash Separator (2400 x*Magnification)

Source: Hawaii Institute of Geophysics

* Please note that the illustration(s) on this page has been reduced 10% in printing.

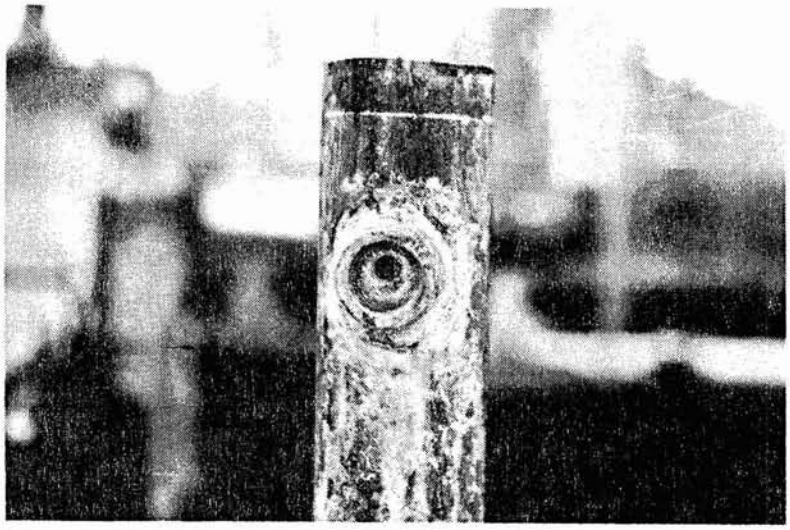

Figure 4-11. 1/2" Nipple on 3" Brine Line from Flash Separator

Source: Hawaii Institute of Geophysics

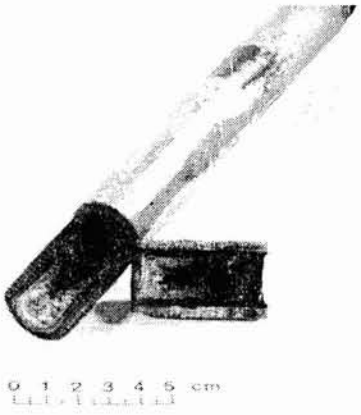

Figure 4-12. Cutaway of 1/2" Pipe off 3" Brine Line

Source: Hawaii Institute of Geophysics

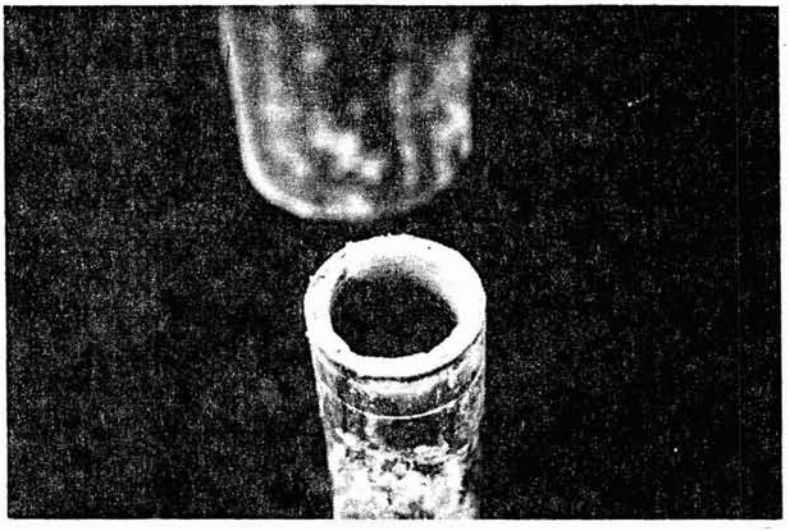

Figure 4-13. Scale Deposits in 3" Brine Piping 10 Feet From Separator

Source: Hawaii Institute of Geophysics

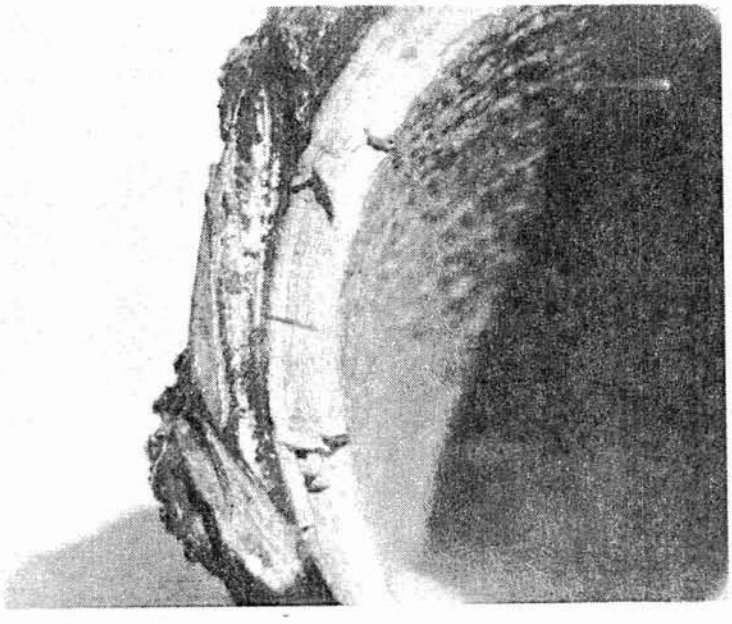

Figure 4-14. Gross Morphology of Deposit on 3" Brine Piping 10 Feet From Separator. Scale material is primarily silica approximately 0.5 cm thick.

Source: Hawaii Institute of Geophysics

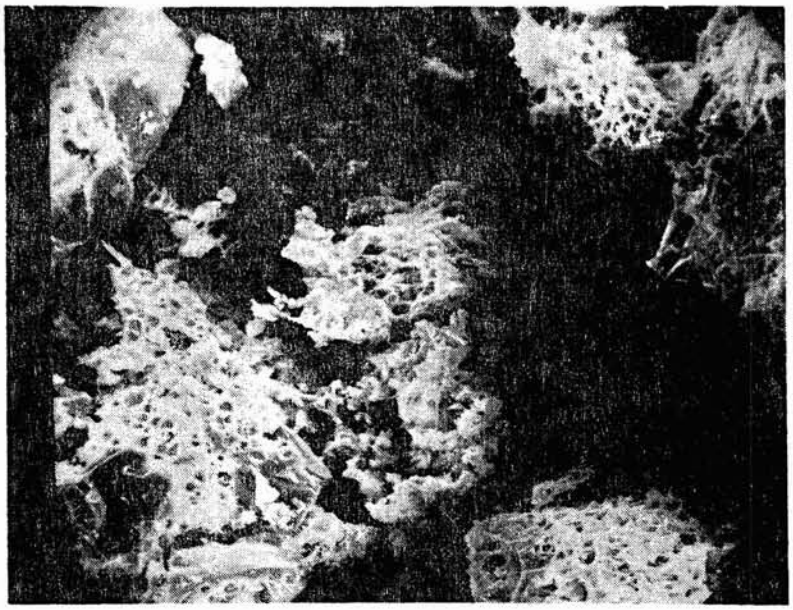

Figure 4-15. Micromorphology of Silica Scale - Outer Layer, Brine Line 10' from Separator (500 x* Magnification)

Source: Hawaii Institute of Geophysics

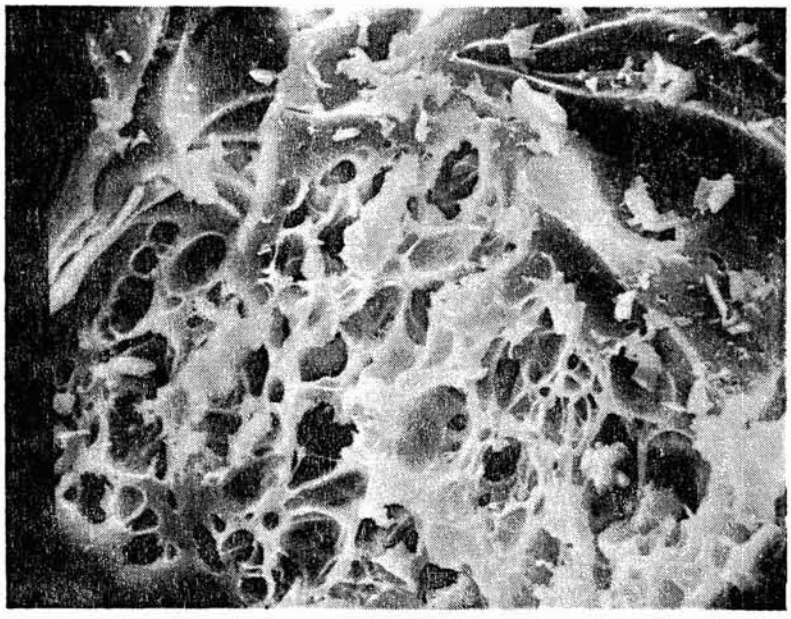

Figure 4-16. Micromorphology of Silica Scale - Outer Layer, Brine Line 10' from Separator (2000 x* Magnification)

Source: Hawaii Institute of Geophysics

* Please note that the illustration(s) on this page has been reduced 10% in printing.

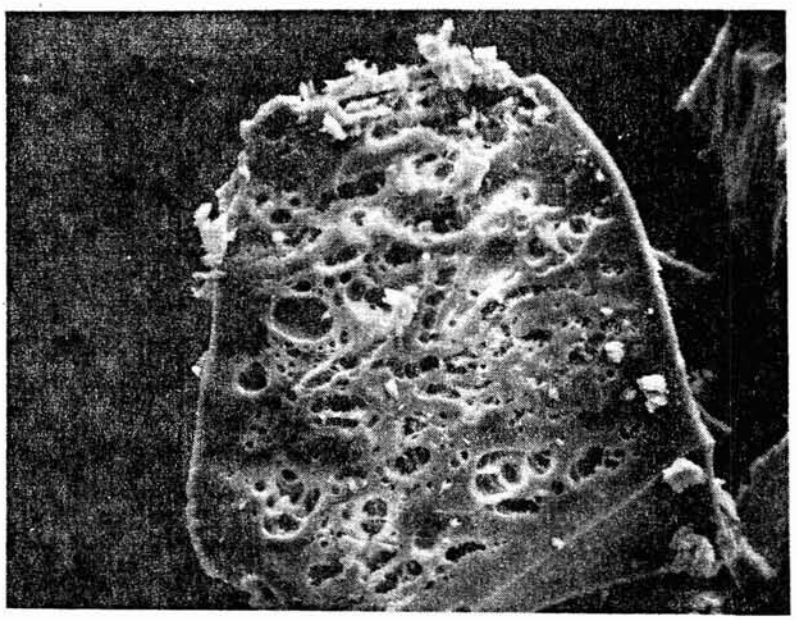

Figure 4-17. Micromorphology of Silica Scale - Inner Layer, Brine Line 10' from Separator (600 x* Magnification)

Source: Hawaii Institute of Geophysics

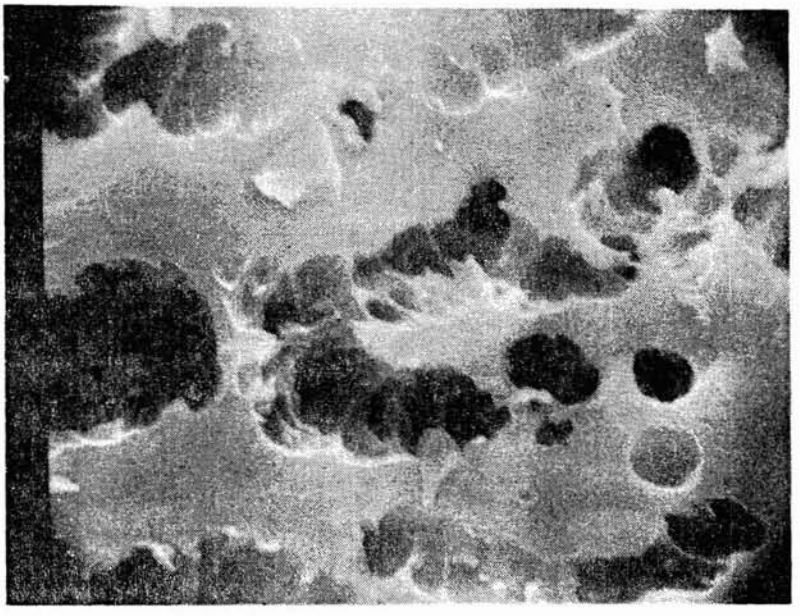

Figure 4-18. Micromorphology of Silica Scale - Inner Layer, Brine Line 10' from Separator (6000 x* Magnification)

Source: Hawaii Institute of Geophysics

* Please note that the illustration(s) on this page has been reduced 10% in printing.

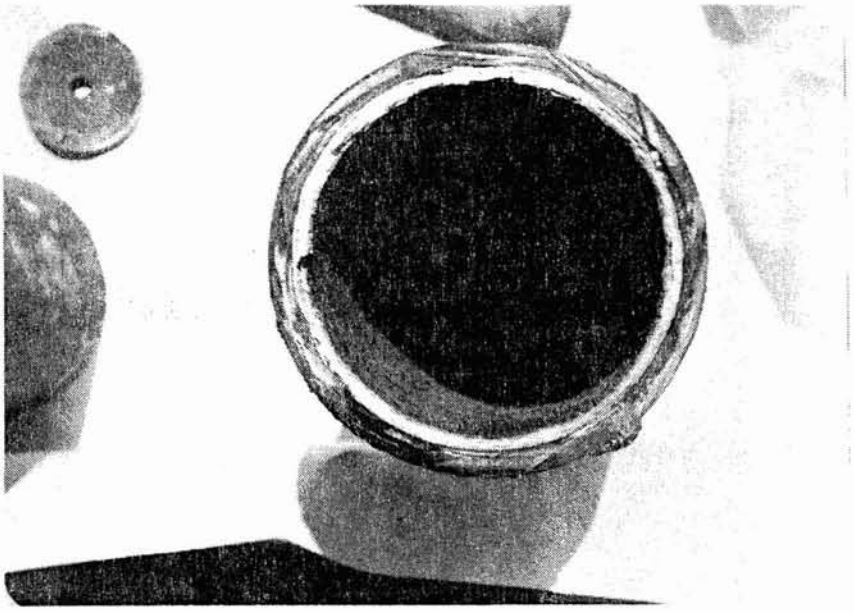

Figure 4-19. Scale Deposits in 3" Brine Line 80 feet from Separator. Scale is silica approximately 0.3 cm thick.

Source: Hawaii Institute of Geophysics

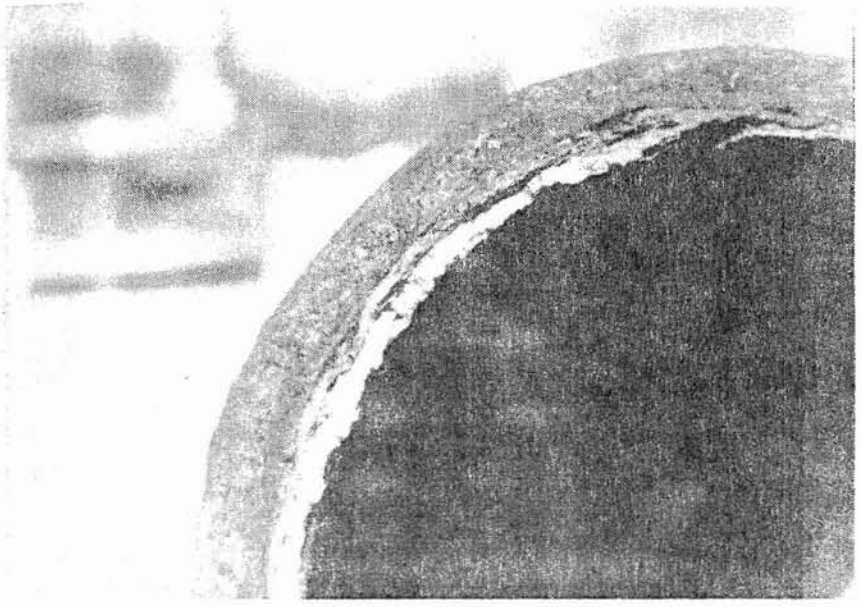

Figure 4-20. Scale Deposits in 3" Brine Line 175 ft. from Separator. Scale material is silica approximately 0.2 - 0.3 cm thick.

Source: Hawaii Institute of Geophysics

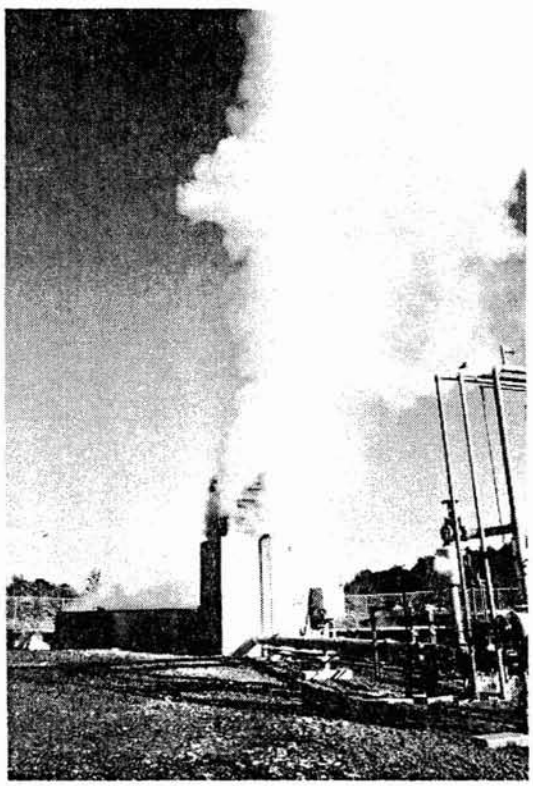

Figure 4-21. Brine Muffler Box

Source: Hawaiian Electric Co., Inc.

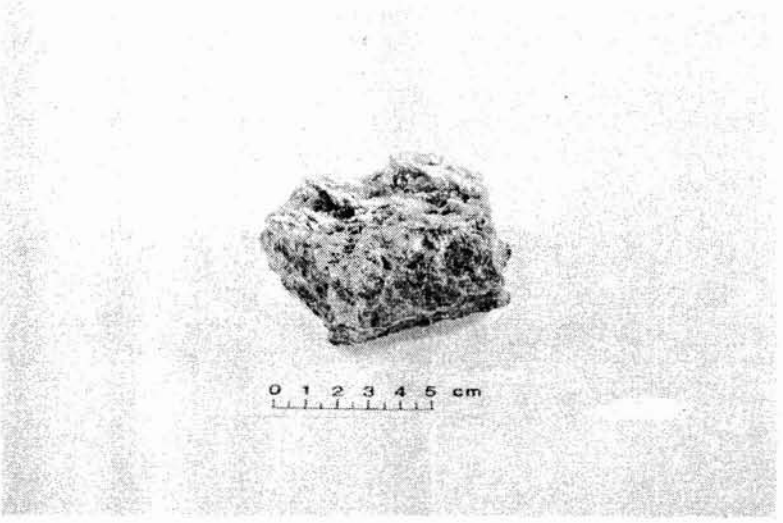

Figure 4-22. Silica Deposits on Muffler Box Discharge Line. Scale is silica, 2-3 cm thick. Note denser texture.

Source: Hawaii Institute of Geophysics

Figure 4-23. Silica Deposits - Brine Retention Pond. Silica is approximately 10 cm thick. Note variable texture.

Source: Hawaii Institute of Geophysics

Figure 4-24. Silica Deposits - Brine Retention Pond (Close-up)

Source: Hawaii Institute of Geophysics

Figure 4-25. Micromorphology of Silica Scale - Brine Retention Pond (550 x* Magnification)

Source: Hawaii Institute of Geophysics

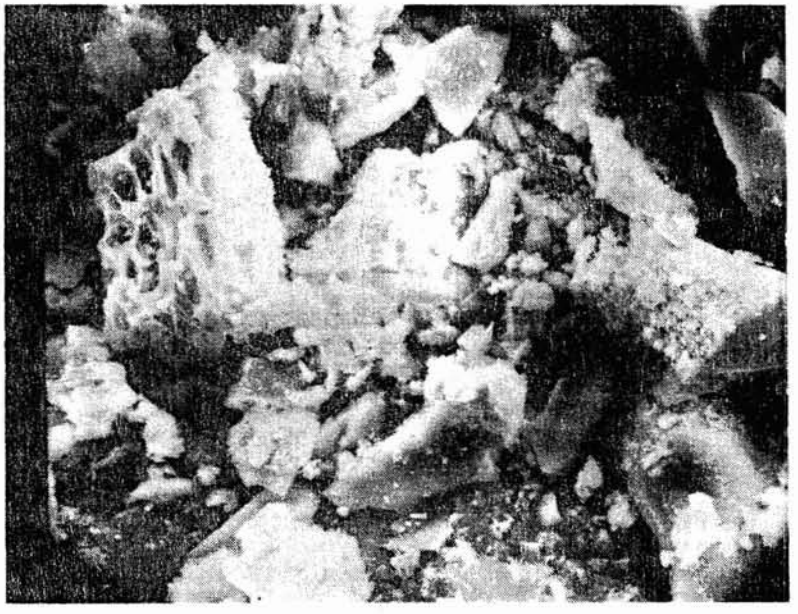

Figure 4-26. Micromorphology of Silica Scale - Brine Retention Pond (1100 x* Magnification)

Source: Hawaii Institute of Geophysics

* Please note that the illustration(s) on this page has been reduced 10% in printing.

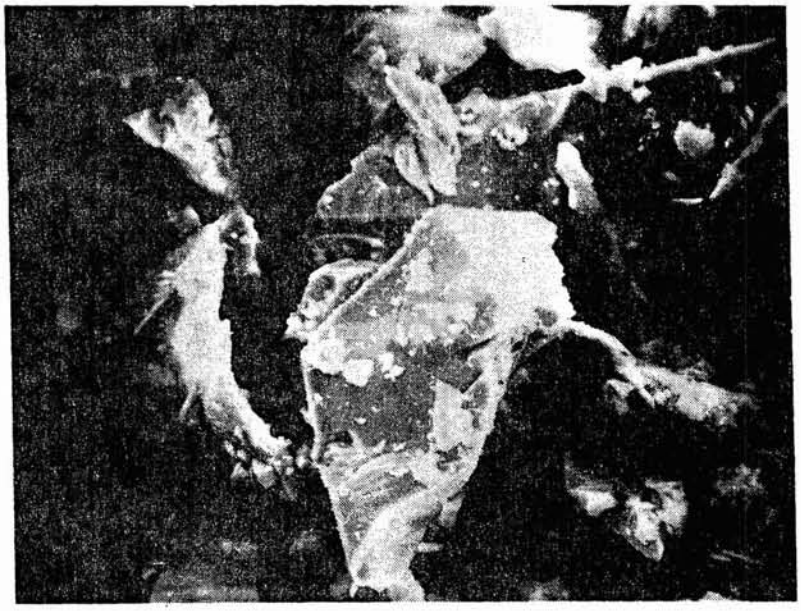

Figure 4-27. Micromorphology of Silica Scale - Brine Retention Pond (600 x* Magnification)

Source: Hawaii Institute of Geophysics

Figure 4-28. Micromorphology of Silica Scale. Brine Retention Pond (2400 x* Magnification)

Source: Hawaii Institute of Geophysics

* Please note that the illustration(s) on this page has been reduced 10% in printing.

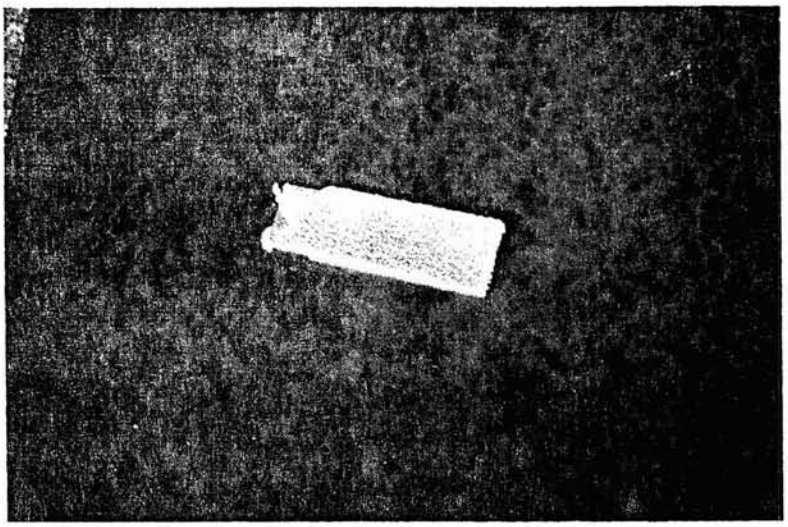

Figure 4-29. Progress of Silica Deposition in Retention Pond, Sample 1. Slides are 2.5 cm x 7.5 cm. Scale thickness is variable to approximately 0.4 cm.

Source: Hawaii Institute of Geophysics

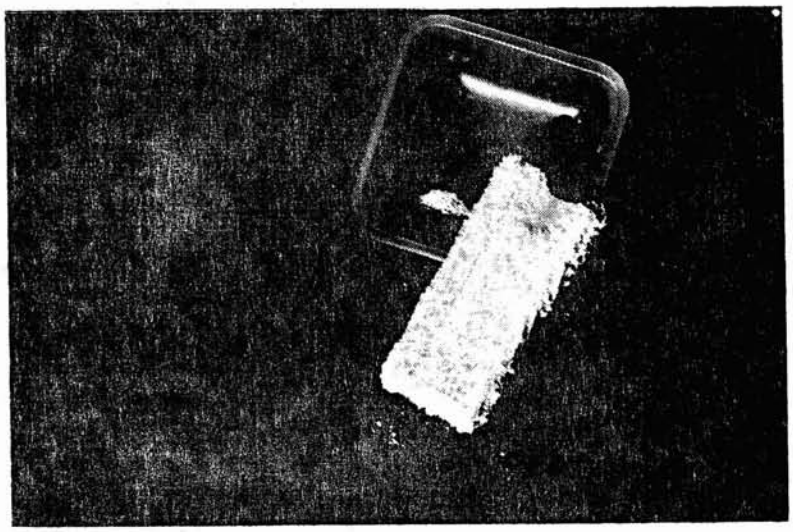

Figure 4-30. Progress of Silica Deposition in Retention Pond, Sample 2. Scale thickness is variable from 0.1 to 0.4 cm.

Source: Hawaii Institute of Geophysics

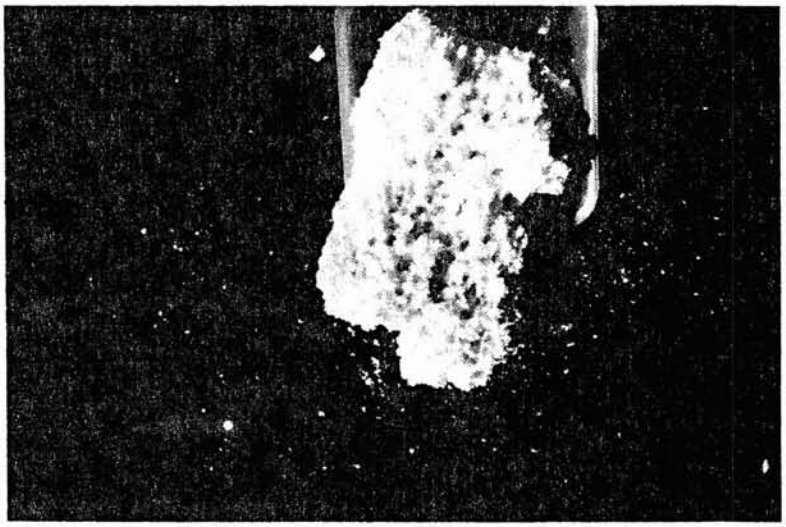

Figure 4-31. Progress of Silica Deposition in Retention Pond, Sample 3. Scale thickness ranges to nearly 1 cm.

Source: Hawaii Institute of Geophysics

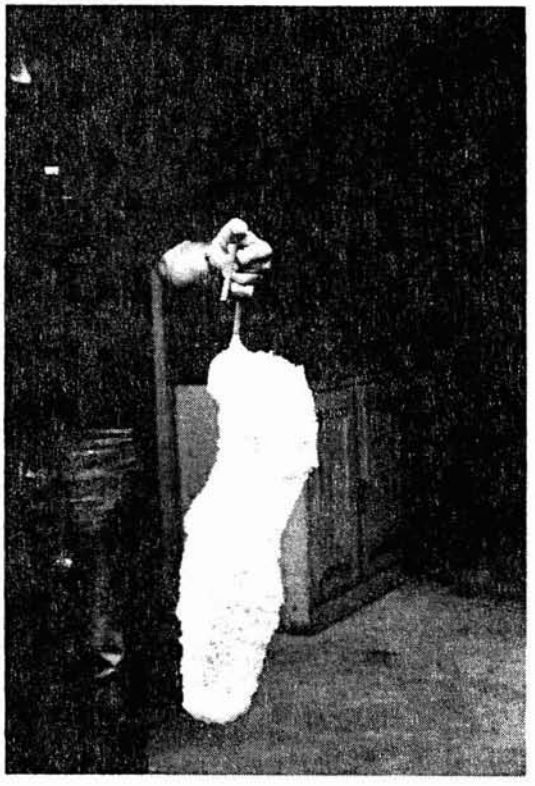

Figure 4-32. Progress of Silica Deposition in Retention Pond, Sample 4. Scale thickness ranges to 10-15 cm.

Source: Hawaii Institute of Geophysics

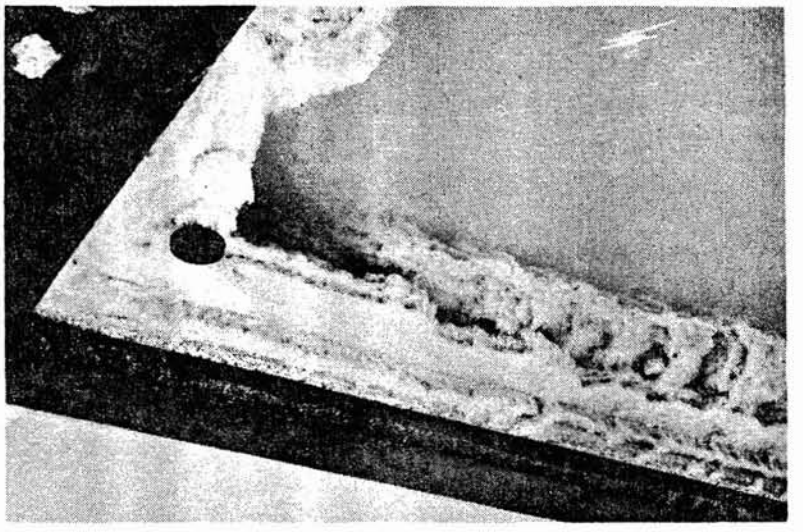

Figure 4-33. Brine Retention Pond - Corner

Source: Hawaii Institute of Geophysics

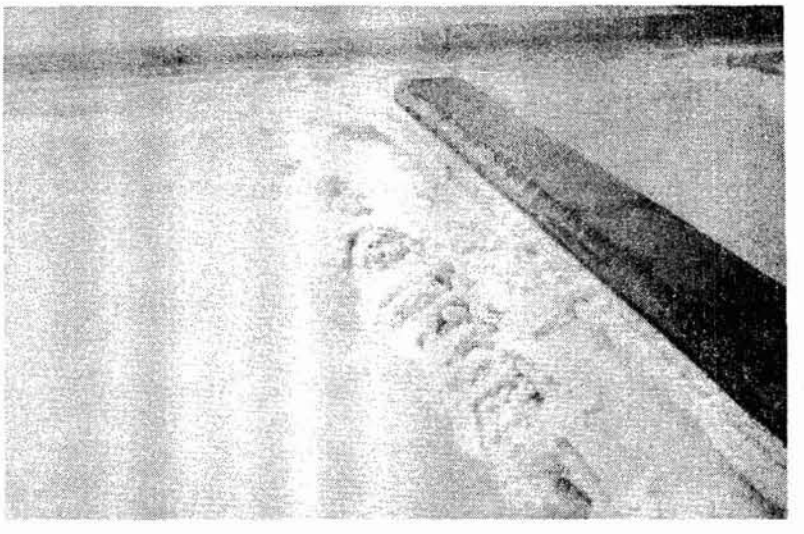

Figure 4.34. Brine Retention Pond - Baffle

Source: Hawaii Institute of Geophysics

Section 5

PLANT OPERATIONAL HISTORY

PLANT DESCRIPTION

The plant consists of an Elliot single inlet steam turbine operating at 5800 rpm which drives a 3000 kWe, 3750 kVA, 1800 rpm air-cooled generator manufactured by Ideal Electric through an Elliot speed reducer. Steam design conditions are 175 psia at 370°F and 51,475 lbs/hr (12.3 kg/cm^2 at 188°C and 23,349 kg/hr).

This six-stage turbine has a compartmental type steam chest with a total of 29 nozzles. Each turbine stage has an inter-stage, manually controlled drain that exits to a condensate flash tank located below the floor which is vented to the main condenser. The turbine exhausts upward through a 40-inch (1.02 m) diameter exhaust pipe at 4 inches Hg absolute (0.14 kg/cm^2) back pressure to a surface condenser by Graham.

The main condenser is designed to operate at an absolute pressure of 4 inches Hg (0.14 kg/cm^2). The steam is condensed and the non-condensable gas (N.C.G.) is drawn off by a two-stage ejector and discharged to the hydrogen sulfide (H_2S) abatement system. The condensate is treated with caustic which is injected and mixed in a static pipeline mixer, and pumped through a carbon steel pipeline to the cooling water return header. The condensate makes up the cooling water losses, due to the evaporative cooling process, by mixing with the cooling water on its return to the cooling towers (manufactured by Marley). About 3300 gpm (750 m^3/hr) is required for the cooling water requirements. Since the condensate supplies more make-up water than required, excess water is by-passed to the percolation ponds for disposal.

The hydrogen sulfide abatement system is a packaged unit by John Zink Co. The H_2S that is ejected from the condenser is burned in an incinerator and the combustion gases pass through an absorber column where the sulfur dioxide is scrubbed with a mixture of water and caustic soda.

OPERATING EXPERIENCES

The plant was initially energized on July 18, 1981. After this initial operation of the plant, numerous operating problems were encountered with the turbine-generator, hydrogen sulfide abatement systems, and the speed control and trip valves. This delayed the plant commercial operation date to March 1982 when the Hawaii Electric Light Company, Inc. (HELCO) assumed the responsibility to operate and maintain the plant under contract with the State of Hawaii.

Since March 1982 the plant has operated as a base load unit with an availability factor of 93% (Table 5-2). During this period, the unit did not run for 870 hours of which 463 hours were due to forced outages and the remainder for scheduled maintenance. The numbers of forced outages caused by the various malfunctions are as shown in Table 5-1 below.

TABLE 5-1

FORCED OUTAGE FREQUENCY

	Number of Occurrences	Total Forced Outage Hours	Percent of Forced Outage Hours
1. H_2S Abatement System	6	348	75.2
2. Plant Electrical System	4	46	9.9
3. Turbine System	5	32	6.9
4. Trans. & Dist. System	3	12	2.6
5. Cooling Tower	1	16	3.5
6. Steam Separator	2	6	1.3
7. Miscellaneous	2	3	0.6
	23	463	100.0

TABLE 5-2

HGP-A RUNNING HOURS AND NET KWHRS PRODUCED

Month	Running Hrs.	Month Hrs.	Net KWHR Prod	Avg. Net KW Output
3-82	433	744	866.1×10^3	2000
4-82	634	720	1447.0	2282
5-82	742	744	1788.0	2409
6-82	720	720	1744.0	2422
7-82	732	744	1790.1	2445
8-82	691	744	1257.9	1820
9-82	709	720	1800.0	2539
10-82	741	744	1869.7	2523
11-82	686	720	1722.3	2511
12-82	740	744	1840.7	2487
1-83	744	744	1887.1	2536
2-83	611	672	1570.4	2570
3-83	740	744	1903.6	2572 max
4-83	669	720	1713.4	2561
5-83	739	744	1890.0	2558
6-83	501	720	1269.3	2534
7-83	730	744	1839.7	2520
	11562	12432	28199.2	

Time Avail = 93%

Corrected Max Net Capacity Due to Reduced Steam Flow is 2572 KW

Corrected Max Gross Capacity Due to Reduced Steam Flow is 2822 KW

Avg. Plant Load for Auxiliary = 250 KW

The major outages caused by the H_2S abatement system were the result of excessive backpressure in the absorber column (2 outages for 166 hours and 5 hours to clean the absorber column) and a broken blower fan (148 hours for repairs). The remaining outages were caused by other system malfunctions.

The scrubber backpressure problem was due to insufficient air for complete oxidation of H_2S in the incinerator resulting in the deposition of elemental sulfur in the packed column. It should be noted that the incinerator malfunction was primarily the result of incorrect engineering specifications that resulted in underdesign of the air supply blowers. This has been corrected. In addition, an emergency scrubber has been installed so that the John Zink scrubber problems no longer cause turbine outages and hydrogen sulfide abatement can be continued.

The outages caused by the power plant electrical system were primarily due to a breaker fault (36 hours), loose wires and relay malfunctions.

The outages caused by the steam turbine system were the result of low oil pressure (21 hours to clean the systems), low condenser vacuum, vibration (twice) and governor repairs.

The single trip caused by the cooling tower was a result of failures in the control wiring to the fan breakers.

In spite of the initial lengthy outages resulting from the John Zink scrubber failures, the overall forced outage rate during the initial 17 months of operation was approximately 4%. This is not excessive for a plant that is manned only one shift per day and also generally had a low restart priority on the system.

Section 6

CONCLUSIONS AND RECOMMENDATIONS

GENERAL

The data obtained from the overhaul of HGP-A Geothermal Wellhead Power Plant provided information from which a plant, using the same resource, can be designed to minimize scale and corrosion of the plant equipment caused by geothermal fluid. This will greatly benefit the owner/operator of future geothermal power plants by reducing operating costs and increasing plant efficiency.

In general, the results of the inspection and overhaul program found that two distinct types of scale formation are occurring; i.e., silicate and metal sulfide. The silica type scale predominates in the brine system and the metal sulfides are found primarily in the steam system. The rate of deposition and scale morphology were found to be strongly influenced by the chemical conditions present in the steam and brine systems. The data suggest that the major chemical controls on scale formation at the HGP-A facility are brine salinity and pH in the brine system and the intermittent access of air (oxygen) to the steam system.

BRINE FLUID HANDLING AND DISPOSAL

Brine fluid must be kept under pressure to keep entrained gases in solution. A reduction in pressure releases these gases, primarily CO_2, which shifts the pH of the fluid. This change in pH causes the precipitation of silica from solution which can seal off surface or underground disposal of the brine. Thus, it appears that the best disposal method of the brine would be to inject it, under pressure, into the ground to a level above the first geothermal production zone.

All brine handling drain valves should be of ball-type construction and all stop valves should be of butterfly design with 316L stainless steel construction of all wetted parts. Control valves may be of butterfly design but the packing

must be pressurized with domestic water to keep the buildup of silica out of that area.

All brine disposal lines should be paralleled with a standby line to allow the brine system to operate continuously when maintaining that line. Provisions must be made to drain, purge and layup the standby line with domestic water.

CONTROLS AND INSTRUMENTATION

Copper tubing should not be used for geothermal applications since it corrodes very quickly in the presence of even low concentrations of H_2S. Type 316L stainless steel and ultra-violet ray proof plastic tubing have proven to be practical for all exterior locations. A high quality plastic is adequate for interior locations where it is not exposed to ultra-violet light.
The use of 316L stainless steel or hydrogen sulfide gas-proof plastic is recommended for all control valve internals exposed to geothermal fluids, steam or gas. The valve steam packing gland area must be pressurized with domestic water to prevent silica buildup which could result in immobility of the rotating or sliding surfaces of the valve. In addition, frequent exercising of the valves will prevent the valves from sticking.

The exterior of each control apparatus must have a durable finish that is highly resistant to sulfate action. Any surface on which water is permitted to stand will be subject to deterioration through sulfate action. Water shield covers are highly recommended for all apparatus and gauges.

Pressure gauge interiors should not be exposed directly to geothermal brines, steams or gases. Stainless steel housed diaphragm seals are essential for gauge longevity when exposed to geothermal fluids.

CORROSIVE FACTORS

Silica in the HGP-A geothermal fluid was found to be present at concentrations greater than normally found in sea water and chloride at concentrations less than in sea water. When hot geothermal brines are flashed to the atmosphere, the pH increases which causes the silica to precipitate. The presence of chlorides and sulfides allows concentrated corrosive attack on most metals when the brines are in contact with atmospheric oxygen.

Leakage of air at the turbine low pressure glands and valve packings located at the vacuum part of the system permits oxygen to enter the system and react with hydrogen sulfide to form sulfurous and sulfuric acids. These acids are very corrosive to most metals, especially those containing nickel and copper.

METALS

Sulfide stress cracking (SSC) can cause catastrophic failure in pressure parts when in contact with liquids containing dissolved H_2S. Lower temperatures and low pH help accelerate this action.

Stainless steels of the martensitic and ferritic type are also very susceptible to SSC. Austenitic stainless steels, with low carbon content, tend to have a greater immunity, as do low strength steels.

Titanium alloys exhibit good resistance to stress corrosion cracking (SCC) when the natural protective film remains intact.

Internal exfoliation of steam lines poses the greatest threat of steam turbine corrosion. Exfoliation is due to sulfidation of the steam line internal surfaces which in turn produces an iron sulfide material which falls off (exfoliates) and is carried by the steam flow into the turbine nozzles and the wheels. The resulting erosion and erosion-sponsored corrosion will cause permanent loss of turbine output. Steam blanketing during shutdown will help reduce the internal pipe corrosion by the prevention of oxygen intrusion. Oxygen corrosion of the steam line internals during plant shutdown forms iron oxide which also can damage the turbine. To minimize such damage, close monitoring and frequent inspections are mandatory. It has been found that large capacity, dual strainers placed ahead of the trip valves can help alleviate this problem.

Elastomers such as those used in pump seat "O" rings, have failed due to their being incompatible with the geothermal brine fluids. The least stable are elastomers made of silicones, nitrile rubber and bisphenol-cured fluoroelastomers. Those compounded with EPDM rubber "ethylene-propylene-diene monomer", perfluoroelastomer and ethylene-propylene copolymer are acceptable.

Proper design and material selection will greatly reduce corrosion of the plant equipment and thereby reduce the cost of operation and maintenance.

MAIN STEAM SYSTEM

Moisture Separator

It is believed that iron oxide deposits are the result of oxygen intrusion during plant shutdown. A valve in the main steam line after the moisture separator should be installed so that it can be kept under steam blanket conditions during shutdowns.

The inlet and outlet perforated plates should be made of 316L stainless steel to prevent these plates from becoming a source of iron sulfide and oxide. In addition, a freeblow, quick-acting valve should be installed in the bottom drain of the moisture separator to keep it from plugging.

Main Steam Line

Main steam lines should be sloped to a cupped drain. Steam traps are not effective.

Control Valves

The valves wide open mode of operation at HGP-A does not subject these valves to the normal wear and tear which turbine control valves usually experience. Butterfly valves are not recommended for throttling service due to their high energy losses. A more appropriate control valve for maximum utilization of the resource supply in this case would be the use of individual poppet valves for each nozzle block compartment.

Without exception, main stop valves for steam must have stainless steel trim, and in all cases where geothermal steam or fluid comes in contact with valve packing, that packing must not contain carbon or graphite. Where water is present, carbon and graphite can cause severe pitting of the stainless steel; teflon packing is preferred.

Small valves handling steam or brine water must be made of stainless steel, and whenever possible, should be a high quality ball design made of 316L stainless steel and packed with teflon. Silicones, nitrile rubber and bisphenol-cured fluoroelastomer packing are not acceptable.

Gate-type stop valves should never be used on the brine system. Ball and butterfly types are acceptable.

All valves must be exercised periodically to avoid immobility due to silica accumulation. Injecting potable water at packing and grease points will keep silica build-up under control.

Plastic ball valves of proper material are acceptable on low pressure and low temperature fluid and gas piping systems. FRP and plastics exhibit a higher coefficient of expansion than steel so precautions must be made to accommodate this factor.

Steam Turbine

The nozzle block restrictions did not appreciably affect the turbine output. Undoubtedly, the many short outages and restarts have kept these passageways sufficiently clear for maintenance of capability. Periodic water washing of the turbine at stage two is believed to have aided in maintaining capability. Turbines should be equipped with steam atomized nozzles in each steam chest compartment for water washing.

The large and sturdy spindle blades have withstood the steam resource chemicals very well. Although pitting was not a serious problem for this low pressure turbine, blade metallurgy could probably be improved to help reduce the pitting action which apparently varies with steam passage through the stages. Scale accumulation in all parts of the turbine was predominantly pyrite. In general, scale deposition did not appear to be as large a factor as was originally anticipated and thus, the blade design, having generous blade openings and a low number of blades per wheel, could be re-evaluated to better optimize resource utilization.

Scaling on the diaphragm blades was less than expected and did not appreciably affect the capability of the turbine. Pitting on the diaphram blades was more severe than it was on the turbine blades. Scale deposition along the slip-fit facings between the diaphragms and their seats in the turbine casing had a tendency to wedge the diaphragms in place. Removal of the diaphragm sections from the casing seats required the greatest single manpower effort of the overhaul operation. During reassembly, the diaphragms were reset with teflon

tape to prevent a metal-to-metal lock up. The results of this experiment will be determined at the next overhaul.

The turbine exhaust pipe was relatively clean. However, the turbine glands were severely scaled and may require shutdown and removal for cleaning on an annual basis.

CONDENSER

The steam side of the condenser was clean. The condenser hotwell was also clean with some soft loose iron sulfide deposits on the floor and should not require opening for cleaning on a frequent basis in the future.

On the water side of the condenser a porous iron oxide coating, and pitting, was evident on the bottom three-fourths section of the tube interior. The source of the iron oxide is the extensive carbon steel cooling water piping used for this plant. The pitting of the tubes is believed to be the result of exposure of the condenser to stagnant cooling water during the period of August to December 1981 when power plant operations were suspended due to a turbine failure. When the system was opened in January 1982 for cleaning, the tube interiors were heavily coated with anaerobic bacteria slime. Proper maintenance of the algicide and biocide treatment of the cooling water must be done to prevent this bacterial growth. The cooling water system contained only one, 1" drain valve for the elevated condenser. Suitable numbers and sizes of drain valves must be provided to allow draining of the condenser during periods of plant shutdown.

HEAT EXCHANGERS

Slime-fouling affects the heat transfer of the apparatus. Cooling water systems should not contain carbon steel piping since it can be a source of iron oxide which can be deposited on the interiors of heat exchanger tubes. Generous drains should be provided so that the system can be drained during any outages over 48 hours to prevent pitting of the tubes.

Section 7

BIBLIOGRAPHY

Baughman, E. C. HGP-A Single Stage Direct Flash Geothermal Power Plant First Overhaul Assessment Part II. August 1983.

Baughman, E. C. Two-Day Shutdown of March 20 and 21, 1984. Interoffice Correspondence. April 27, 1984.

Rogers Engineering Co., Inc. HGP-A Wellhead Generator, Proof-Of-Feasibility Project, 3 MW Wellhead Generator. Plant Data Manual, Volume I. 1981.

Thomas, D. Status Summary of the HGP-A Generator Facility. 1983

Kroopnick, P., R. W. Buddemeier, D. Thomas, L. S. Lau and D. Bills, "Hydrology and Geochemistry of a Hawaiian Geothermal System," HGP-A: Hawaii Institute of Geophysics Technical Report No. 78-6. 1978

Mottle, M.J., and H. D. Holland. Chemical Exchange During Hydrothermal Alteration of Basalt by Seawater - I. Experimental Results for Major and Minor Components of Seawater. 1978

Mottle, M.J., H.D. Holland, and R.F. Corr. Chemical Exchange During Hydrothermal Alteration of Basalt by Seawater - II. Experimental Results for Fe, Mn, and Sulfur Species. 1979

EPRI AP-4342

Below are five index cards that allow for filing according to the four cross-references in addition to the title of the report. A brief abstract describing the major subject area covered in the report is included on each card.

EPRI

EPRI AP-4342
RP1195-12
Final Report
December 1985

Chemistry, Scale, and Performance of the Hawaii Geothermal Project-A Plant

Contractor: Hawaii Electric Light Company, Inc.

A two-and-a-half-year monitoring study of a geothermal power plant showed that the chemistry of the resource fluid strongly influenced power plant performance. Changes in the fluid chemistry—such as higher salinity and lower pH—substantially increased the rate of scale formation and corrosion in plant components. 124 pp.

EPRI Project Manager: M. E. McLearn

Cross-References:
1. EPRI AP-4342 2. RP1195-12 3. Geothermal Power Systems Program 4. Geothermal Power Plants

ELECTRIC POWER RESEARCH INSTITUTE
Post Office Box 10412, Palo Alto, CA 94303 415-855-2000

EPRI AP-4342

EPRI

EPRI AP-4342
RP1195-12
Final Report
December 1985

Chemistry, Scale, and Performance of the Hawaii Geothermal Project-A Plant

Contractor: Hawaii Electric Light Company, Inc.

A two-and-a-half-year monitoring study of a geothermal power plant showed that the chemistry of the resource fluid strongly influenced power plant performance. Changes in the fluid chemistry—such as higher salinity and lower pH—substantially increased the rate of scale formation and corrosion in plant components. 124 pp.

EPRI Project Manager: M. E. McLearn

Cross-References:
1. EPRI AP-4342 2. RP1195-12 3. Geothermal Power Systems Program 4. Geothermal Power Plants

ELECTRIC POWER RESEARCH INSTITUTE
Post Office Box 10412, Palo Alto, CA 94303 415-855-2000

RP1195-12

EPRI

EPRI AP-4342
RP1195-12
Final Report
December 1985

Chemistry, Scale, and Performance of the Hawaii Geothermal Project-A Plant

Contractor: Hawaii Electric Light Company, Inc.

A two-and-a-half-year monitoring study of a geothermal power plant showed that the chemistry of the resource fluid strongly influenced power plant performance. Changes in the fluid chemistry—such as higher salinity and lower pH—substantially increased the rate of scale formation and corrosion in plant components. 124 pp.

EPRI Project Manager: M. E. McLearn

Cross-References:
1. EPRI AP-4342 2. RP1195-12 3. Geothermal Power Systems Program 4. Geothermal Power Plants

ELECTRIC POWER RESEARCH INSTITUTE
Post Office Box 10412, Palo Alto, CA 94303 415-855-2000

GEOTHERMAL POWER SYSTEMS PROGRAM

EPRI

EPRI AP-4342
RP1195-12
Final Report
December 1985

Chemistry, Scale, and Performance of the Hawaii Geothermal Project-A Plant

Contractor: Hawaii Electric Light Company, Inc.

A two-and-a-half-year monitoring study of a geothermal power plant showed that the chemistry of the resource fluid strongly influenced power plant performance. Changes in the fluid chemistry—such as higher salinity and lower pH—substantially increased the rate of scale formation and corrosion in plant components. 124 pp.

EPRI Project Manager: M. E. McLearn

Cross-References:
1. EPRI AP-4342 2. RP1195-12 3. Geothermal Power Systems Program 4. Geothermal Power Plants

ELECTRIC POWER RESEARCH INSTITUTE
Post Office Box 10412, Palo Alto, CA 94303 415-855-2000

GEOTHERMAL POWER PLANTS

EPRI

EPRI AP-4342
RP1195-12
Final Report
December 1985

Chemistry, Scale, and Performance of the Hawaii Geothermal Project-A Plant

Contractor: Hawaii Electric Light Company, Inc.

A two-and-a-half-year monitoring study of a geothermal power plant showed that the chemistry of the resource fluid strongly influenced power plant performance. Changes in the fluid chemistry—such as higher salinity and lower pH—substantially increased the rate of scale formation and corrosion in plant components. 124 pp.

EPRI Project Manager: M. E. McLearn

Cross-References:
1. EPRI AP-4342 2. RP1195-12 3. Geothermal Power Systems Program 4. Geothermal Power Plants

ELECTRIC POWER RESEARCH INSTITUTE
Post Office Box 10412, Palo Alto, CA 94303 415-855-2000